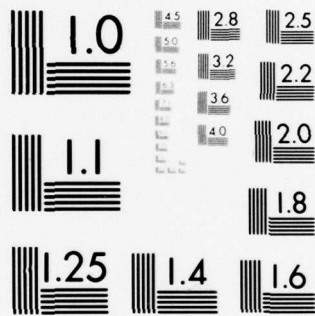| OF |
AD
A063398

END
DATE
FILMED
3-79
DDC

MICROCOPY RESOLUTION TEST CHART

NATIONAL BUREAU OF STANDARDS-1963-A

LEVEL (12)

AD A063398

Use of Drag Measurements to Improve Short-Term Orbit Prediction

B. K. CHING and D. R. HICKMAN
Space Sciences Laboratory
The Ivan A. Getting Laboratories
The Aerospace Corporation
El Segundo, Calif. 90245

use

D D C
RECEIVED
JAN 16 1979
C

20 December 1978

Interim Report

79 01 15 005

This interim report was submitted by The Aerospace Corporation, El Segundo, CA 90245, under Contract No. F04701-78-C-0079 with the Space and Missile Systems Organization, Contracts Management Office, P.O. Box 92960, Worldway Postal Center, Los Angeles, CA 90009. It was reviewed and approved for The Aerospace Corporation by G. A. Paulikas, Director, Space Sciences Laboratory. Gerhard E. Aichinger was the project officer for Mission-Oriented Investigation and Epxerimentation (MOIE) Programs.
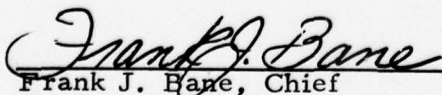
This report has been reviewed by the Information Office (OI) and is releasable to the National Technical Information Service (NTIS). At NTIS, it will be available to the general public, including foreign nations.

This technical report has been reviewed and is approved for publication. Publication of this report does not constitute Air Force approval of the report's findings or conclusions. It is published only for the exchange and stimulation of ideas.

Gerhard E. Aichinger
Project Officer

FOR THE COMMANDER

Frank J. Bane, Chief
Contracts Management Office

REPORT DOCUMENTATION PAGE		READ INSTRUCTIONS BEFORE COMPLETING FORM
1. REPORT NUMBER SAMSO-TR-78-144	2. GOVT ACCESSION NO.	3. RECIPIENT'S CATALOG NUMBER
4. TITLE (and Subtitle) USE OF DRAG MEASUREMENTS TO IMPROVE SHORT-TERM ORBIT PREDICTION		5. TYPE OF REPORT & PERIOD COVERED Interim rept.
		6. PERFORMING ORG. REPORT NUMBER TR-0079(4960-04)-1
7. AUTHOR(s) Barbara K. Ching and David R. Hickman		8. CONTRACT OR GRANT NUMBER(s) F04701-78-C-0079
9. PERFORMING ORGANIZATION NAME AND ADDRESS The Aerospace Corporation El Segundo, Calif. 90245		10. PROGRAM ELEMENT, PROJECT, TASK AREA & WORK UNIT NUMBERS
11. CONTROLLING OFFICE NAME AND ADDRESS Space and Missile Systems Organization Air Force System Command Los Angeles, Calif. 90009		12. REPORT DATE 20 December 1978
		13. NUMBER OF PAGES 83
14. MONITORING AGENCY NAME & ADDRESS(if different from Controlling Office)		15. SECURITY CLASS. (of this report) Unclassified
		15a. DECLASSIFICATION/DOWNGRADING SCHEDULE

16. DISTRIBUTION STATEMENT (of this Report)

Approved for public release; distribution unlimited.

17. DISTRIBUTION STATEMENT (of the abstract entered in Block 20, if different from Report)

18. SUPPLEMENTARY NOTES

19. KEY WORDS (Continue on reverse side if necessary and identify by block number)

Orbit Prediction
Drag Measurements
Calorimeter Measurements
Aerodynamic Drag on Satellites

20. ABSTRACT (Continue on reverse side if necessary and identify by block number)

The improvement in short-term orbit prediction that results from the use of real-time drag measurements to determine the initial vehicle vector has been studied using orbit simulation calculations. Realistic time-dependent behavior of the drag force was provided by the use of calorimeter data from an actual flight. The study was limited to a specific class of low-altitude orbits and to average conditions of magnetic activity. In five samples of calorimeter data, RMS errors in a 3-rev predict span were reduced by OVER

19. KEY WORDS (Continued)

$\geq$ OR =

$\geq$ OR =

20. ABSTRACT (Continued)

factors ≥ 2 and ≥ 3 in the radial and intrack components, respectively, caused solely by the improvement in the initial vector of the predict span. Errors that remain despite the utilization of a near-perfect starting vector could only be caused by improperly modeled drag effects. Because such effects are likely to be the limiting factor in prediction accuracy, improved capability of density prediction will be necessary to meet stringent mission requirements. Until reliable density forecasting capability becomes a reality, the "persistence" feature of the atmosphere can be exploited to improve short-term prediction. In four out of five cases studied, prediction based on the last orbit of drag data in the fit span reduced errors significantly in the predict span.

PREFACE

We wish to thank Mr. Willard Downs III and Ms. Lena Whittaker for their excellent support in the orbit simulation calculations.

79 01 15 005

CONTENTS

TABLES

FIGURES

I.   INTRODUCTION

It seems self-evident that the use of actual measurements of aerodynamic drag on a satellite rather than a force model based on an atmospheric model would provide improved capability for post-flight orbit reconstruction and near-term ephemeris prediction. However, in order to justify the use of drag-measuring devices on an operational basis, a decision would have to be made as to whether the improved capability was sufficiently great to warrant the additional expense. This means, of course, that one must be able to define what constitutes a "sufficient" improvement and also have quantitative data upon which to base a decision.

The purpose of the study reported here was to obtain such quantitative information. Realistic conditions were achieved by using calorimeter data from an actual flight. However, in order not to obscure the interpretation of the results, it was necessary to assume that the calorimeter data were "perfect," i.e. that any errors in orbit fitting or predicting were due to factors other than drag-measurement errors. In this sense, the results of the study are indicative of the "best" possible performance that should be expected and that in actual practice one would have to allow for errors of measurement.

This study proceeded along two general lines: (1) simulated orbit calculations using the TRACE program, and (2) evaluation of the relationship between prediction errors and the drag model. The latter effort included an analysis of the drag data in search of systematic patterns of behavior that might be used to improve predictive capability.

In Section II we shall describe in detail the objectives and logistics of the orbital calculations, while in Section III we will present the results and discuss the relationship between orbit prediction errors and the predictive drag model. A summary of the findings along with reservations and recommendations will be presented in Section IV.

II.   ORBIT SIMULATION STUDIES

1.   Objective and Method

The basic objective of this phase of the study was to determine the errors in 3-rev predictions that would typically result from the use of in situ drag measurements as opposed to the operational approach which relies on the 'DENSEL model to define the drag force. It is assumed that the drag data (in this case calorimeter measurements) are available only in the 6-rev period immediately preceding the 3-rev predict span and that these data may be used to derive (1) the vehicle position and velocity vector at the start of the predict span, and (2) a drag-force model for the predict span.

To obtain the "error" one must, of course, have a "reference" trajectory representing the "true" world. The reference trajectory was specified by using 9-revs of calorimeter data to represent the drag force along with a nominal geopotential model and initial conditions suitable for a low-altitude orbit.

The sequence of TRACE calculations in shown in Fig. 1. First, a 9-rev reference trajectory was generated by TRACE. Artificial tracking data with random noise added were generated during the first 6-revs. The tracking station locations, data type and rate, sigmas, etc. were taken to be representative of the ACES network.

The second step in the procedure was to use the simulated tracking data to obtain a 7-parameter orbit fit over the first 6-revs. In the flow-chart, t_1 and t_2 are the start and stop times of the fit span. Orbit fitting was done using 'DENSEL (the operational model) and also using

-11-

calorimeter data. The fitted orbits were differenced with respect to the reference orbit, yielding radial, intrack, and crosstrack errors. (It is to be noted that since the same calorimeter data are used to generate the reference trajectory and obtain an orbit fit, the resulting fit necessarily represents the best possible fit one might realistically hope for. The only factor that precludes a "perfect" fit is the random noise in the tracking data.)

The third step in the procedure involved predicting ahead for 3-revs (time t_2 to t_3 in the flowchart of Fig. 1) using the fitted vector at t_2 to initialize the predictions. The predicted and reference trajectories were differenced. Several different drag models were tested in the predict span: (1) 'DENSEL, (2) a model that represented the average of all 6-revs of calorimeter data in the fit span, called Model B, and (3) a model that represented the calorimeter data of only the last rev of the fit span, called Model C. Models B and C were actually smoothed and edited versions of the raw calorimeter data. The manner by which the calorimeter data were smoothed and then transformed to working density models is described in detail in a preliminary report (Ref. 1).

In the calorimeter data base that was available for our use, only 5 sets of 9 consecutive orbits of data were found. The study reported here is based on only those 5 sets. In an operational sense it would be quite simple to devise a routine to handle cases of missing data.

For each of the 5 sets of data the following combinations of drag models were used to fit and predict:

INPUT
DRAG MODEL

TRACE

CALORIMETER
DATA

REFERENCE TRAJECTORY
time t_1 to t_3

Simulated
Tracking data
$t_1 - t_2$

ORBIT
DIFFERENCING

OUTPUT

'DENSEL,
CALORIMETER

ORBIT FITTING
$t_1 - t_2$

Initial
Conditions
At t_2

ORBIT
DIFFERENCING

OUTPUT

'DENSEL,
CALORIMETER
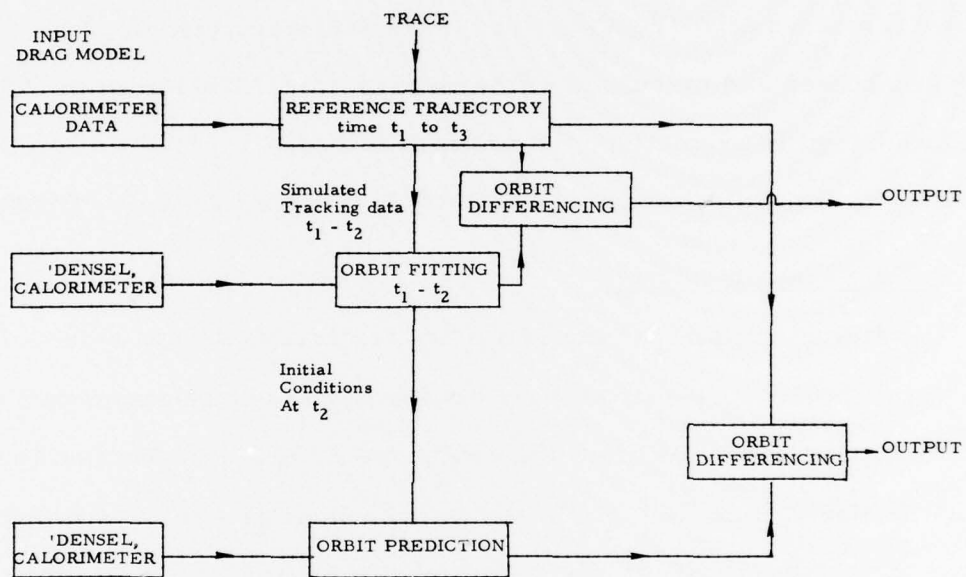
ORBIT PREDICTION

Fig. 1.   Flow Chart of Orbit Simulation Tests

1.   'DENSEL; 'DENSEL (operational method)

2.   Calorimeter data; Model B

3.   Calorimeter data; Model C

4.   Calorimeter data; 'DENSEL.

In a few instances other combinations of models were tested. Such cases
will be identified and discussed in the next section. Whenever the 'DENSEL
model was used in prediction, the ballistic factor ($C_D A/W$) was scaled
according to the drag parameter obtained in the orbit fit with 'DENSEL.

2.   Orbit Characteristics

Initial conditions for the reference trajectories were selected so
as to reconstruct as closely as possible the actual orbits corresponding to
the calorimeter data. Briefly, the orbits were near-circular and low-
altitude (roughly 68 by 200 nmi), sun-synchronous (i ~ 96°), and with
perigee at middle latitudes. In one set of calculations we tested two
different initial values of the right ascension of the ascending node. This
had the effect of calling different tracking stations into play. The results
of this change were insignificant relative to other effects being studied
and, therefore, will not be given further consideration in this report.

The orbit numbers of the data samples and other pertinent infor-
mation are given in Table 1.

TABLE 1. Orbit Characteristics of the Data Samples

Sample Number	Orbit Numbers	Perigee Height (nm)	Perigee Latitude (deg)	Apogee Height (nm)
1	179-187	69	42	217
2	325-333	69	46	210
3	502-510	69	44	208
4	761-769	72	52	205
5	792-800	72	56	206

3.   Calorimeter Data Base

The data base for this study consisted of calorimeter measurements of the aerodynamic heating on a low-altitude satellite obtained over a period of slightly less than 2 months. Roughly 300 data passes were acquired during this interval, but only 5 sets of 9 consecutive orbits contained sufficient coverage about perigee to be useful for the orbit-simulation calculations. However, all useful passes of data were included in studies related to atmospheric be-behavior. An example of a fitted pass of data is shown in Fig. 2.

The fundamental premise of this study is that the atmospheric density derived from the heat flux data is a "perfect" representation of the true atmosphere. This assumption is, of course, not very realistic since our knowledge of the vehicle drag coefficient and the surface thermal accommodation coefficient (along with their altitude dependences) is slightly less than perfect. Further, uncertainties associated with the measurements   were unknown to us. These factors, therefore, must be considered to be outside the scope of the present study, and the results to be presented necessarily reflect optimum conditions.
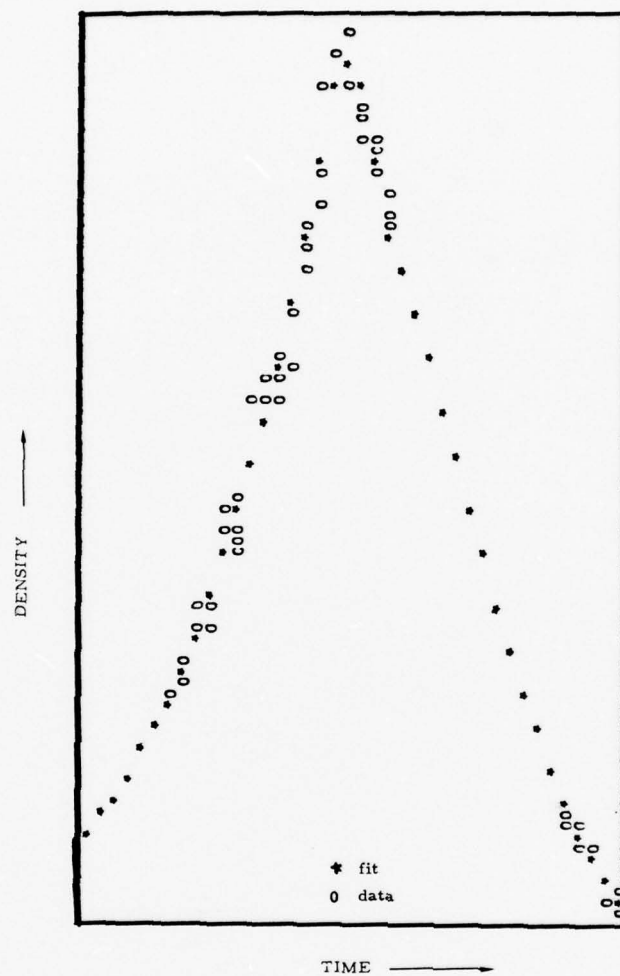
Fig. 2. Example of Calorimeter
Data Fitting

III.   RESULTS AND INTERPRETATION

1.   TRACE Calculations

Graphs of the intrack and radial residuals for the five data sets are presented in Appendix A. For each data set there are four combinations of fit-and-predict drag models as discussed previously. In the graphs the thick vertical line separates the fit and predict intervals; arrows along the lower horizontal axis indicate the perigee positions within the predict span.

Root-mean-square errors in the predict span are presented in Table 2. Errors at perigee are given in Tables 3a and 3b for the radial and intrack components, respectively. Without exception, orbit-fitting with calorimeter data resulted in better fits than the operational model and, thus, provided better starting vectors for the predict spans. RMS-errors of the radial component in the predict span were typically a factor of 2 or better when calorimeter data were used; the improvement in the RMS-error of the intrack component was typically a factor of 3 or more.

Focusing on the errors at perigee (Tables 3a, 3b) we can make the following observations:

1.   With but one exception (fit with calorimeter data, predict with MODC), the average absolute radial error at perigee was less when calorimeter data were used in the fit than when 'DENSEL model was used.

2.   The average absolute radial error at perigee was significantly less than the RMS-error over the predict span regardless of what model was used to fit or predict.

-19-

TABLE 2. RMS Errors (in feet) in the Predict Span

Predict Span Rev. No.	*CALOR/ MOD B	CALOR/ MCD C	CALOR/ 'DENSEL	'DENSEL/ 'DENSEL
185 - 187 radial intrack	288 2828	113 562	149 1415	418 5877
331 - 333 radial intrack	97 768	52 380	110 1073	258 3739
508 - 510 radial intrack	249 2666	233 738	434 4848	1107 14,720
767 - 769 radial intrack	309 1775	174 438	250 1194	470 3086
798 - 800 radial intrack	57 561	47 400	41 105	219 1919

* CALOR/MODB means calorimeter data were used in the fit span, Model B in the predict span.

TABLE 3a. Summary of Radial Errors (feet) at Perigee

Predict Span Rev. No.	CALOR/ MOD B	CALOR/ MOD C	CALOR/ 'DENSEL	'DENSEL/ 'DENSEL
185	-10	-9	-6	11
186	-12	-26	-7	24
187	-6	-34	-9	26
Abs. Ave.	9	23	7	20
331	11	10	-5	-91
332	64	41	15	-92
333	110	64	26	-94
Abs. Ave.	62	38	15	92
508	-5	4	-24	-123
509	-56	-34	-107	-197
510	-4	1	-71	-208
Abs. Ave.	22	13	67	176
767	-6	6	-21	160
768	28	85	-20	146
769	42	151	-34	136
Abs. Ave.	25	81	25	147
798	9	1	4	81
799	27	5	15	94
800	21	-13	3	78
Abs. Ave.	19	6	7	84

TABLE 3b. Summary of Intrack Errors (feet) at Perigee

Predict Span Rev. No.	CALOR/ MOD B	CALOR/ MOD C	CALOR/ 'DENSEL	'DENSEL/ 'DENSEL
185	-14	1	0	2704
186	1906	-166	1092	5774
187	4942	-1331	2479	9153
Abs. Ave.	2287	499	1190	5877
331	-29	-28	-16	1446
332	-326	362	768	3585
333	-1480	576	1792	5971
Abs. Ave.	612	322	859	3667
508	-11	-4	-10	4056
509	2565	1430	3684	12,125
510	4430	1022	7798	22,384
Abs. Ave.	2335	812	3831	12,855
767	-27	-24	-25	499
768	810	-316	367	1656
769	2354	-1066	1056	3126
Abs. Ave.	1063	469	483	1760
798	-5	7	-5	678
799	-224	-156	69	1628
800	-951	-738	-65	2741
Abs. Ave.	393	300	46	1682

3. The absolute radial error at perigee did not consistently increase with time in the predict span.

4. The average absolute intrack error at perigee was always less using calorimeter data to fit than using the 'DENSEL model.

5. The average absolute intrack error at perigee did not differ significantly from the RMS-error over the predict span.

6. The absolute intrack error at perigee increased with time in the predict span.

7. Radial errors at perigee did not correlate with any of the 3 drag models used in prediction. By constrast, the intrack errors at perigee were always the least for Model C (based on the last rev of calorimeter data in the fit span).

To provide better insight on the relationship between errors and the drag prediction model, we have plotted the RMS-errors and the perigee errors of both the radial and intrack components against the following quantities: (1) the initial error of the predict span, (2) the mean level of the true density in the predict span, and (3) the density variability withing the predict span. In order to avoid ambiguities in interpretation, the drag model used for prediction in all cases was the operational model 'DENSEL.

Figure 3a shows the dependence of the RMS-radial error in the predict span on the initial radial error in the starting vector. The 5 circles on the graph represent the 5 different data sets that were fit with calorimeter data;

-23-
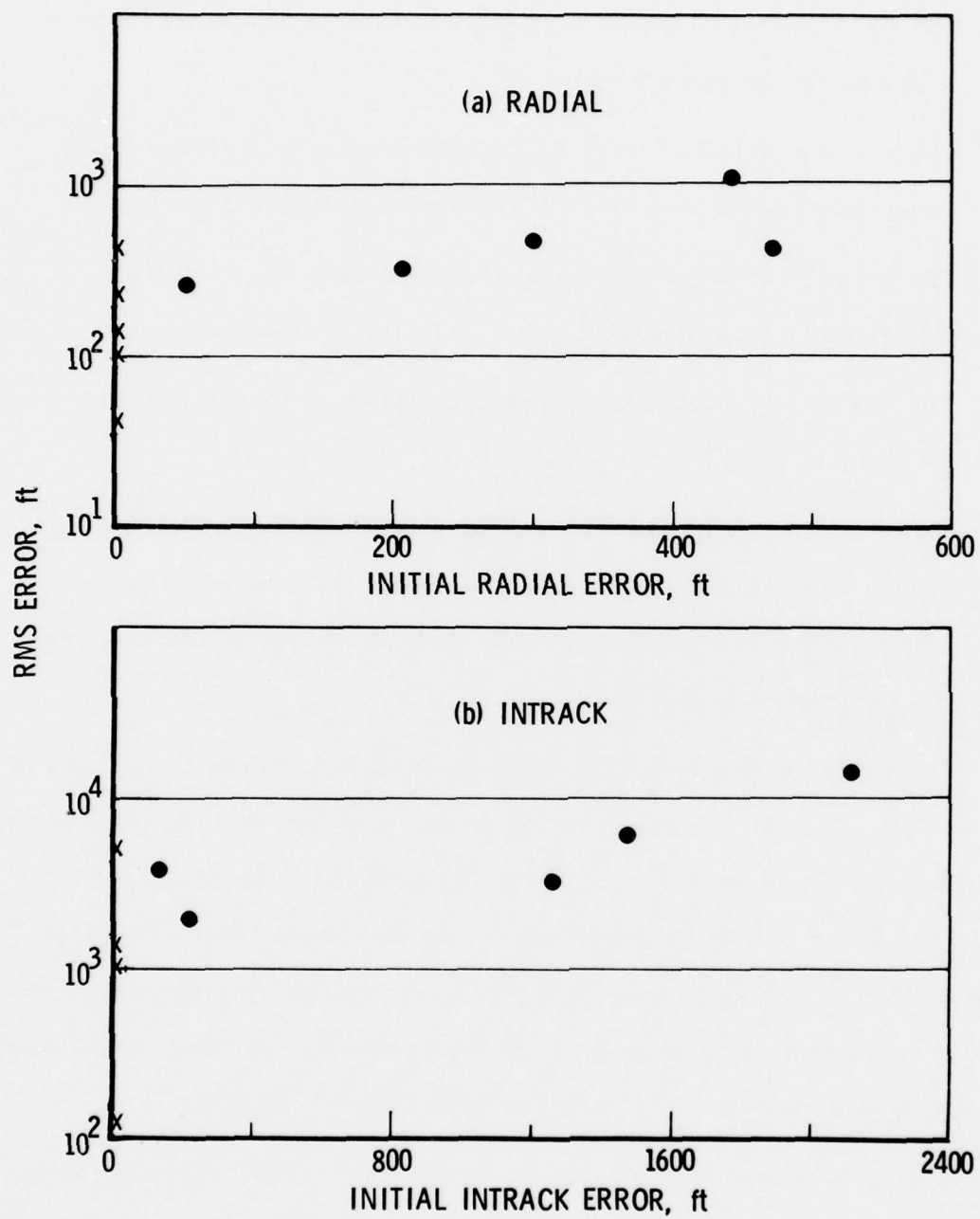
Fig. 3. RMS Error in Predict Span Vs. Initial Error. X denotes
'DENSEL fit; • denotes calorimeter fit.

the X's represent the fits with 'DENSEL. As mentioned previously, all predictions were made with 'DENSEL and the ballistic coefficient was scaled according to the fitted drag parameter. On the scale used for the abscissa, the initial errors in the radial component $|\Delta R_0|$ for the calorimeter fits are indistinguishable and appear to be near-zero. The actual values ranged from a few tenths of a foot to a few feet. Since, however, the RMS-errors were uncorrelated with $|\Delta R_0|$ for the calorimeter cases, we saw no advantage in expanding the scale near zero. In the cases where 'DENSEL was used to fit the tracking data, there is a well-defined relationship between the initial error and the RMS-error. If we were to average calorimeter points, that average (~ 200 ft) would fit in nicely with the other points. Essentially the same remarks may be applied to the intrack component shown in Fig. 3b.

In Figs. 4a and 4b the average of the absolute errors at perigee in the predict span are plotted against the initial errors in the radial and intrack components, respectively. Again, the initial errors corresponding to the calorimeter data fits are so much less than the errors from the 'DENSEL fits that their points are crowded near zero. As before, expansion of the scale near zero would serve no purpose since the errors appeared to be un-correlated. As opposed to Figs. 3a and 3b, there is no well-behaved relationship between the perigee errors and the initial errors in the radial component. The intrack component does exhibit a dependence, but with some scatter.

-25-
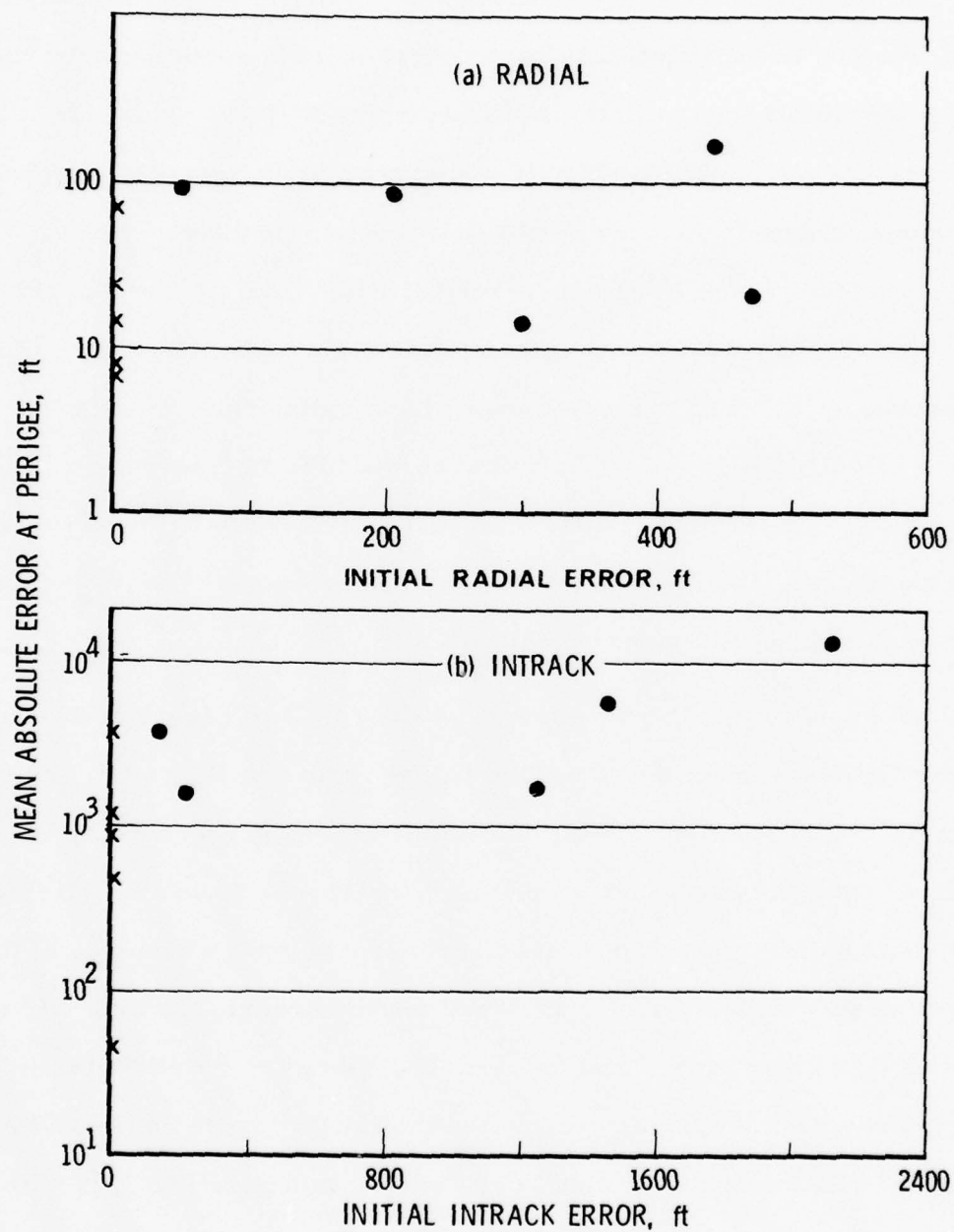
Fig. 4. Mean Absolute Error at Perigee in the Predict Span
Vs. Initial Error

In Figs. 5a and 5b we show the RMS-errors in the predict interval plotted against the mean density of the predict interval. The calorimeter and the 'DENSEL points both show that the RMS-error increases with the mean level of the density, which is intuitively what one would expect.

With regard to the perigee errors, it is seen in Figs. 6a and 6b that the intrack component does increase with the density while the radial component does not.

In Figs. 7a, b and 8a, b we show the RMS and perigee errors against the density variability within the predict interval, the latter being defined as the RMS-deviation from the mean. In all cases we observe a definite tendency for errors to grow with density variability.

To summarize Figs. 3 - 8, we note that intuitively one would expect errors to grow in all cases, i.e., with initial error, with mean density, and with variability in the density. Indeed, this was verified for the RMS-error, which essentially is an average over the entire predict span, and the intrack error at perigee, but not the radial error at perigee. In the latter case only the density variability factor appeared to influence the radial error at perigee in a systematic way.

These orbit simulation studies indicate that both the starting vector of the predict span and the density within the predict span are important factors for good ephemeris prediction. Further, it is not only the mean density that is important, but time-dependent changes as well.
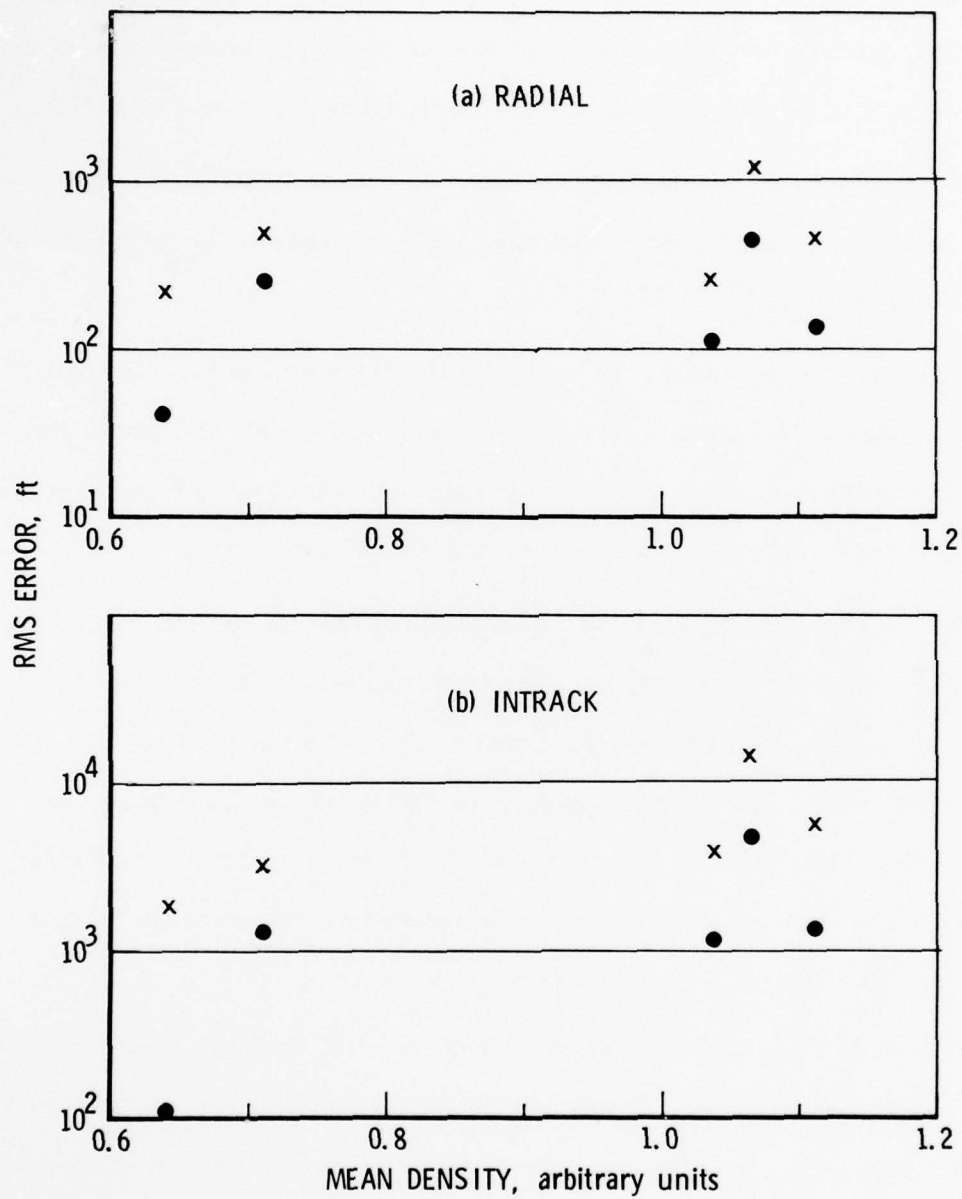
Fig. 5.   RMS Error in Predict Span Vs. Mean Density
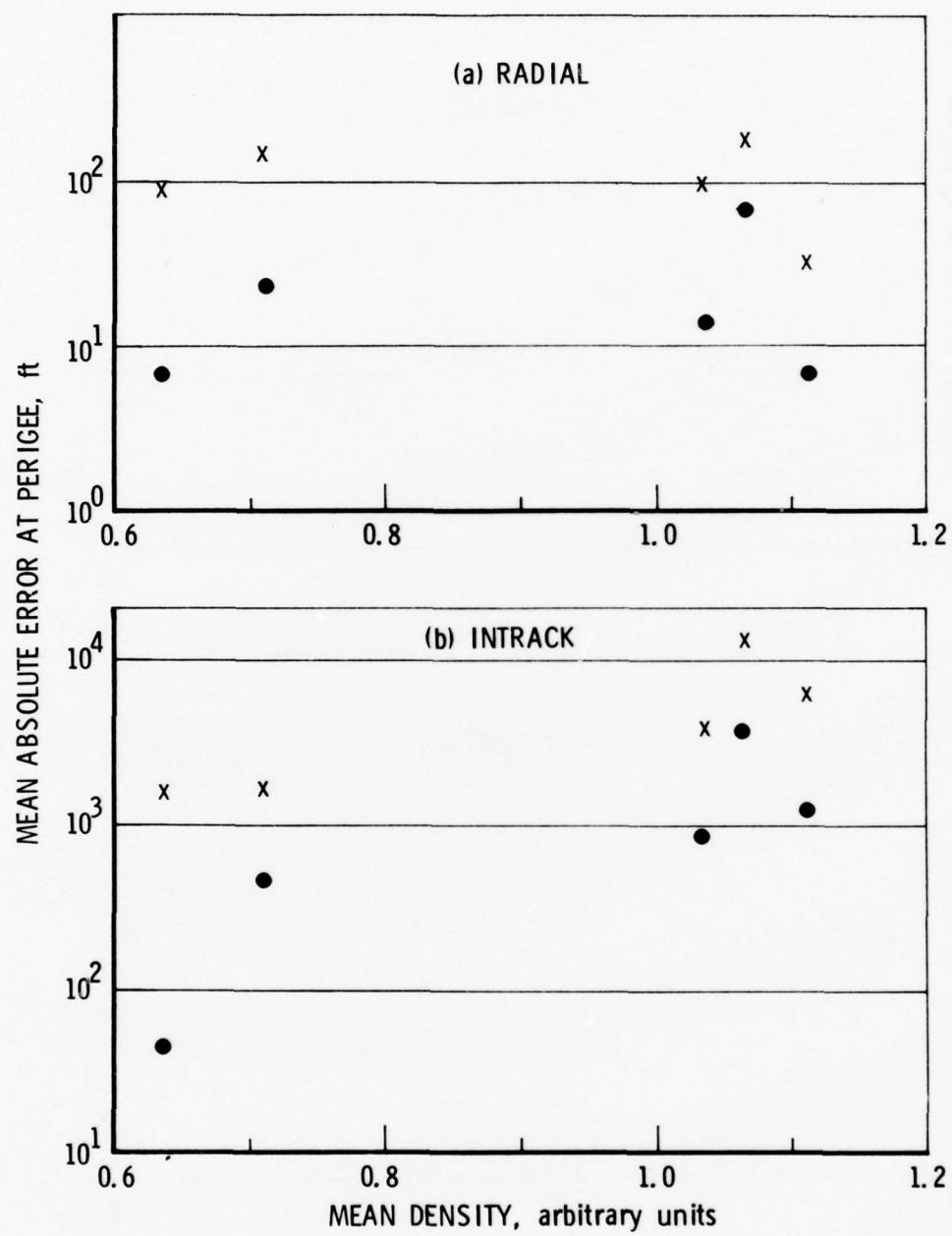
Fig. 6.   Mean Absolute Error at Perigee in the Predict Span
          Vs. Mean Density
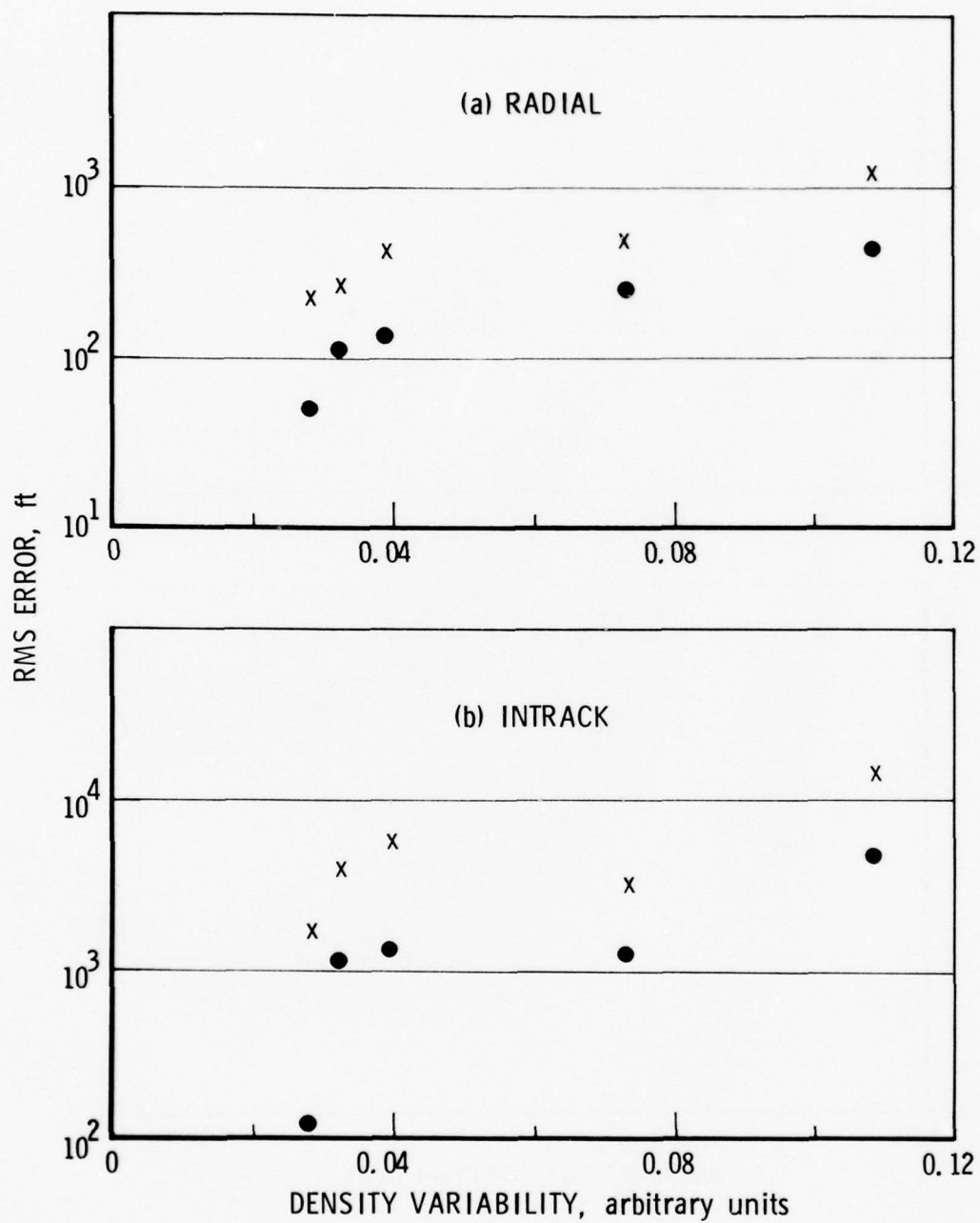
Fig. 7.   RMS Error in Predict Span Vs. Density Variability
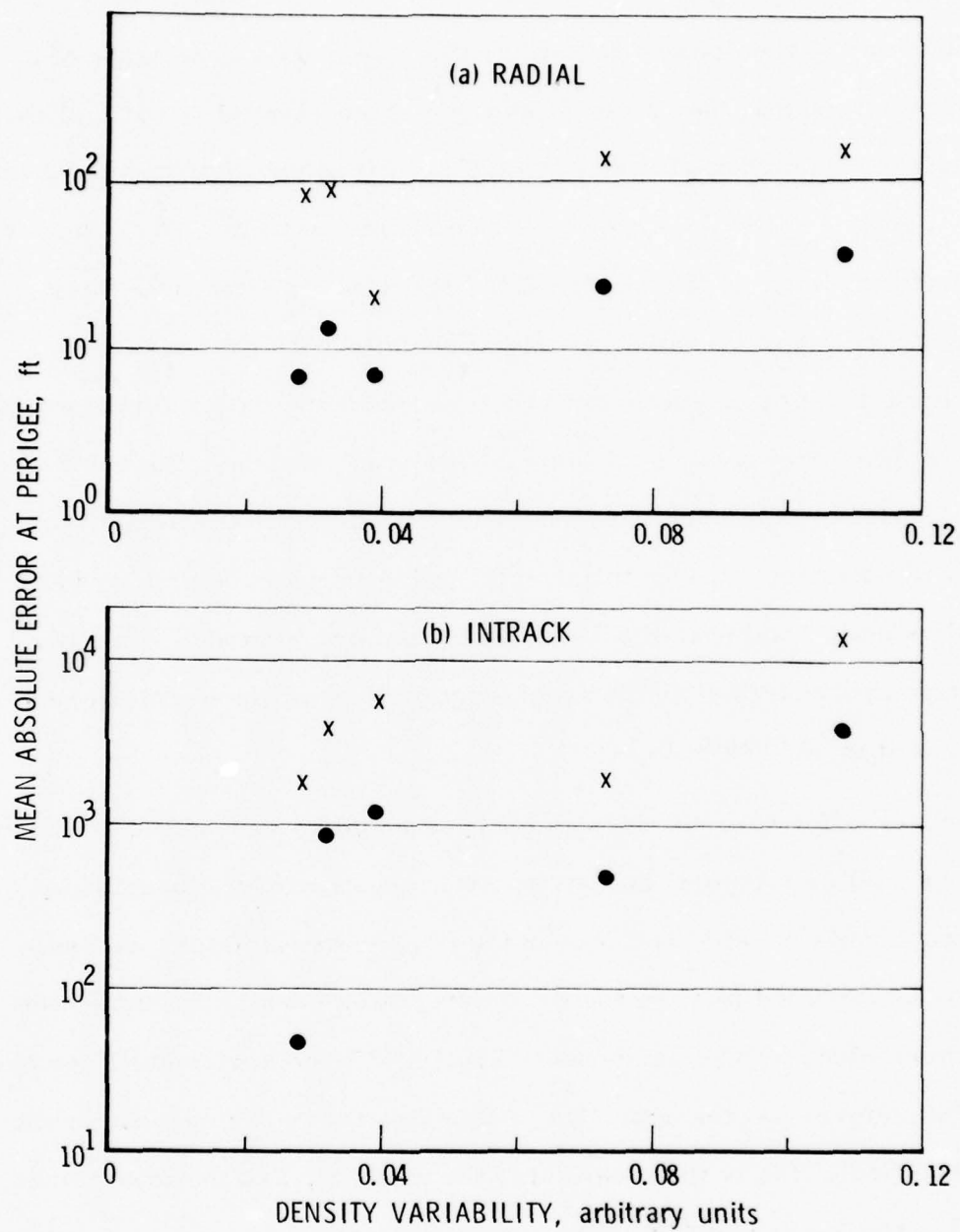
Fig. 8.   Mean Absolute Error at Perigee in the Predict Span
Vs. Density Variability

2.   Atmospheric Studies

At the low perigee altitudes of the orbits under study, very little is known of the density variations that occur on a time scale of a few hours except that they do exist and can be substantial (> 10% of the mean level). At higher altitudes (> 100 nm) it is known that such short-period variations tend to correlate with magnetic activity. With the present set of calorimeter data we found the short-term orbit-integrated density variations to be rather poorly correlated with Kp fluctuations, although the level of magnetic activity throughout the data interval was relatively low. However, on a longer time scale of a day, the orbit-integrated density did show a relationship with daily magnetic activity as illustrated in Fig. 9. (In this and following figures the density has been adjusted to compensate for changes related to altitude. This normalization procedure, which is frequently used in aeronomical studies, is discussed in Appendix B.)

Since orbit-to-orbit density changes could be associated with spatial as well as temporal variations, we investigated the possibility of geographically-related features in the density distribution. A first-cut analysis involved plotting the orbit-integrated density vs longitude of minimum altitude; this is shown in Fig.10. Three horizontal lines are shown for reference: the upper line delineates the upper quartile of the data, the middle line is the mean (also the median), and the lower line delineates the lower quartile. The machine-plot is in a sense misleading since, if more than one point falls within a specified grid, only a single asterisk is shown. Thus, the number of points that should lie between the upper and lower lines is greater than is actually shown.
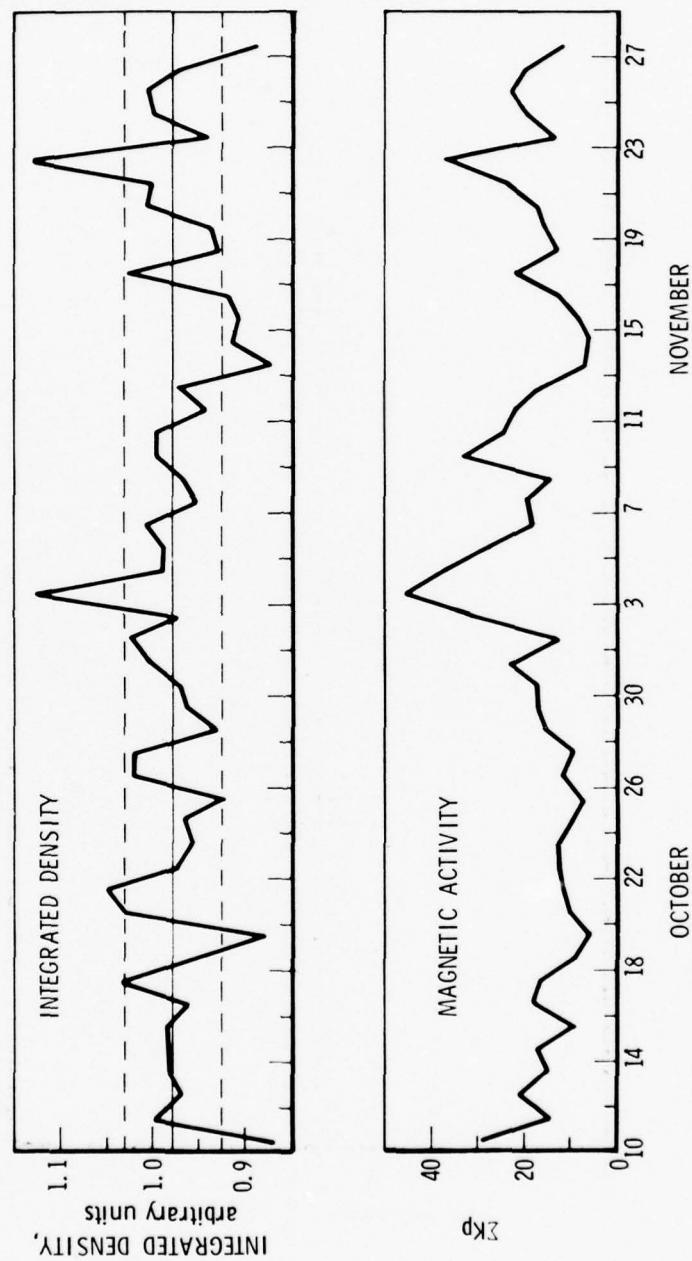
Fig. 9. Daily Average of Orbit-Integrated Density (corrected for differences in perigee height) and Daily Sum of Kp
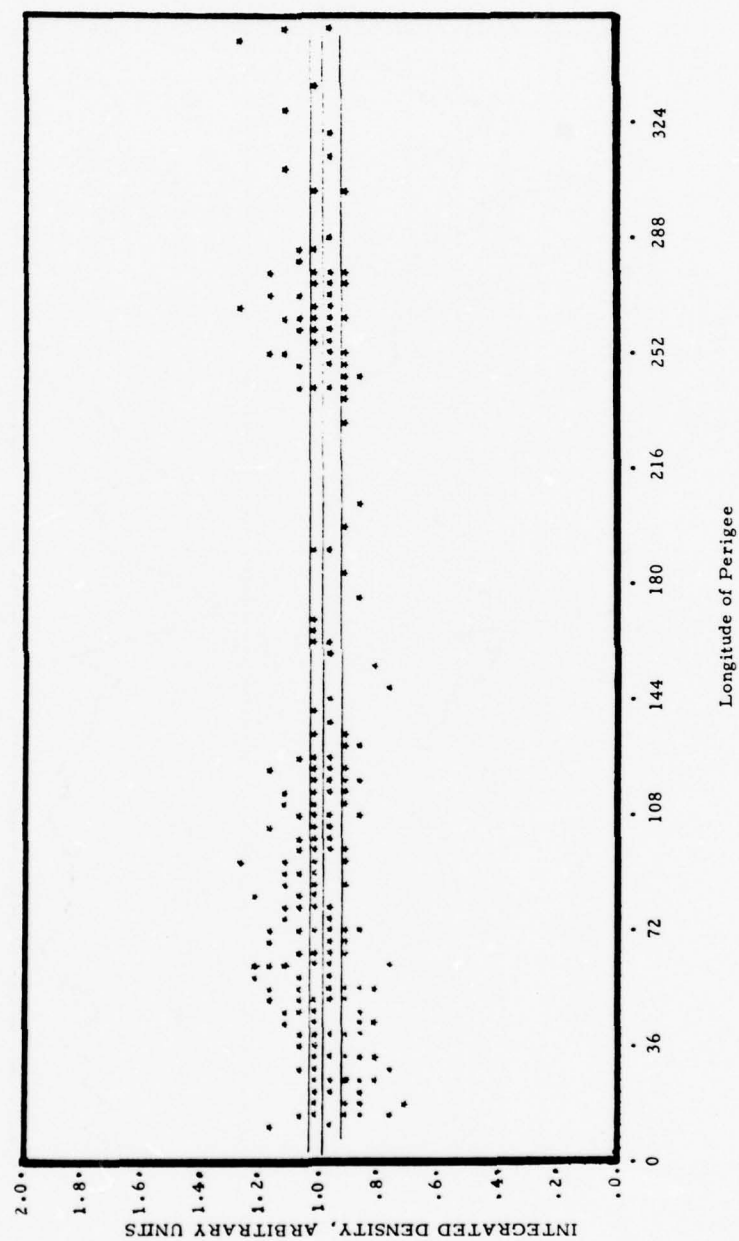
Fig. 10. Altitude-Corrected Orbit-Integrated Density Vs. Longitude of Perigee. Middle horizontal line denotes the average and median value. Upper and lower lines denote upper and lower quartiles of the data.

-34-

The plot indicates that the density near 72°E longitude is greater by about 10% than the density near 20°E. There appears to be a minimum near 20°E longitude, but this is speculative since there are too few points to the west of the apparent minimum. The density in the sector from 144°E to about 240°E also appears to be lower than average; however, again there are too few points to be certain of this feature.

Plotting the density against both latitude and longitude of minimum altitude as in Fig. 11 fails to elucidate matters. Here, circles represent the upper-most quartile; asterisks are used for the upper-middle quartile, plus-signs for the lower-middle quartile, and minus-signs for the lower quartile. From about 35°N to 50°N, where the majority of points exist, the symbols are more or less distributed in buck-shot fashion. There is a definite lack of upper-quartile symbols in the $144-240^\circ$E sector, but as mentioned above the data coverage there was very sketchy. Similarly, there appears to be a zone of high density between 20° and 24°N and a zone of low density between 24° and 30°N; but again the poor data coverage may be biasing the statistics. In all, therefore, where there was good data coverage, there was no well-defined geographically-related structure. Possible regions of "highs" or "lows" were compromised by the paucity of data.

Although no outstanding geographical or magnetic-index related effects were found, it was determined from the calorimeter data base that the density at the heights in question did exhibit a certain degree of what might be called persistence. That is, given the orbit-integrated density for
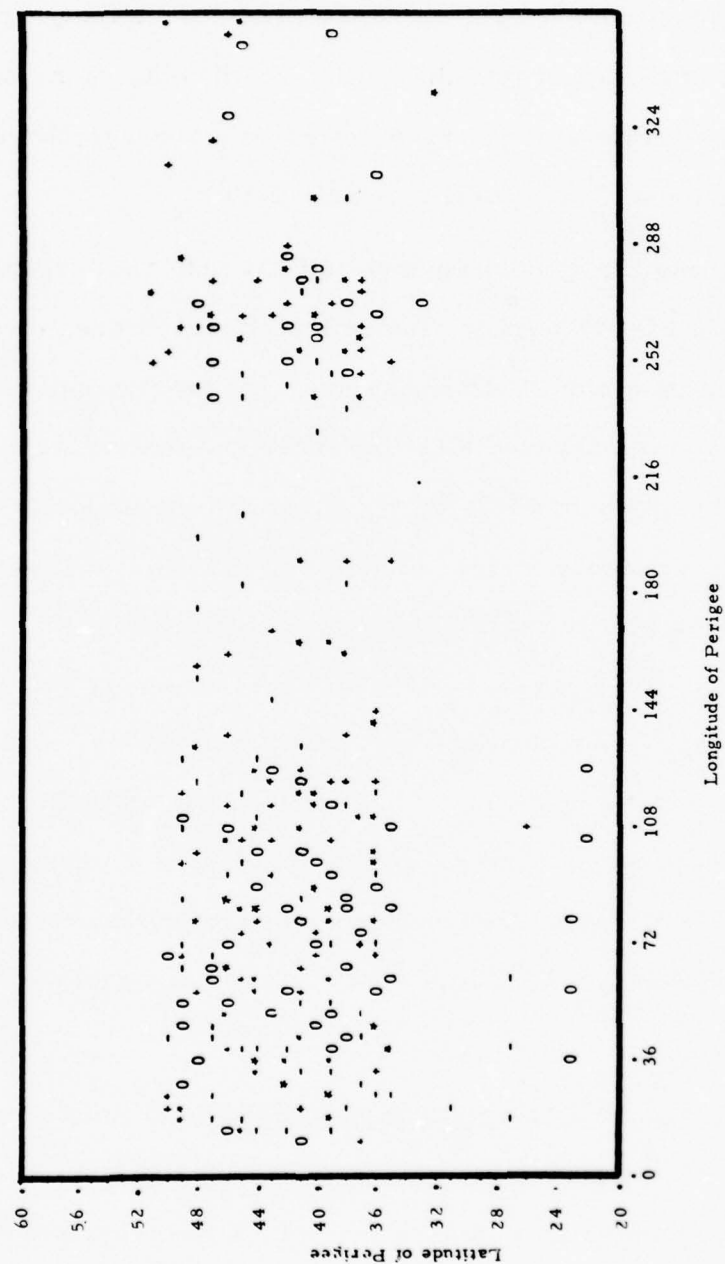
Fig. 11. Distribution of Altitude-Corrected Orbit-Integrated Density in Latitude and Longitude of Perigee: 0 = upper quartile; * = upper-middle quartile; + = lower-middle quartile; - = lower quartile.

a particular orbit, we found that in 68 of 155 cases (44%) the integrated density of the following orbit did not differ by more than $\pm$ 5%. Further, in 88% of the cases, the integrated density was within $\pm$ 15% of that of the preceding orbit. Similarly, in ~ 30% of the cases available for study, the density of the second and third orbits following the given orbit did not change by more than $\pm$ 5%. This "persistence" feature explains why in nearly all our calculations the prediction Model C yielded the lowest errors. Model C, it is recalled, was simply the measured density of the last orbit in the fit span.

3. Further Considerations of Short-Term Prediction

The question of the relative importance of the starting vector as opposed to the accuracy of the drag model in the predict span was investigated by comparing several TRACE runs having different combinations of fit/predict drag models. The comparison was carried out for only one of the five data samples, and so the results must be viewed and interpreted with a fair amount of discretion.

Basically, the purpose was to compare "perfect" with "operational" drag force models, where the "perfect" model was the calorimeter data that were used to generate the reference trajectory, and the operational model was, of course, 'DENSEL. The results are presented in Table 4. Both RMS-errors and perigee errors in the predict span are tabulated. The data sample used was Revs 761-769.

For this particular sample, having either a perfect starting vector or a perfect drag model yielded essentially similar improvements in RMS-errors as compared with the operational approach. On the other hand, the accuracy of the starting vector appears to be important insofar as perigee errors are concerned.

-37-

As mentioned before, we must be careful not to over-interpret the results because we are dealing with a single data set. A cautious conclusion that may be drawn from this exercise is that both the starting vector and the drag model are important, and thus future endeavors to improve short-term orbit prediction should not overlook either of these factors.

Table 4. RMS-Errors and Mean Absolute Errors at Perigee
(in feet) in the Predict Span of Data Set 4 (Revs 767-769)

	'DENSEL/'DENSEL	CALOR/'DENSEL	'DENSEL/CALOR
Radial			
RMS	470	250	257
Perigee	147	58	173
Intrack			
RMS	3086	1194	1960
Perigee	1760	483	1286

An interesting aspect of prediction errors that can be seen in the figures in Appendix A is the complexity and sensitivity of the time-dependent behavior related to different predictive drag models. That is, given a specific starting vector, the drag model affects not only the envelope of the error oscillations, but the phase as well. The source of this complex response can be understood at least qualitatively by examining simplified analytical expressions for the

-38-

orbital perturbations due to air drag. Specifically, the radial distance r
at a position on the orbit where the true anomaly is ϕ is related to the
distance r_o for a drag-free orbit by (Ref. 2, eqn. 88).

$$\frac{1}{r} - \frac{1}{r_o} = \delta \int_0^\phi \left[1 - \cos(\phi - \theta) \right] \frac{(1 + 2e \cos\theta + e^2)^{1/2}}{(1 + e\cos\theta)^2} \rho(\theta) \, d\theta \quad (1)$$

where ρ is the density, e is the eccentricity, and δ is a parameter
similar to the so-called ballistic parameter. From (1), it is straight-
forward to derive the difference in radial distance after one revolution owing
to different density models:

$$\frac{(r_1 - r_2)}{r^2} = -\delta \int_\phi^{\phi + 2\pi} G(\theta, \phi)(\rho_1 - \rho_2) \, d\theta \quad (2)$$

where

$$G(\theta, \phi) = \left[1 - \cos(\phi - \theta) \right] \frac{(1 + 2e\cos\theta + e^2)^{1/2}}{(1 + e\cos\theta)^2} \quad (3)$$

A sketch of the behavior of the function G is shown in Fig. 12. The important
feature is that the phase depends on ϕ, the position in the orbit where the
radial difference is to be evaluated. In essence, the difference in the radial
component (eqn. 2) is the orbit-integrated difference in density weighted by the
function G.

In the simple case where the ratio of the densities (ρ_2/ρ_1) is constant
along the orbit, eqn. (2) may be written
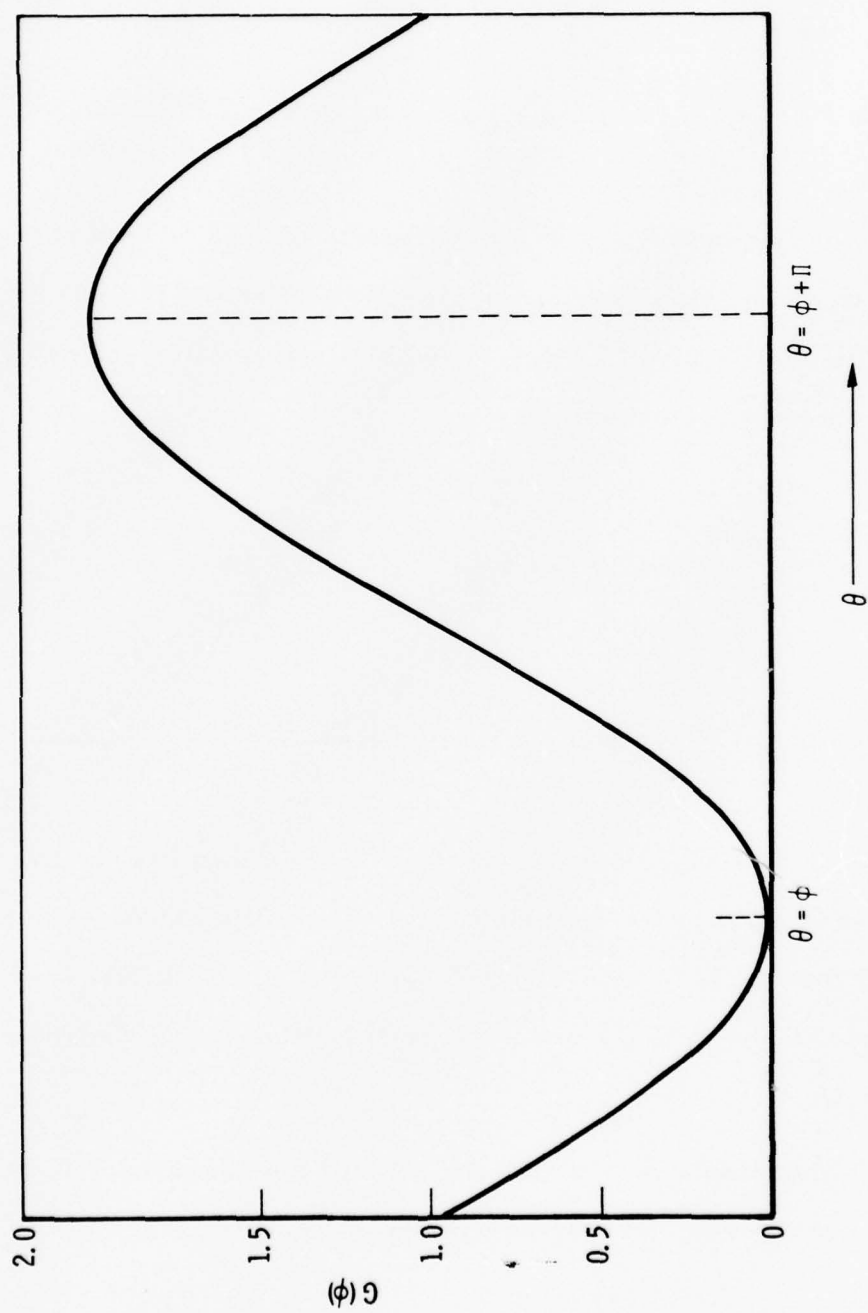
Fig. 12. Variation of Function G with θ, the True Anomaly

$$\frac{r_1 - r_2}{r^2} = -\delta \, \rho_{p1} \left(1 - \frac{\rho_2}{\rho_1} \right) \int_{\phi}^{\phi + 2\pi} G(\theta, \phi) \exp\left[-\beta \, \frac{(1 - \cos\theta)}{(1 + e\cos\theta)} \right] \rho \, d\theta \qquad (4)$$

In deriving (4) we assume that the density is given by

$$\rho = \rho_p \exp\left[-(r - r_p)/H \right]$$

where ρ_p is the density at perigee, r_p is the perigee distance, and H the density scale height; the parameter β in (4) is $r_p e/H$. In this simple case the integral is a positive-definite quantity, and thus the radial difference has the same sign for all ϕ depending on the ratio ρ_2/ρ_1. It is apparent from Fig. 12 and eqn. (4) that for given values of the parameters ρ_2/ρ_1, δ, e, β, and ρ_{p1}, the difference is a minimum at perigee ($\phi = 0$) and a maximum at apogee ($\phi = \pi$). This, of course, is not surprising to anyone with any familiarity with orbital analyses, as it is well known that the perigee height decays very slowly under the action of air drag relative to the decay of apogee.

In the general case represented by eqn. (2), the radial difference depends on the variation of the density difference around the orbit weighted by the function G. It should be noted that even if the orbit-integrated difference in the density is zero, the radial difference can be non-zero because of the function G. It is obvious that under general conditions, where ($\rho_1 - \rho_2$) varies in some complex fashion, it is no straightforward matter to infer the effect on the radial distance. To even predict the sign of the change would require knowledge of the behavior of the density difference around the orbit.

-41-

IV. SUMMARY AND RECOMMENDATIONS

Subject to the constraints and assumptions mentioned earlier, the major results of this study are as follows:

1. Given the tracking coverage of the AOES network, direct measurements of the drag on a low-altitude vehicle allow the orbit to be fit with far greater accuracy than would be obtainable using the operational drag model. RMS-errors in the fit span of the radial, intrack, and cross-track components were < 1 ft, < 10 ft, and < 1 ft, respectively, using drag data, and > 10 ft, > 100 ft, > 10 ft using the 'DENSEL model.

2. The accurate starting vectors obtained with the drag measurements significantly improved the 3-rev prediction capability. Using the 'DENSEL model to predict, we achieved an average reduction in RMS error of a factor of 2 in the radial component and a factor of 4 in the intrack component. The mean absolute error at perigee was reduced by factors of 3 and 4, respectively, for the radial and intrack components.

3. The level of the density and the variability of the density within the predict span affect prediction accuracy. On a short term basis (i.e. orbit by orbit), we found no outstanding correlation between the density and the often-used Kp index of magnetic activity. We also failed to find compelling evidence of permanent geographically-related features in the density. We did find, however, that the statistical "persistence" of the lower thermosphere can be exploited to improve short term orbit prediction.

As emphasized in this report, the results must be interpreted as "optimistic" since no allowances have been made for errors in drag measurements, satellite tracking (other than random errors), or other external force models (i.e. the geopotential). The next obvious test would be to use real, **not** simulated, tracking data in a comparative study of drag data vs operational model.

Although the emphasis of this study has been on satellite-borne measurements of drag, it should be noted that improvement in the starting vector of a prediction interval might also be achieved by improved tracking capability.

A most important issue is the need to improve the drag model predictive capability on the short-term time scale (i.e. an orbital period). Although it was found that the persistence feature of the atmosphere could be exploited in orbit prediction, success is to be expected only on a statistical basis. It must also be noted that the present data base was obtained during a period devoid of major magnetic activity, and so we have not been able to analyze the effects of such disturbances on orbit prediction. Large changes in density taking place on a short-time scale can have profound effects on low-altitude orbits; thus it is important to be able to predict the occurrence and magnitude of such events. A break-through in this area does not appear to be imminent, but since the drag model may become the ultimate limiting factor in orbit prediction, the task should not be readily abandoned.

REFERENCES

1.   B. K. Ching and D. R. Hickman, "A Feasibility Study of the Use of Calorimeter Data in Orbit Fitting and Prediction," The Aerospace Corporation ATM-78(3960-04)-1, November, 1977.

2.   G. E. Cook, D. G. King-Hele, and D. M. C. Walker, "The Contraction of Satellite Orbits Under the Influence of Air Drag. I. With Spherically Symmetric Atmosphere," Proc. Roy. Soc. 257A, 224, 1960.

APPENDIX A. Plots of Orbit Differences

Plots of the radial and intrack errors are shown on the following pages. Figures of the crosstrack error have not been included since this component is generally not a source of significant error.

The drag models used in the fit and predict intervals and the orbit numbers of the data sample are indicated at the top of each graph. Thick vertical lines are used to separate the fit and predict intervals; thick horizontal lines identify the zero-error level. Arrows along the time axis denote the times of perigee.

Prediction density Models B and C (MODB, MODC) were derived from the calorimeter data of the fit spans. Model B was based upon all data in the fit span; Model C was based on only the last orbit.
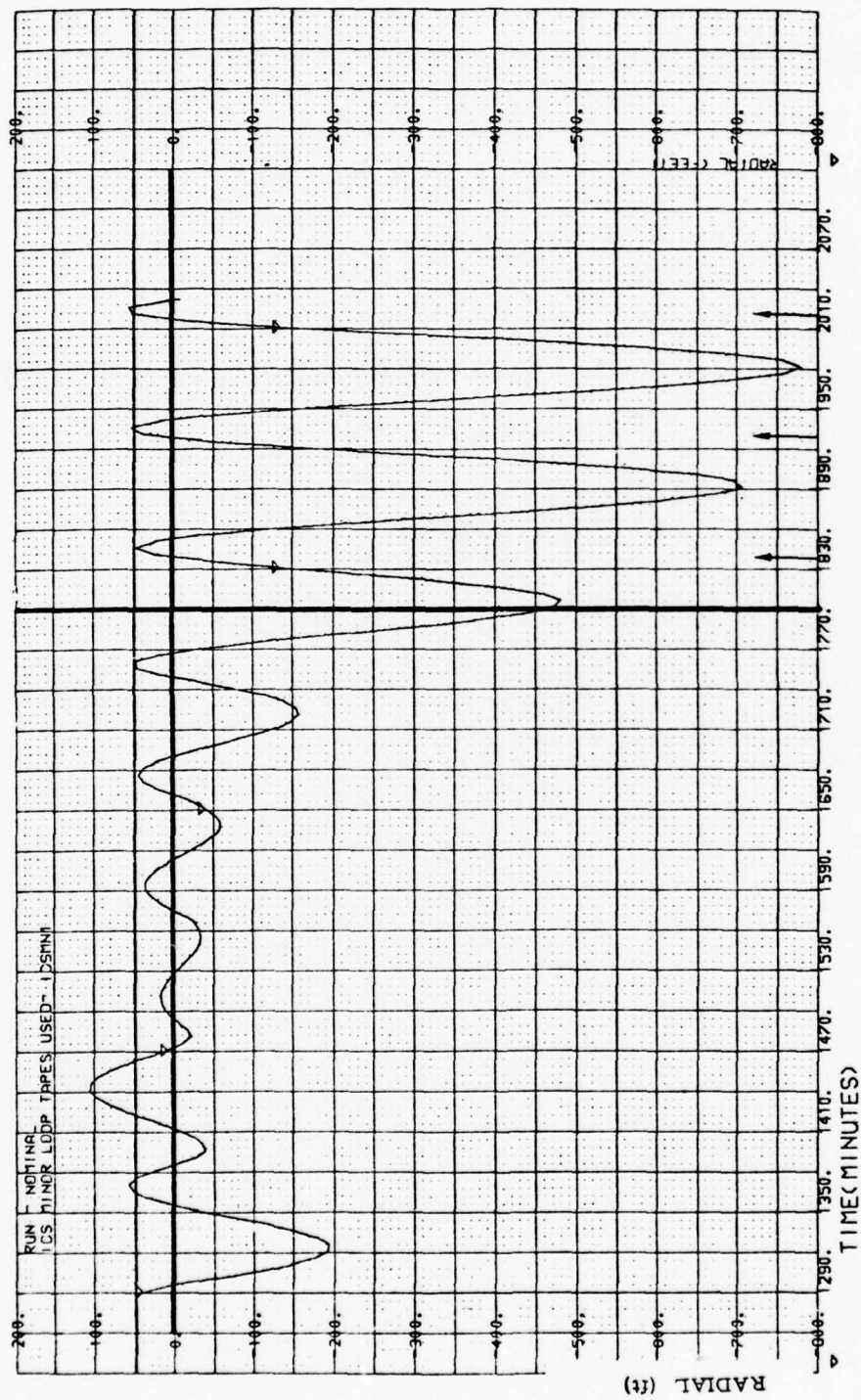
Fig. A-1. 'DENSEL (fit)/'DENSEL (predict) 179-187
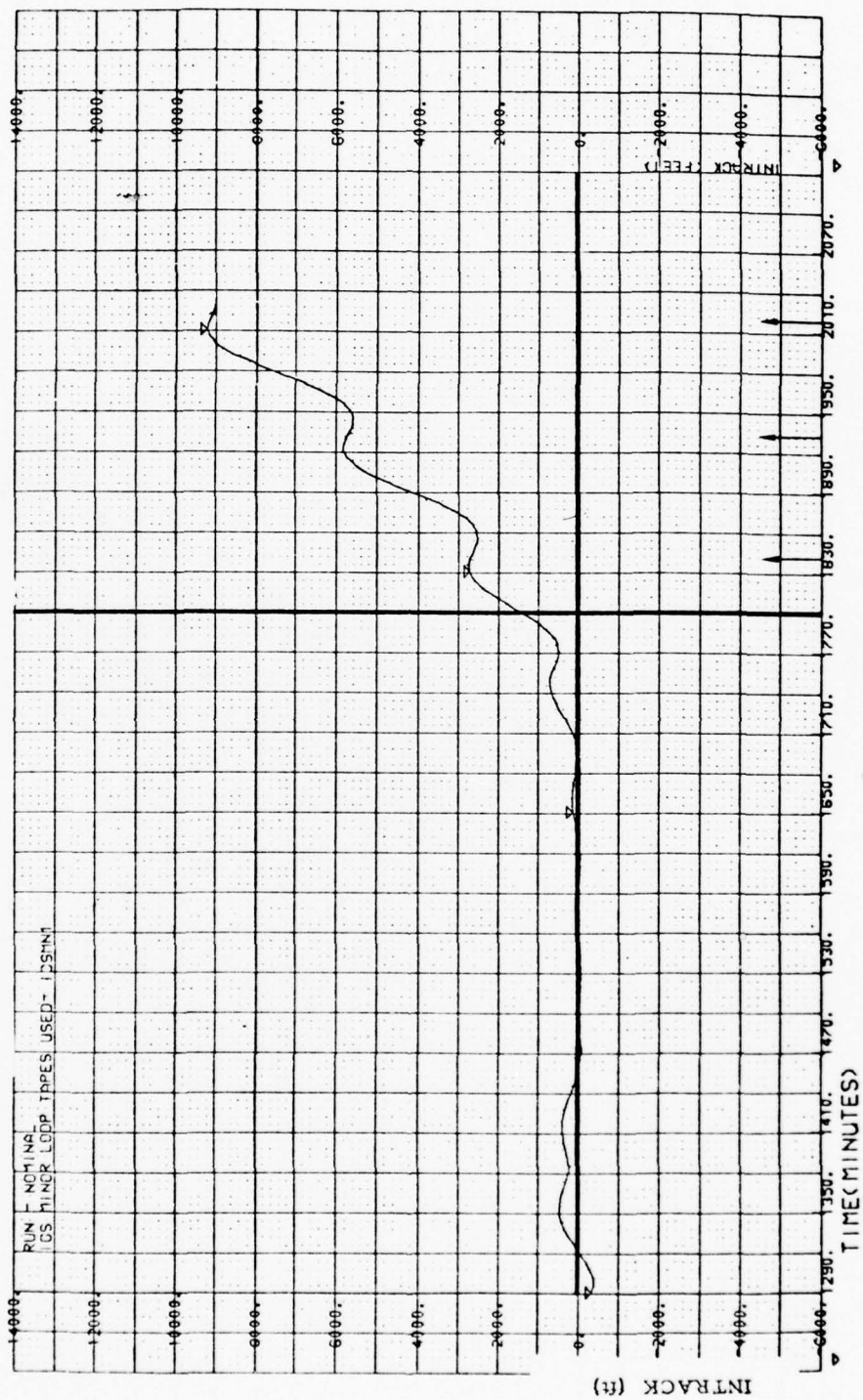
Fig. A-1. 'DENSEL (fit)/'DENSEL (predict) 179-187 (Continued)
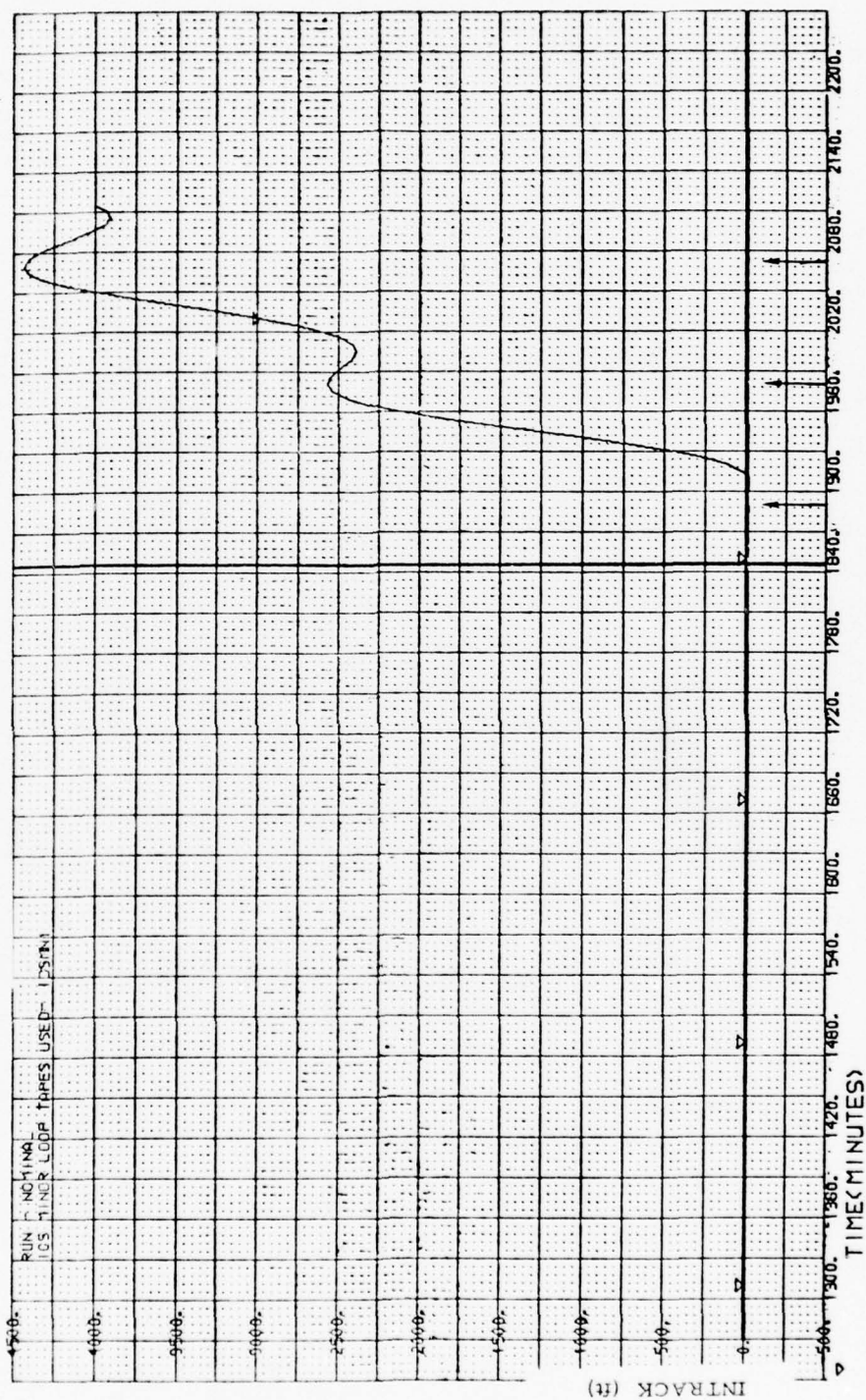
-49-
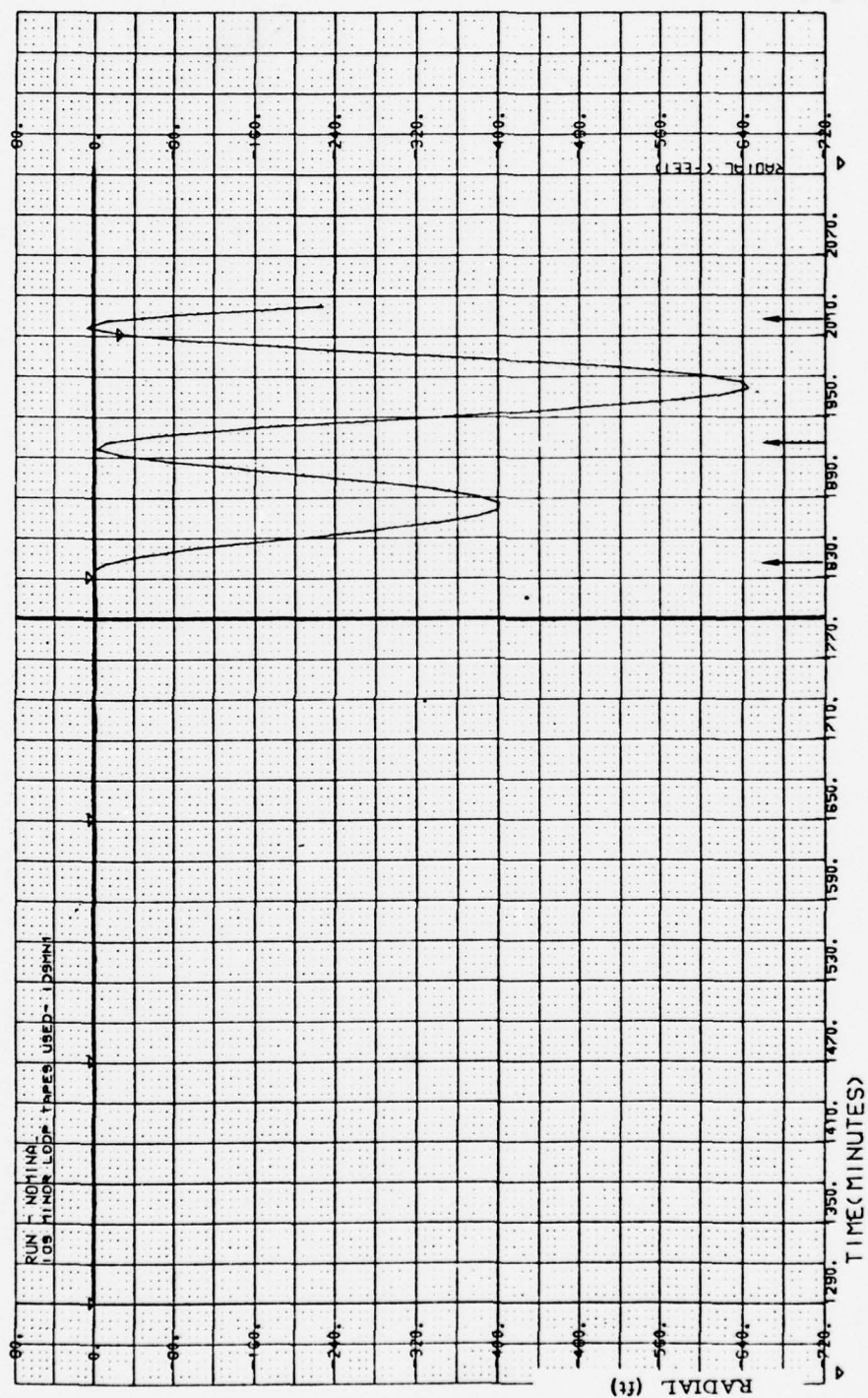
Fig. A-2. Calorimeter (fit)/MODB (predict) 179-187
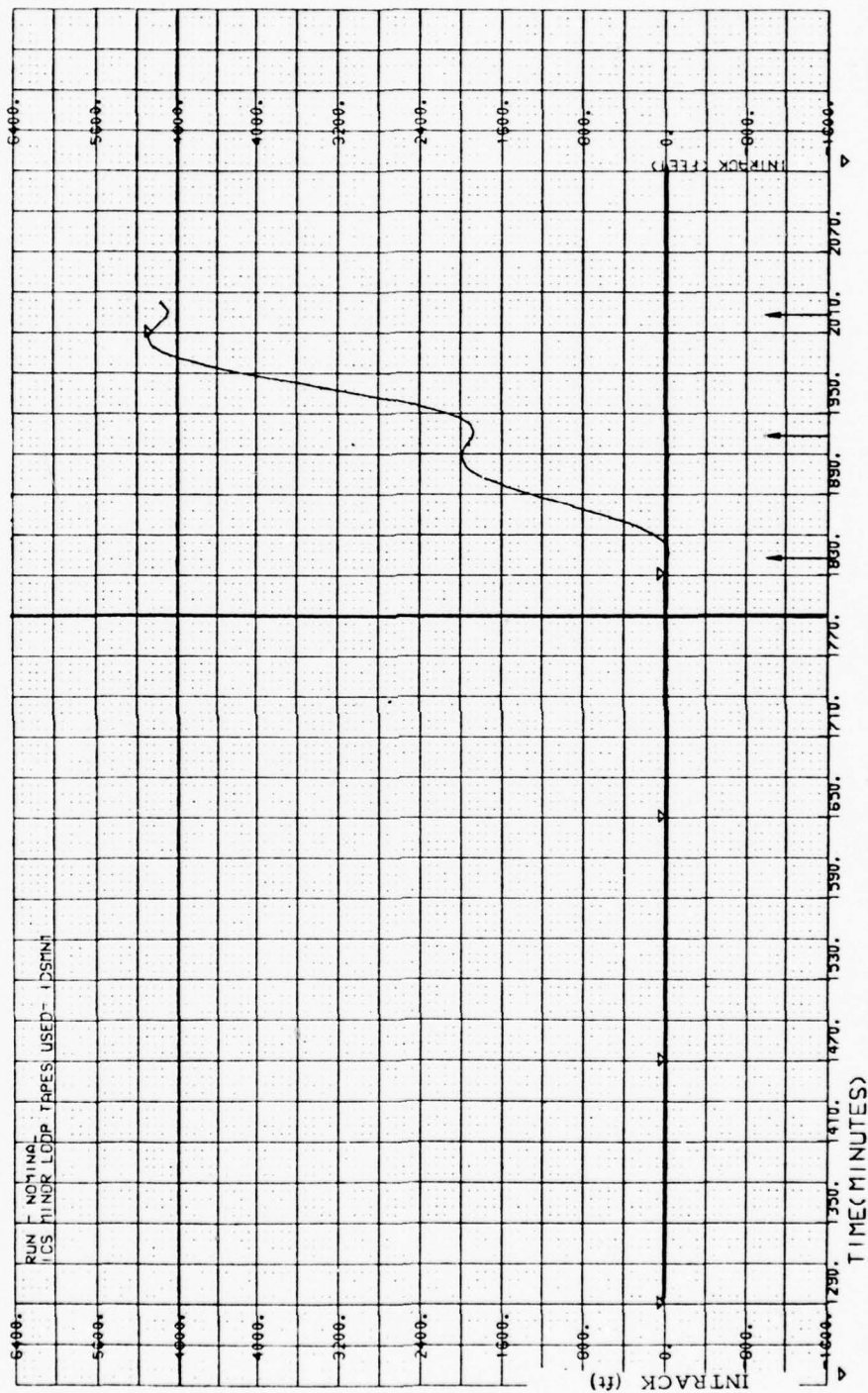
Fig. A-2. Calorimeter (fit)/MODB (predict) 179-187 (Continued)
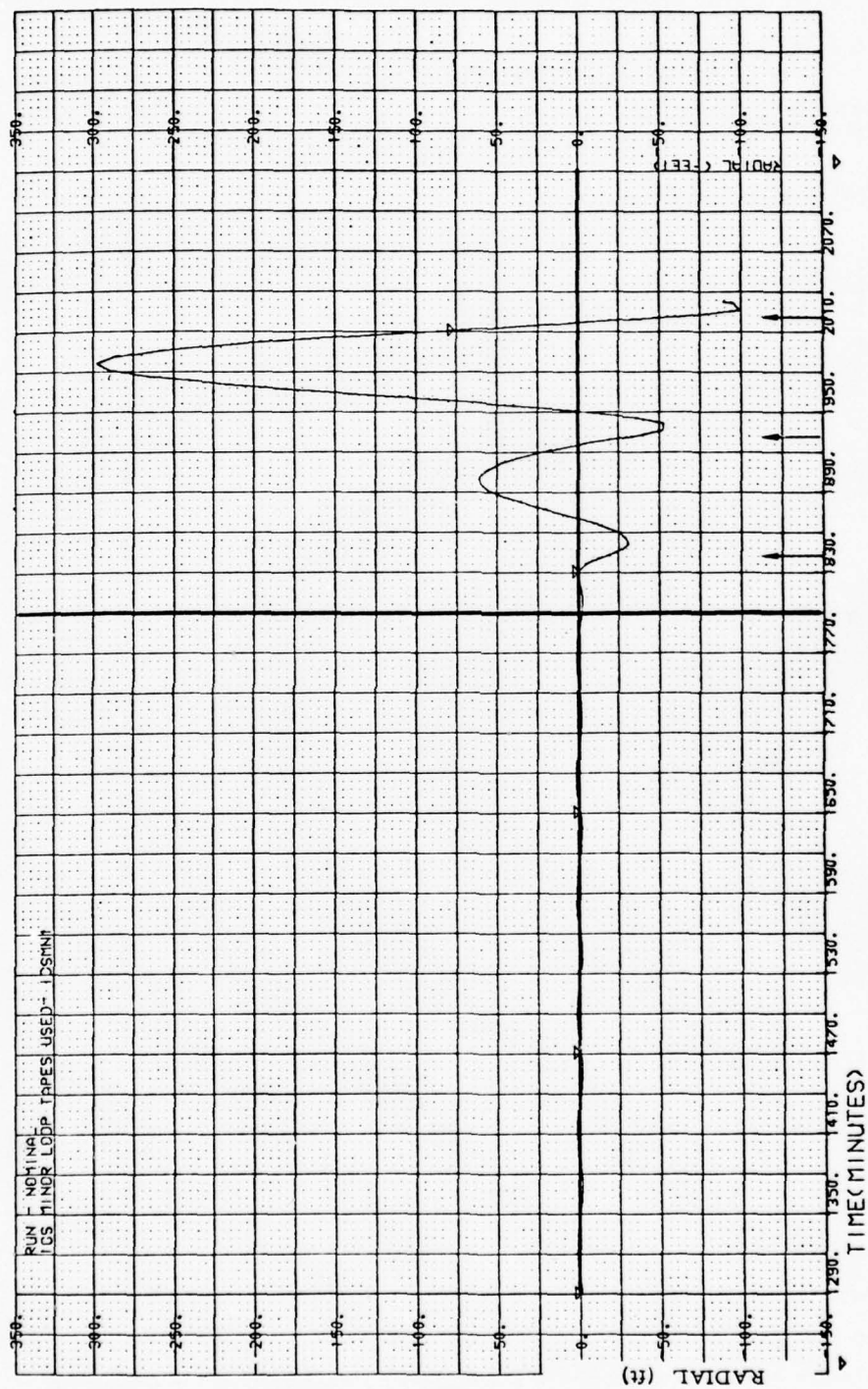
Fig. A-3. Calorimeter (fit)/MODC (predict) 179-187
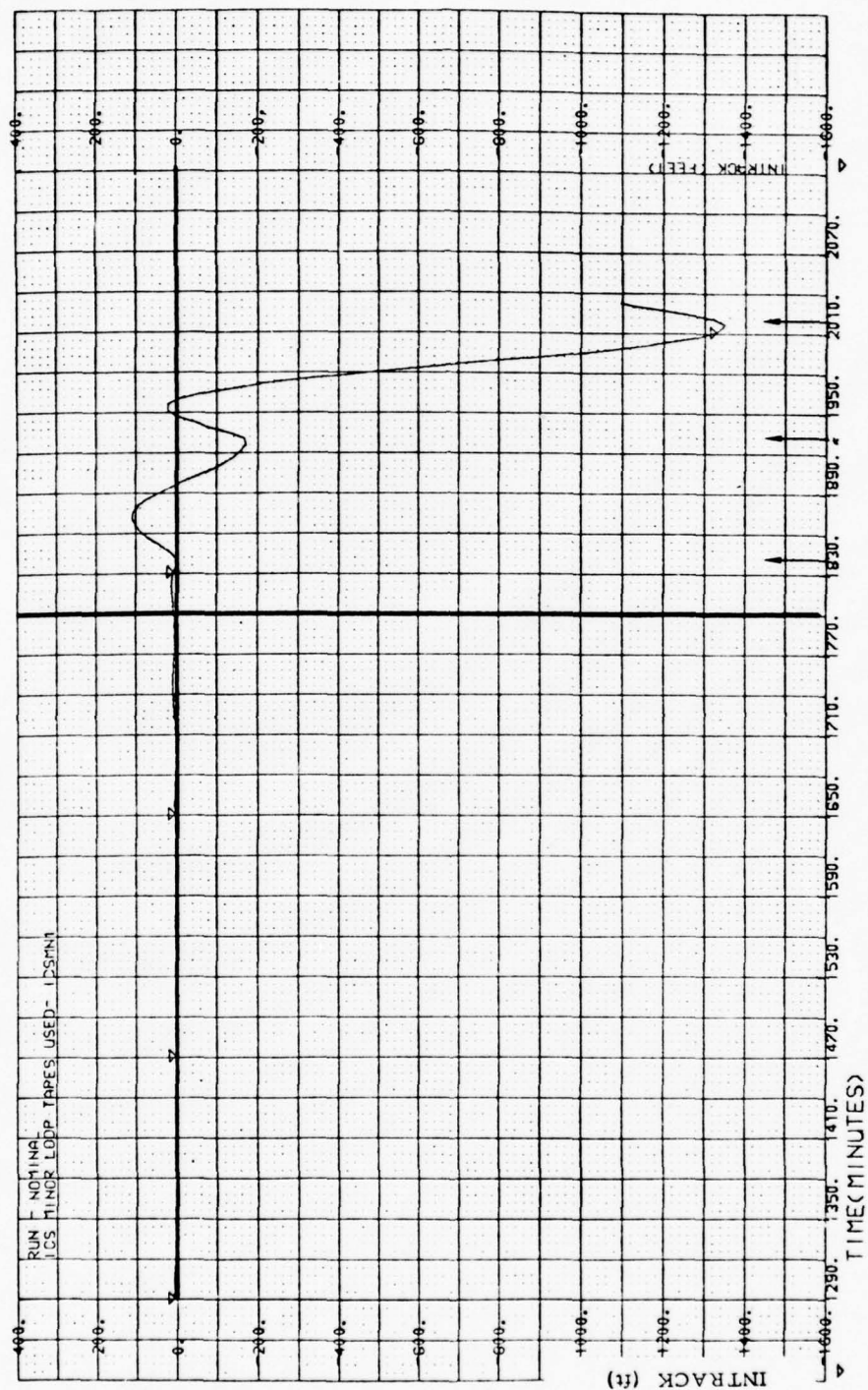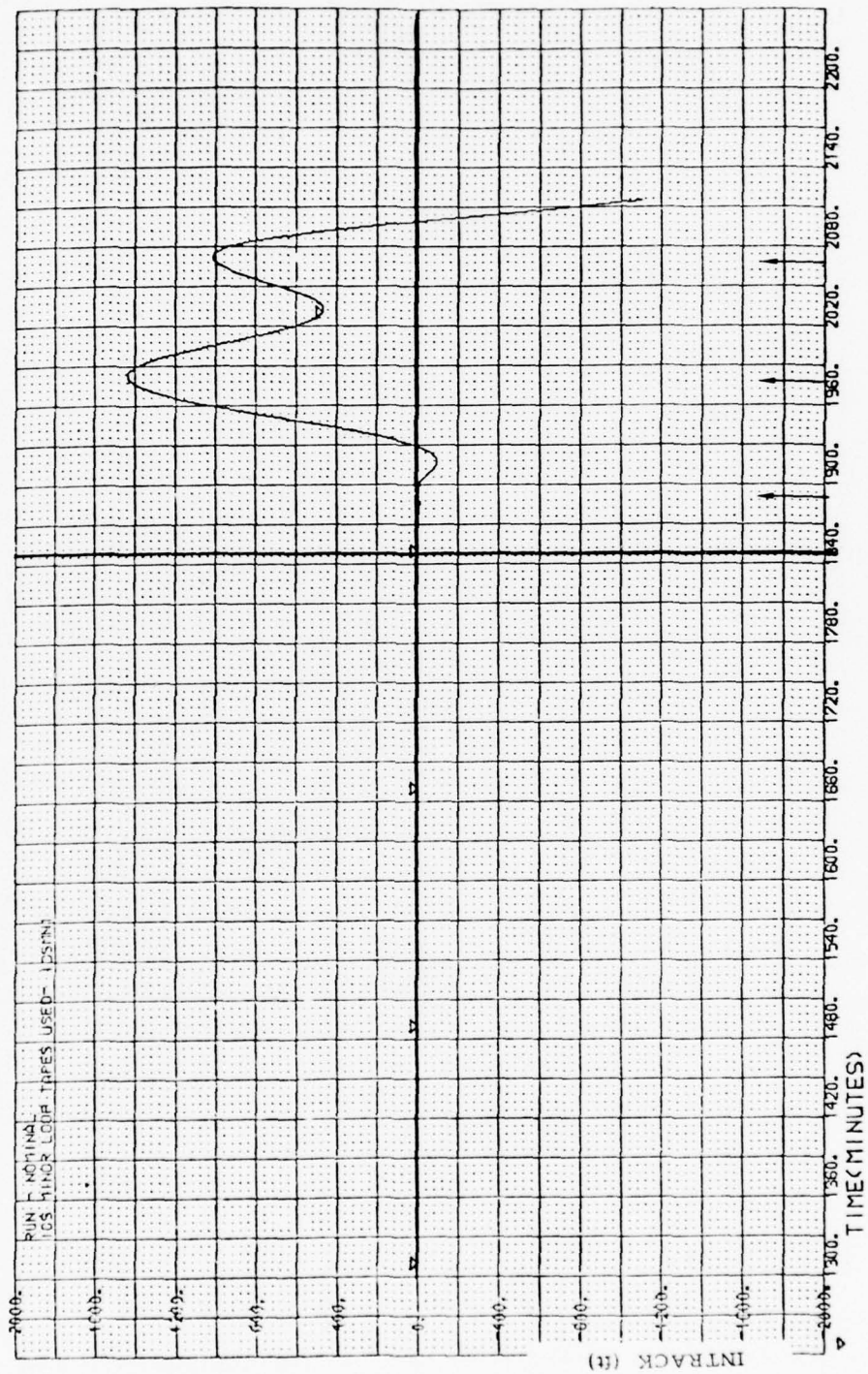
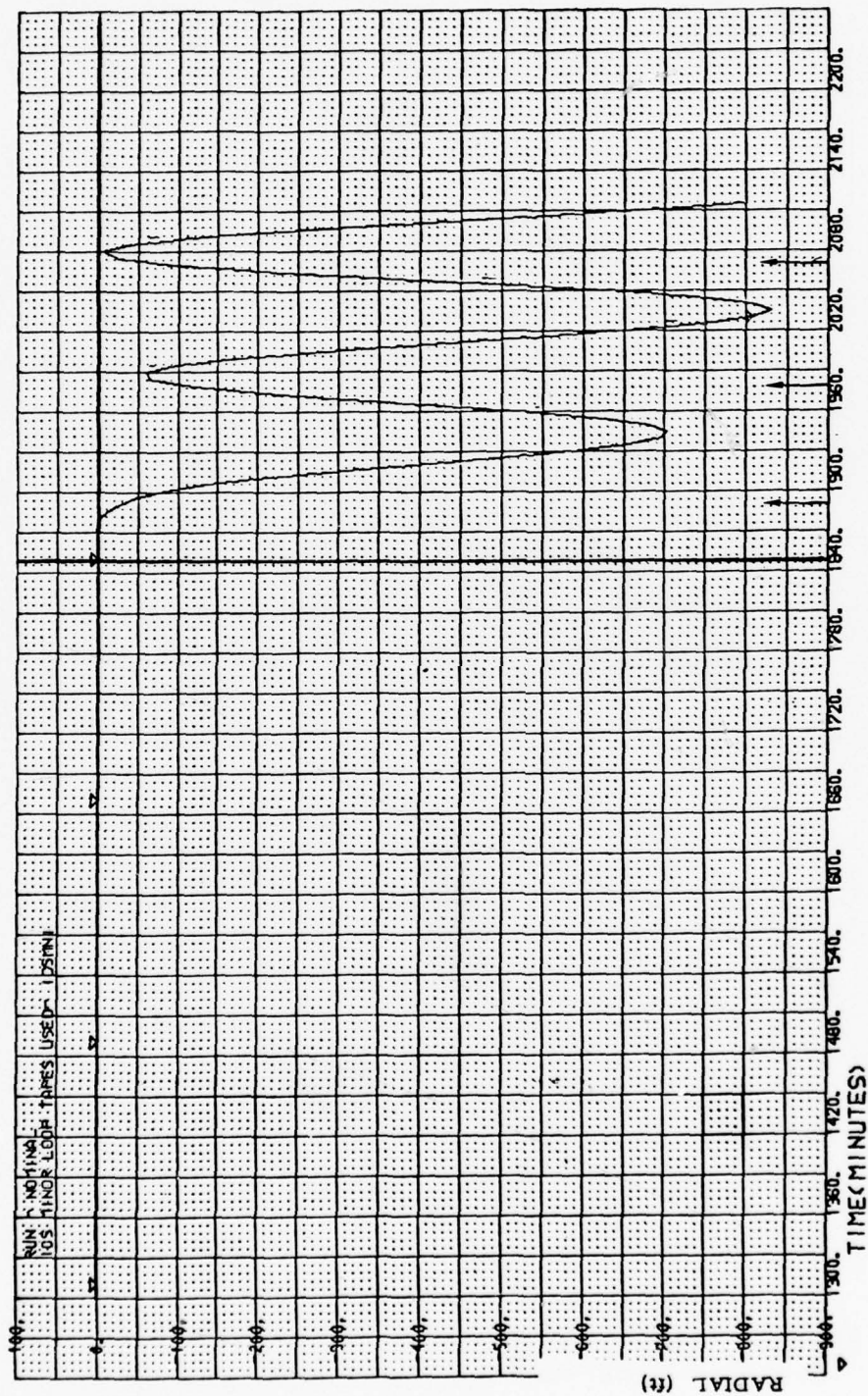Fig. A-3. Calorimeter (fit)/MODC (predict) 179-187 (Continued)

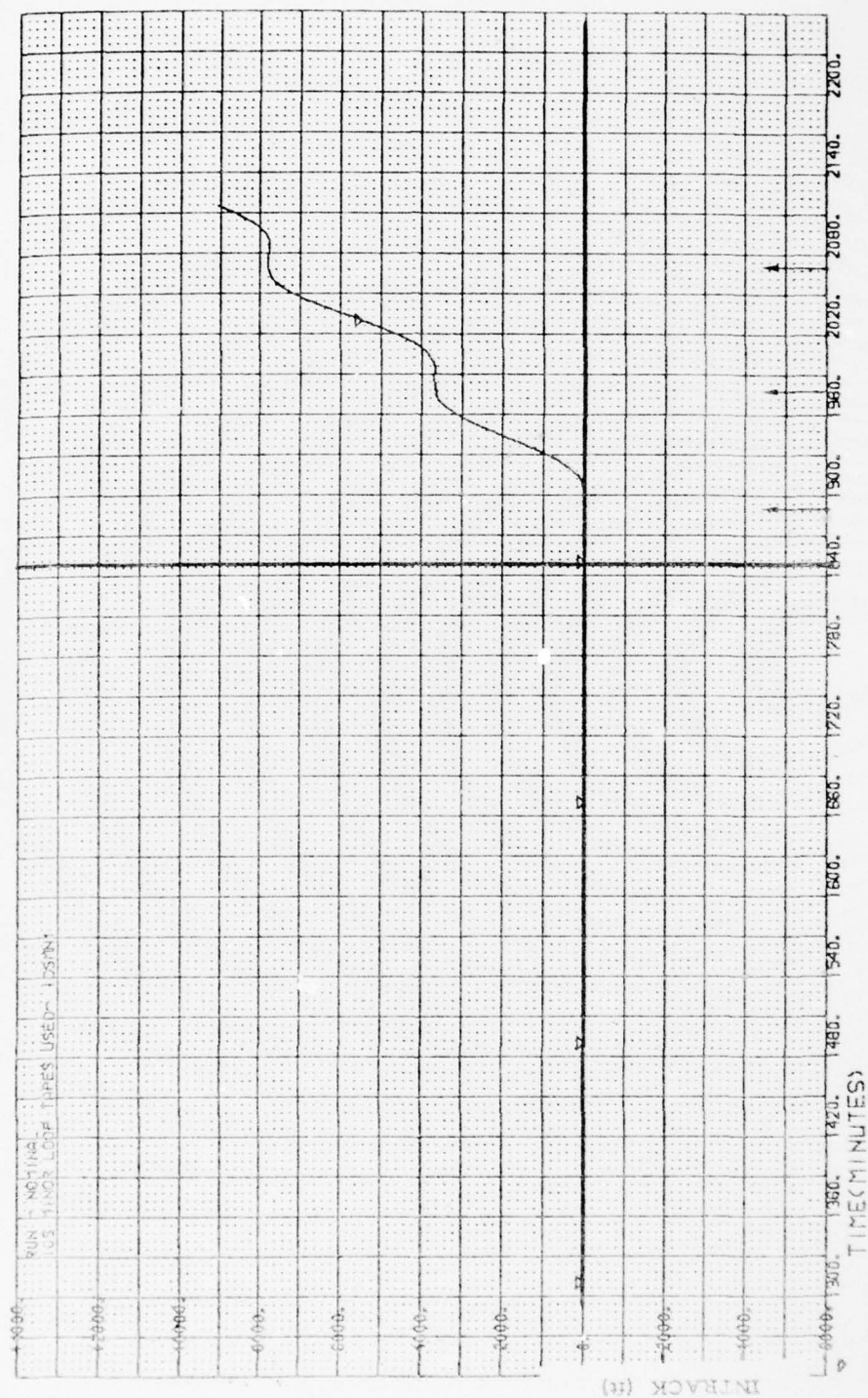-53-
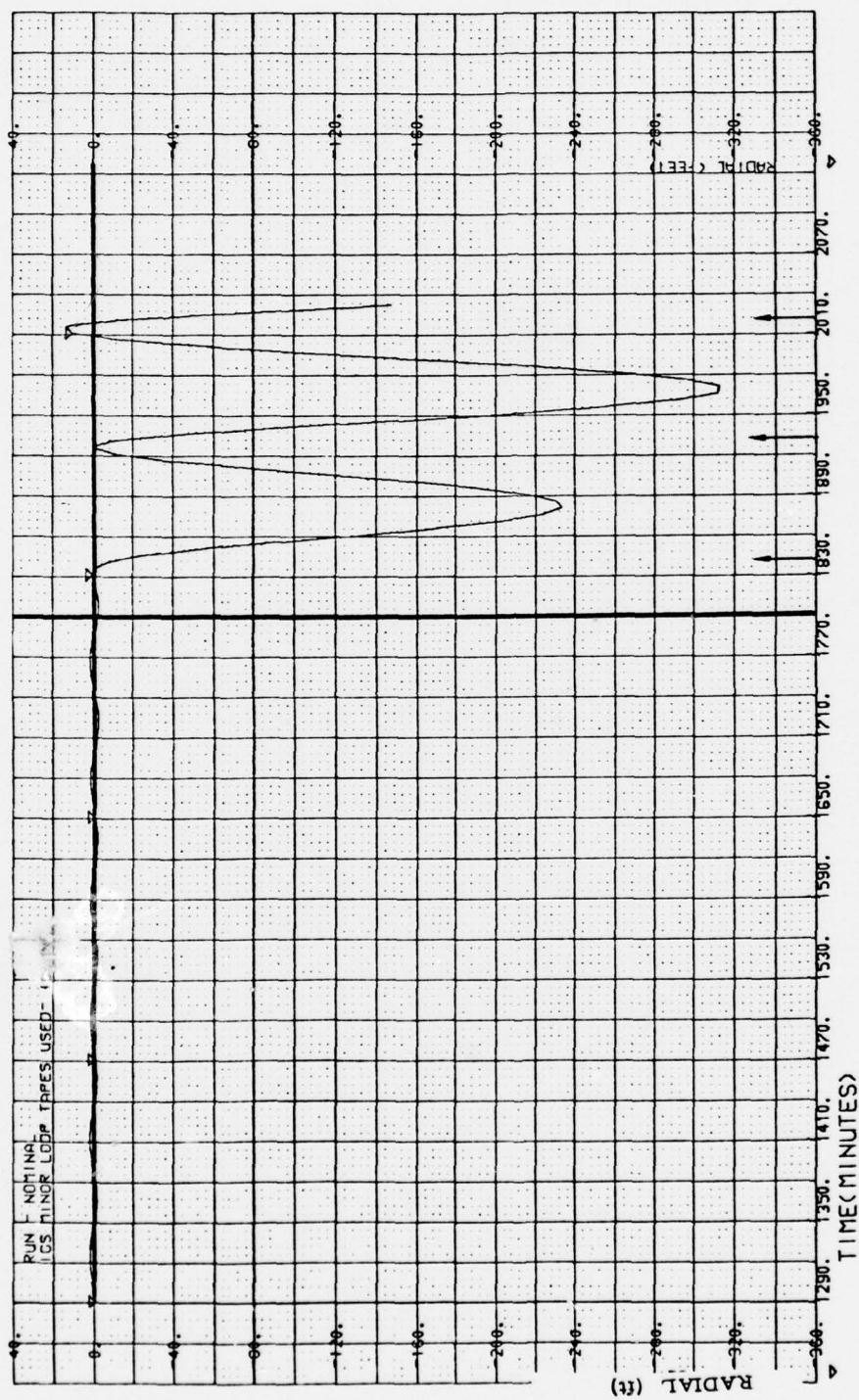
Fig. A-4. Calorimeter (fit)/"DENSEL (predict) 179-187
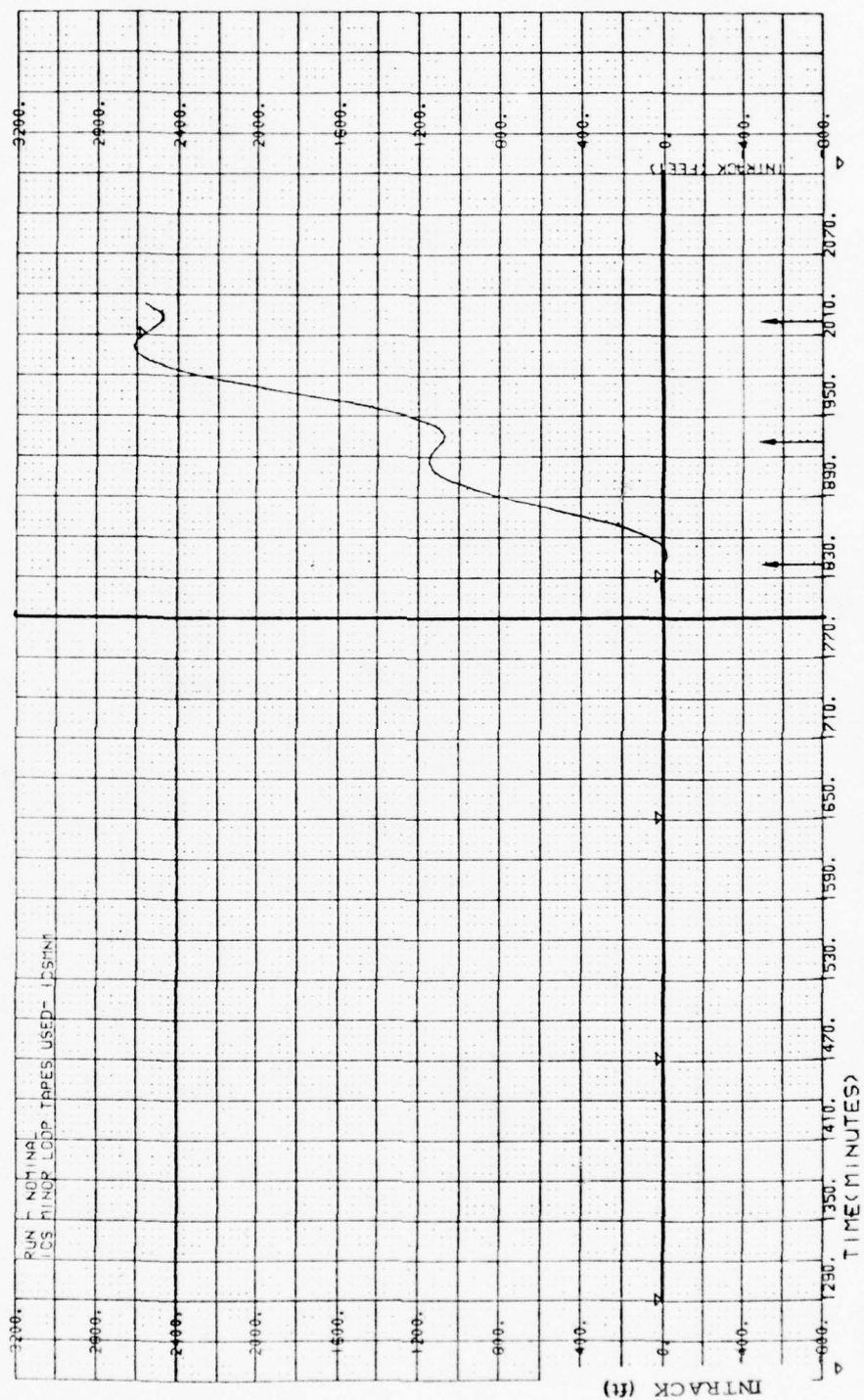
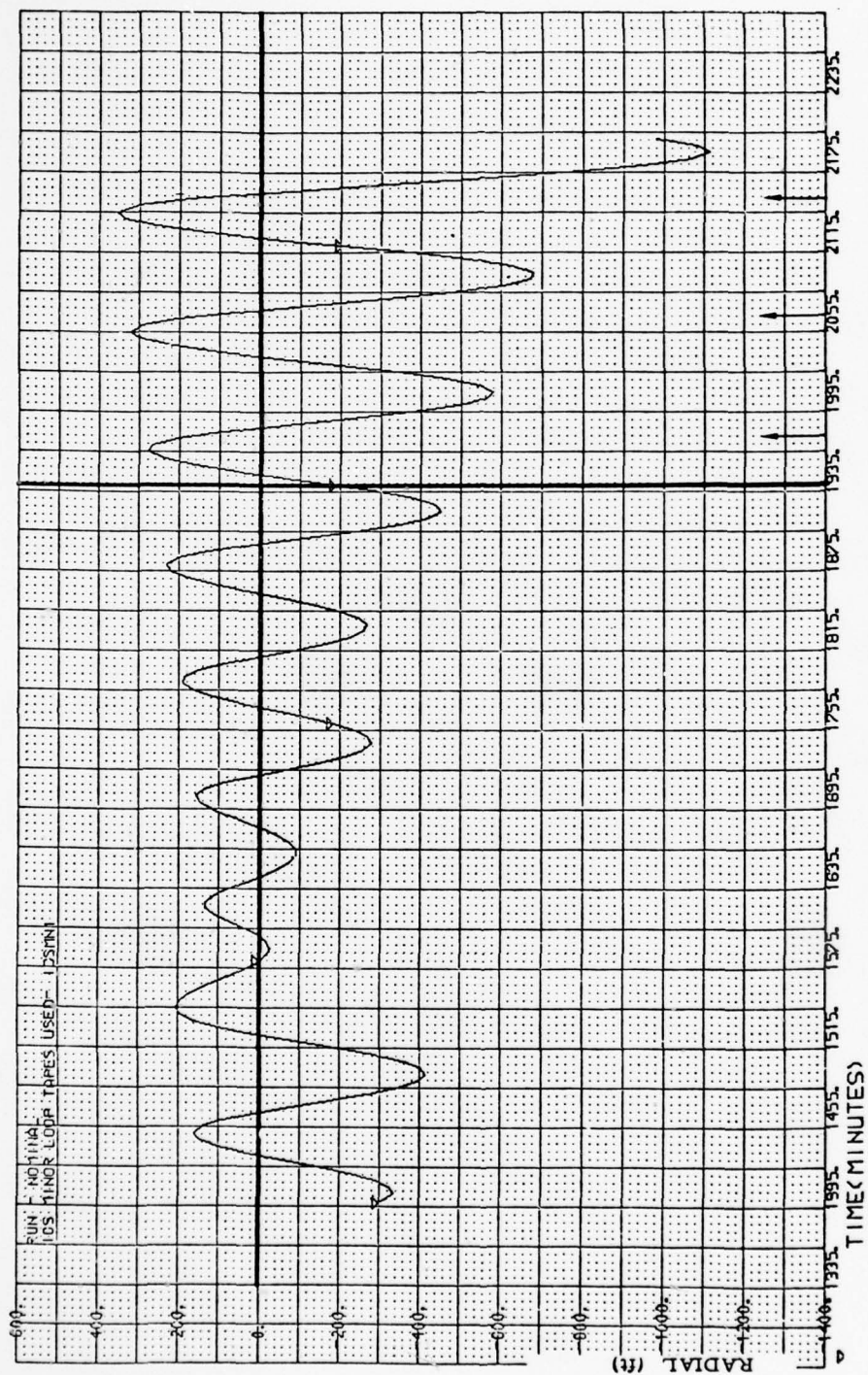Fig. A-4. Calorimeter (fit)/DENSEL (predict) 179-187 (Continued)
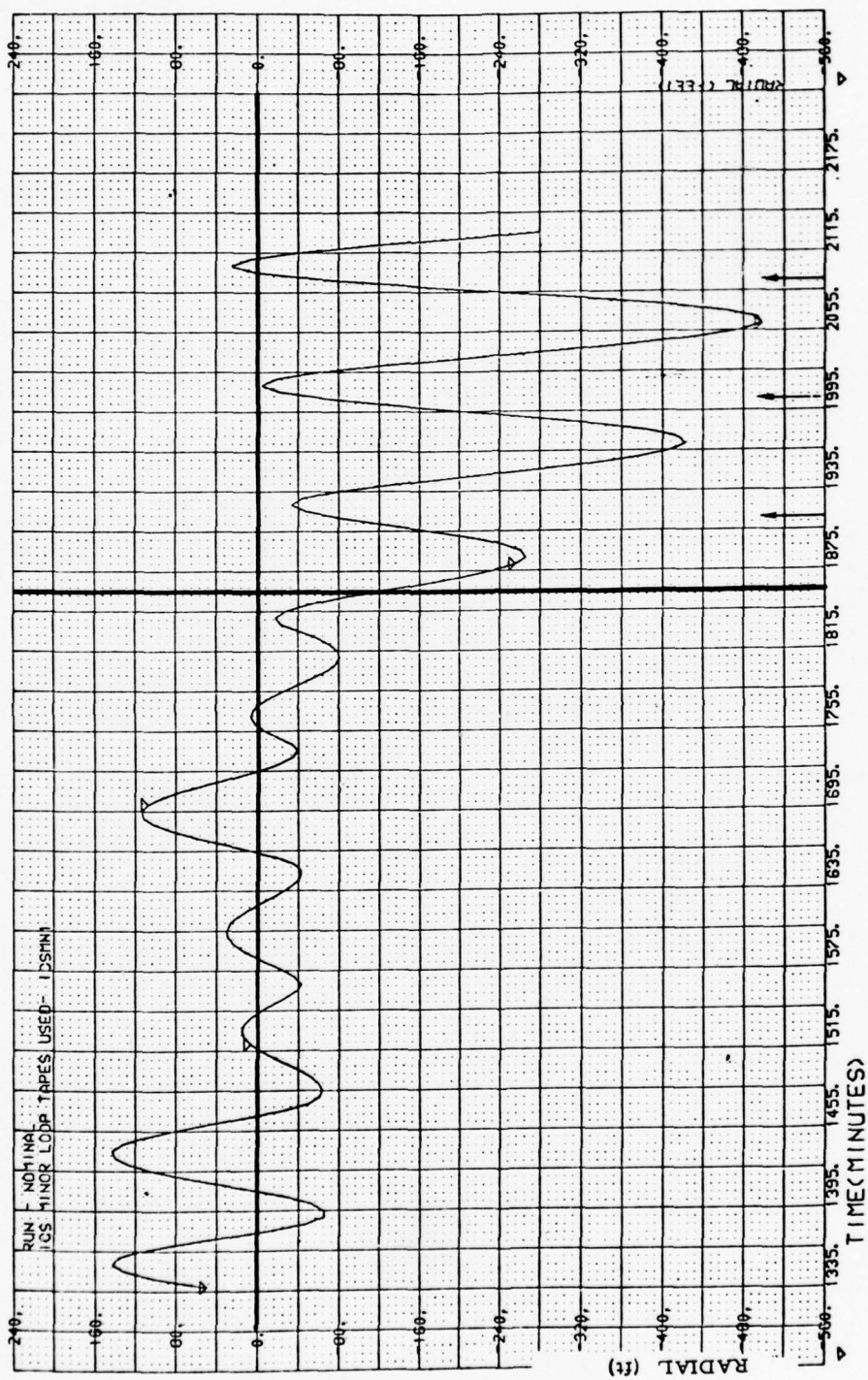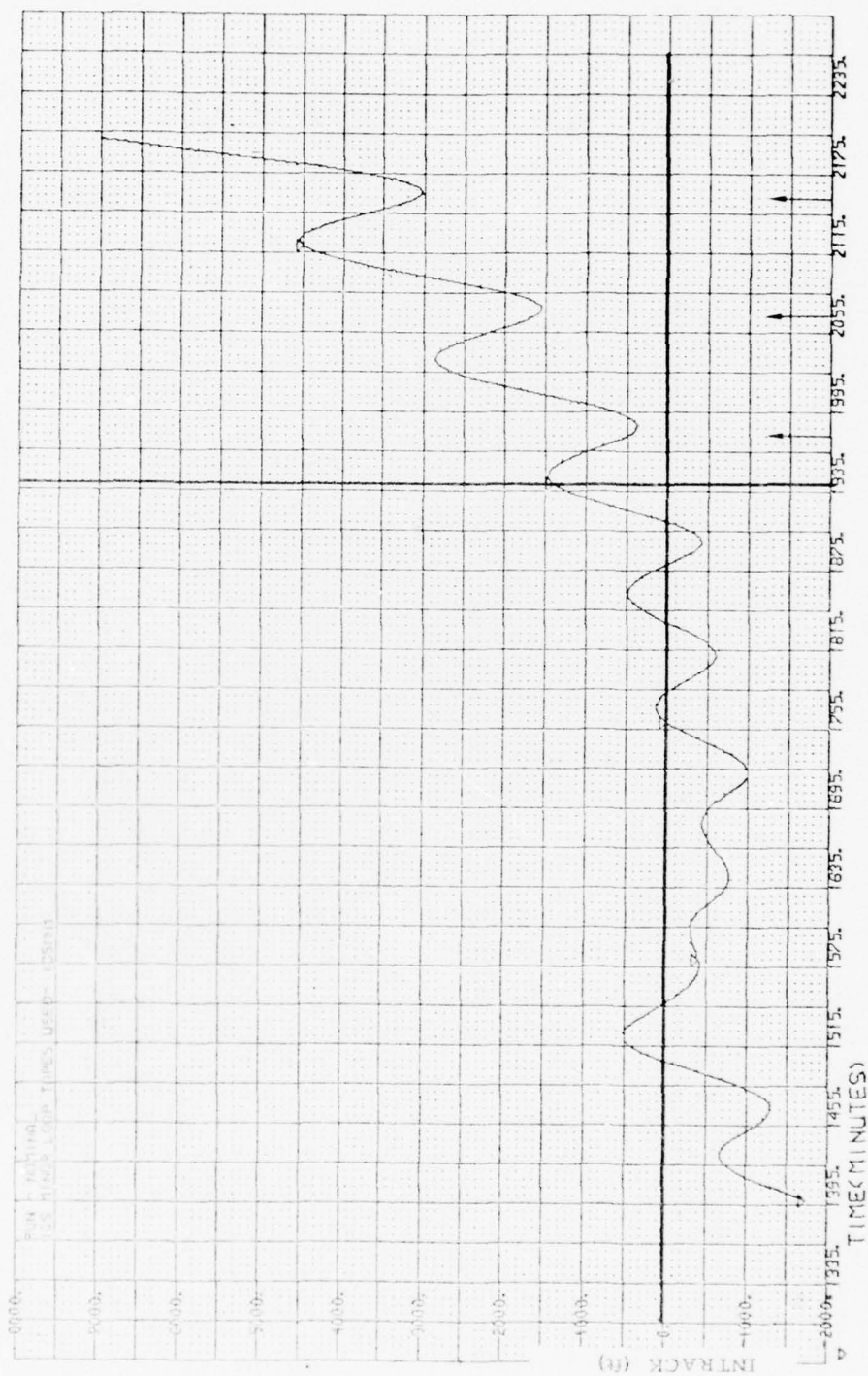
Fig. A-5. 'DENSEL (fit and predict) 325-333
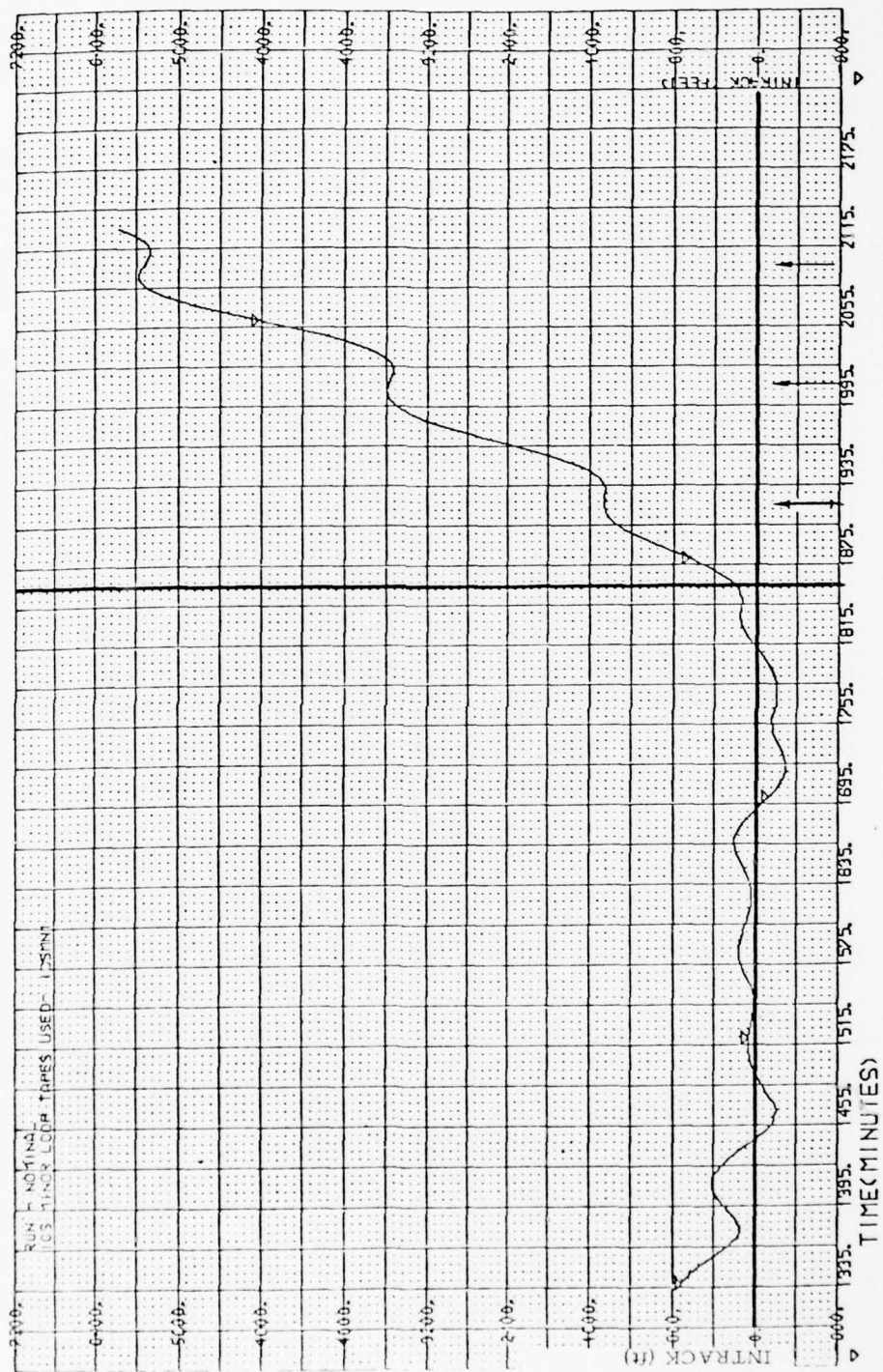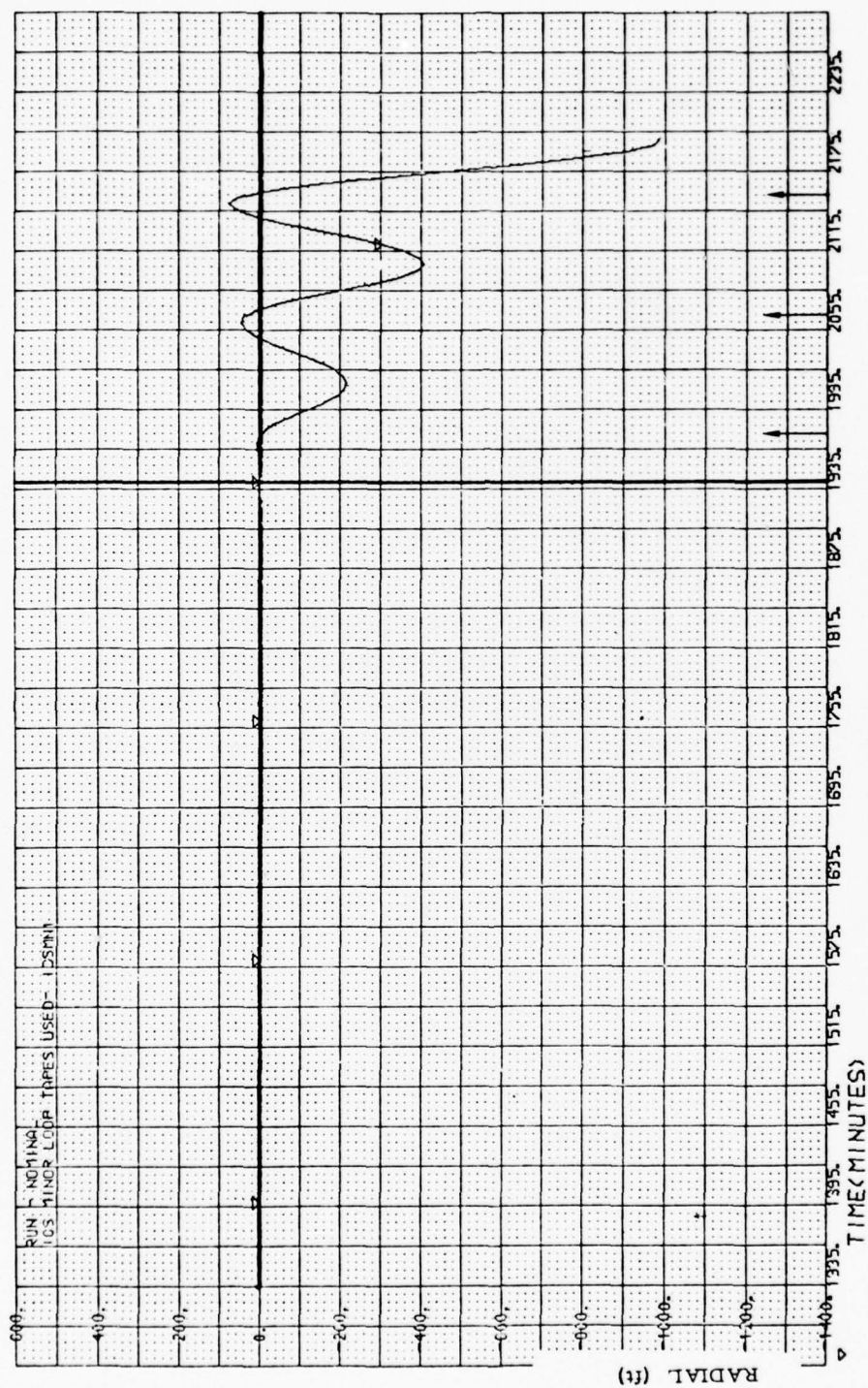
Fig. A-5. 'DENSEL (fit and predict) 325-333 (Continued)
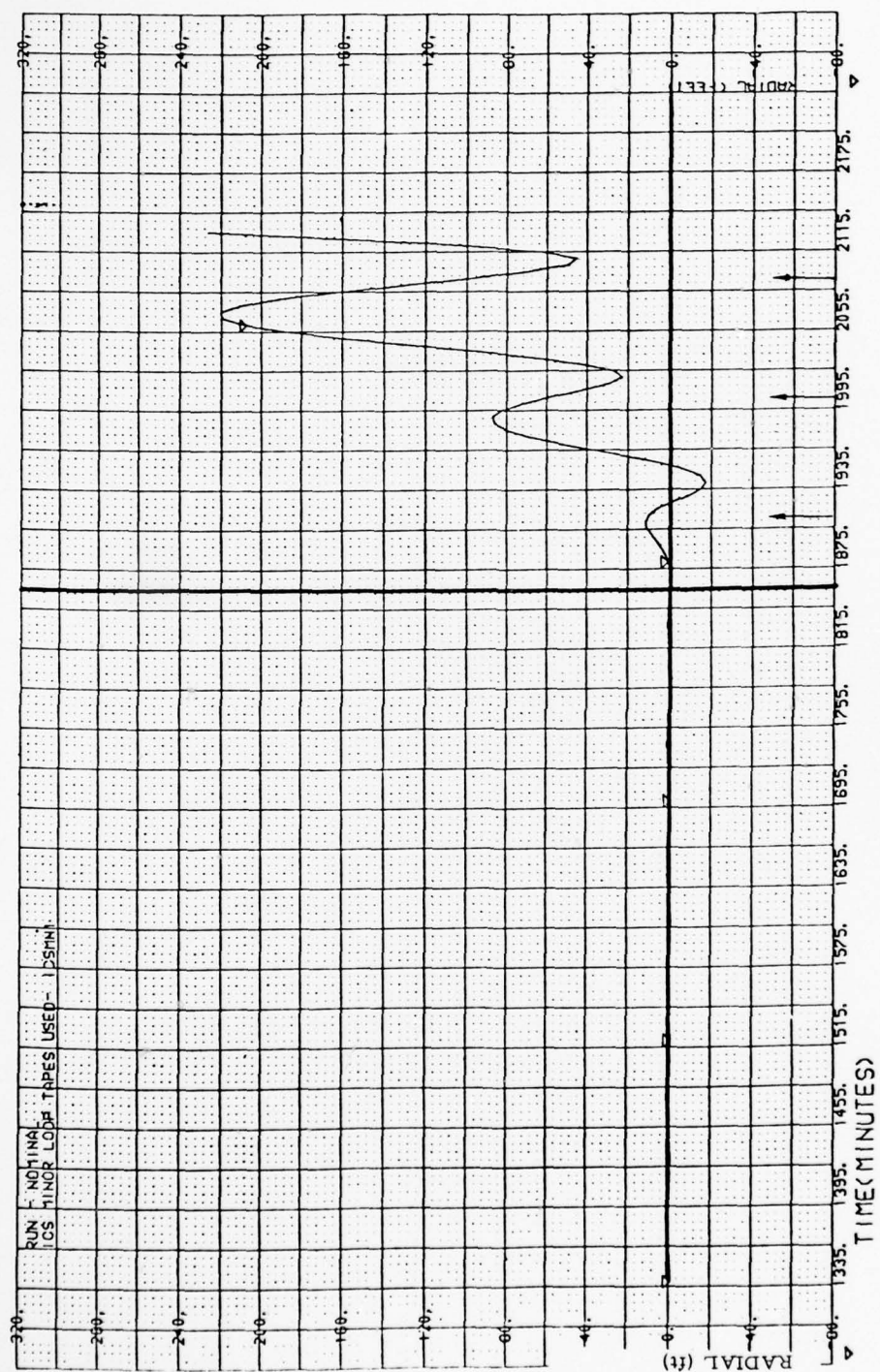
Fig. A-6. Calorimeter (fit)/MODB (predict) 325-333
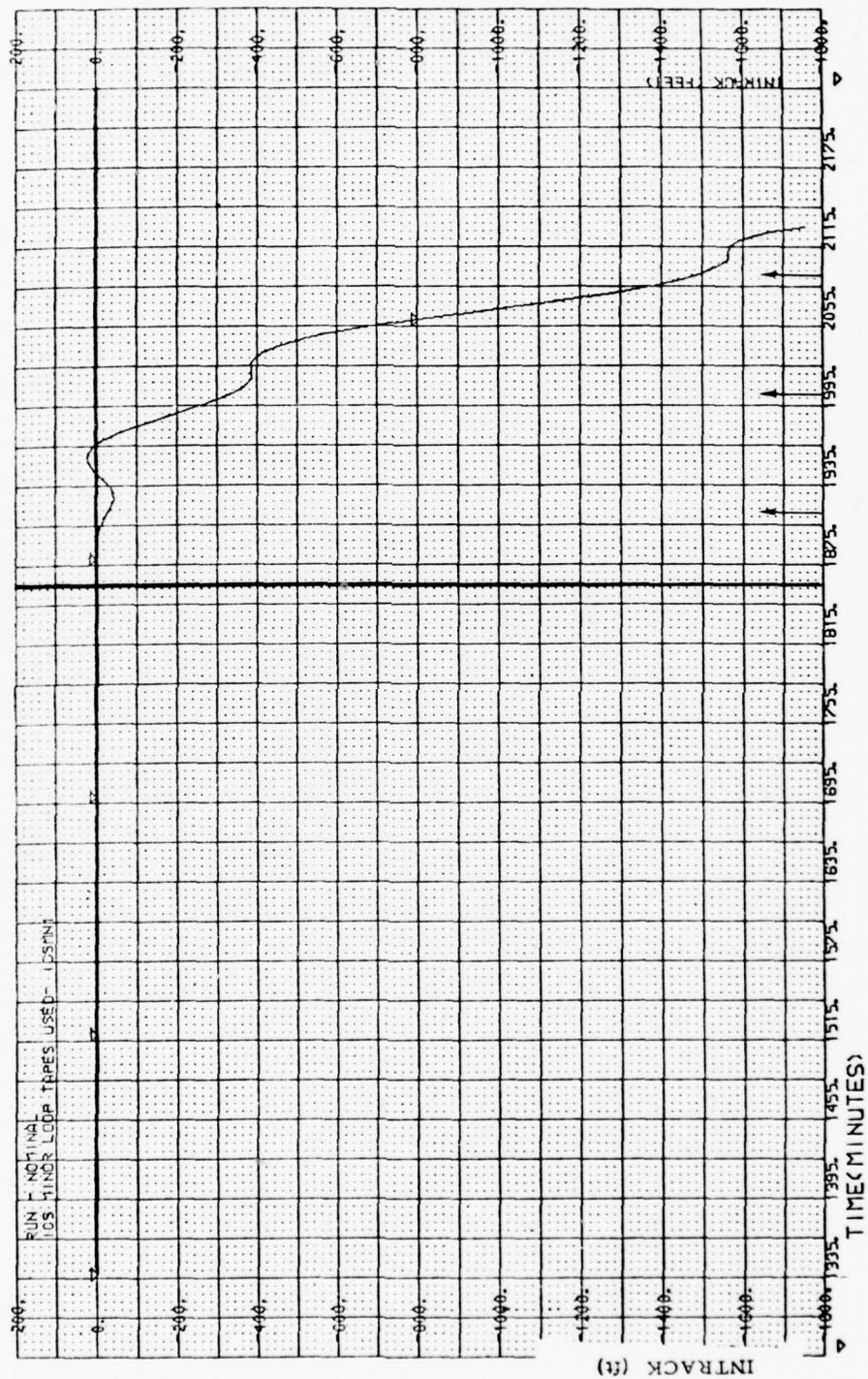
Fig. A-6. Calorimeter (fit)/MODB (predict) 325-333 (Continued)

Fig. A-7. Calorimeter (fit)/MODC (predict) 325-333

-60-
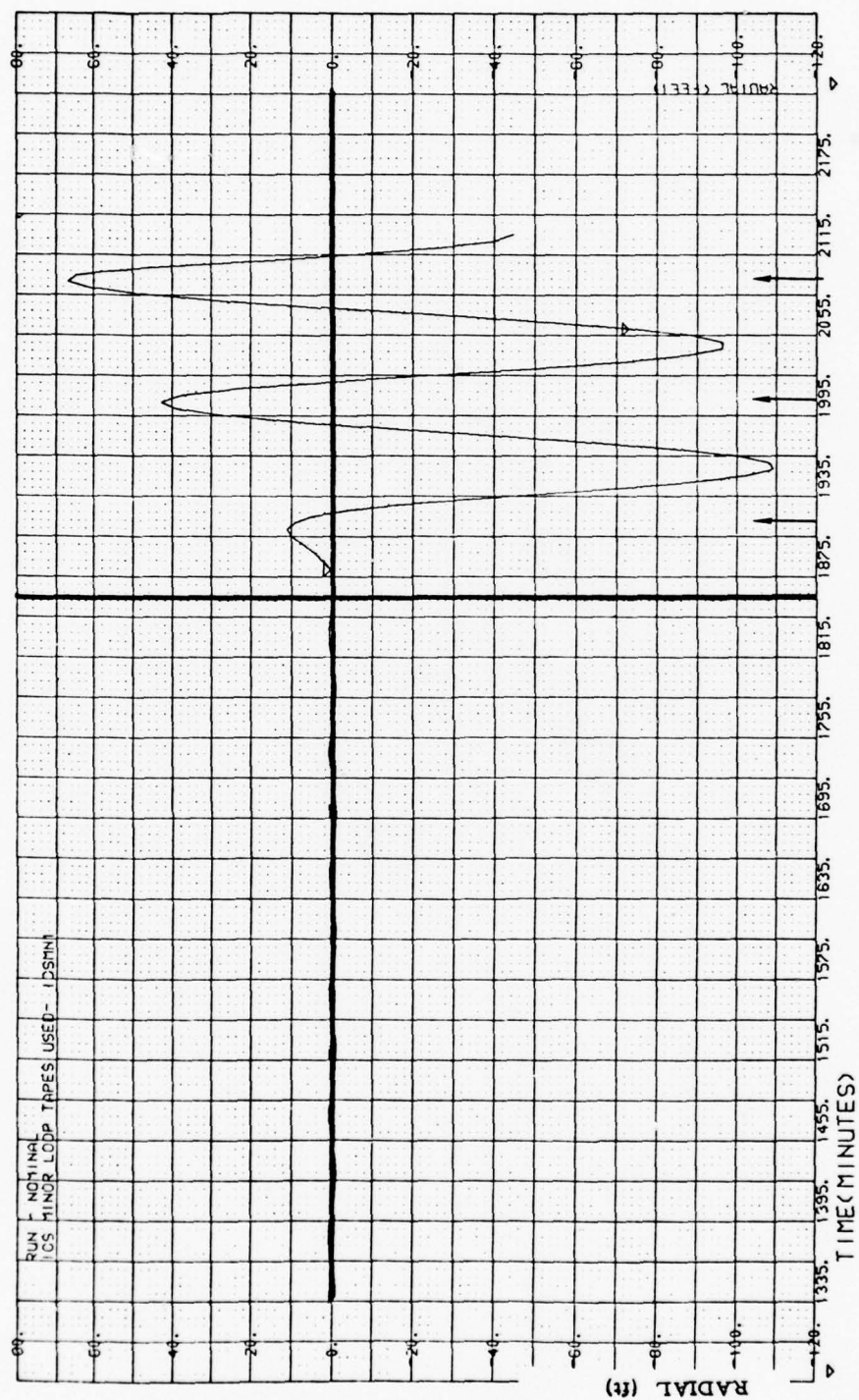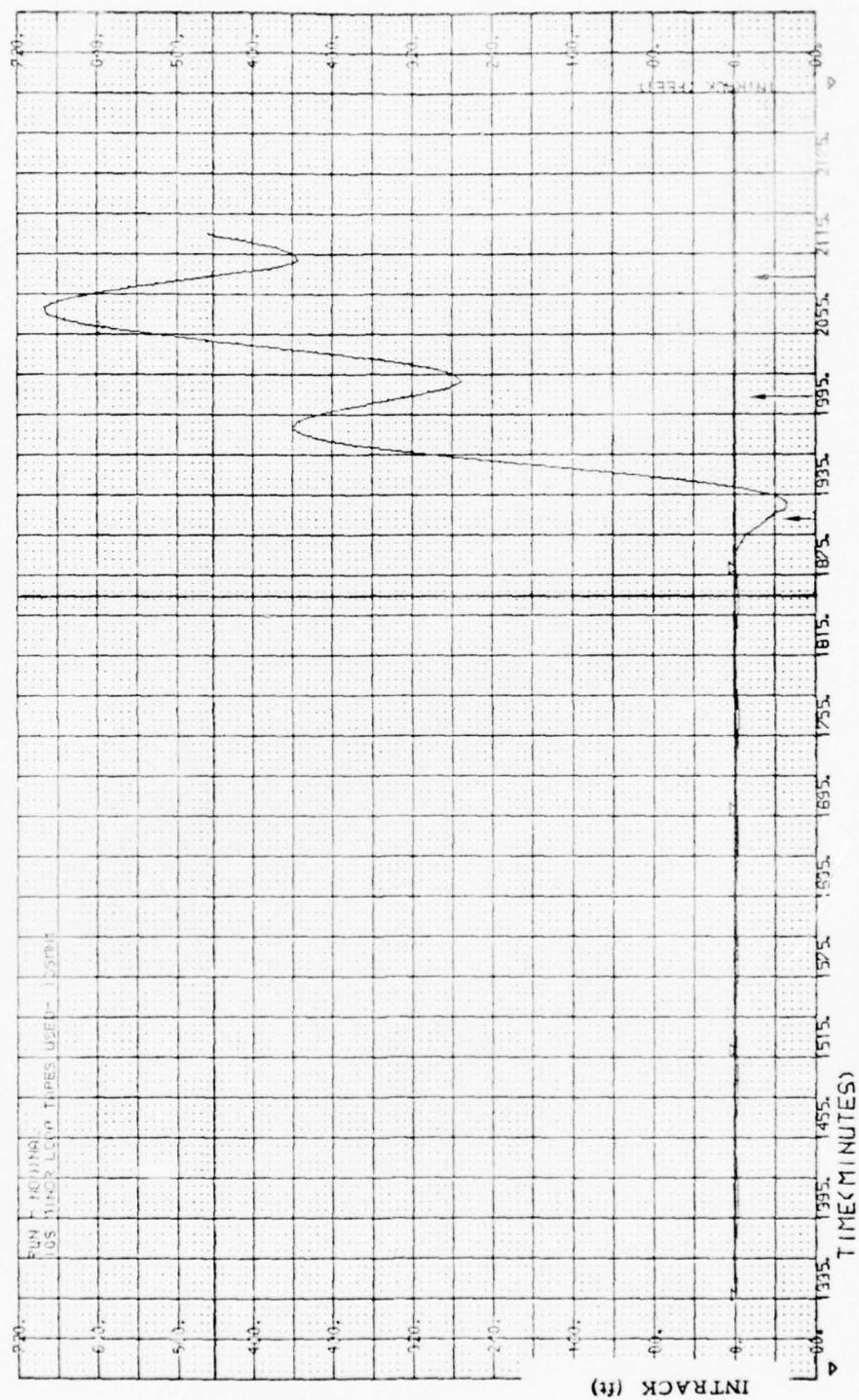
Fig. A-7. Calorimeter (fit)/MODC (predict) 325-333 (Continued)
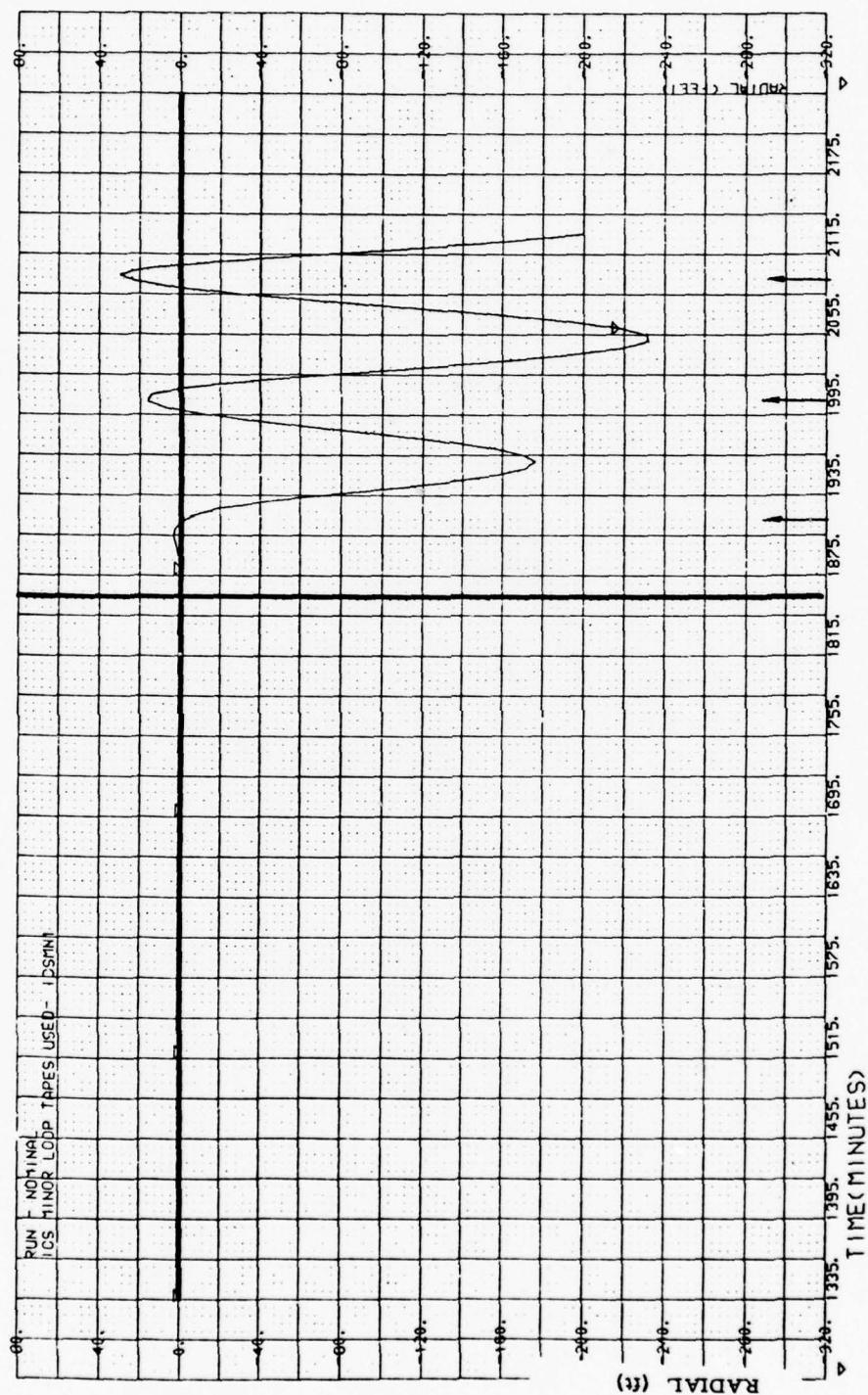
Fig. A-8.   Calorimeter (fit)/'DENSEL (predict) 325-333
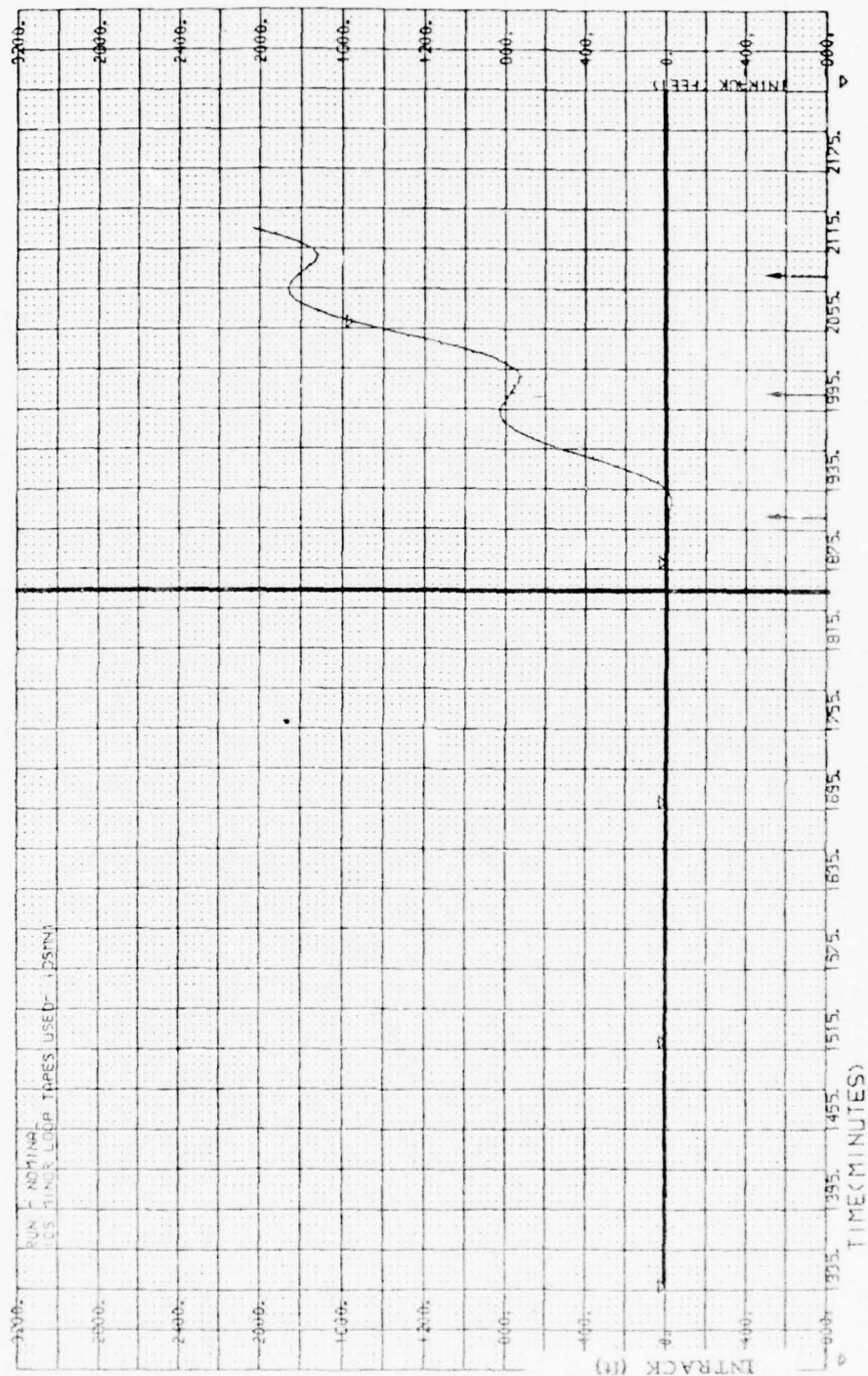
Fig. A-8. Calorimeter (fit)/"DENSEL (predict) 325-333 (Continued)
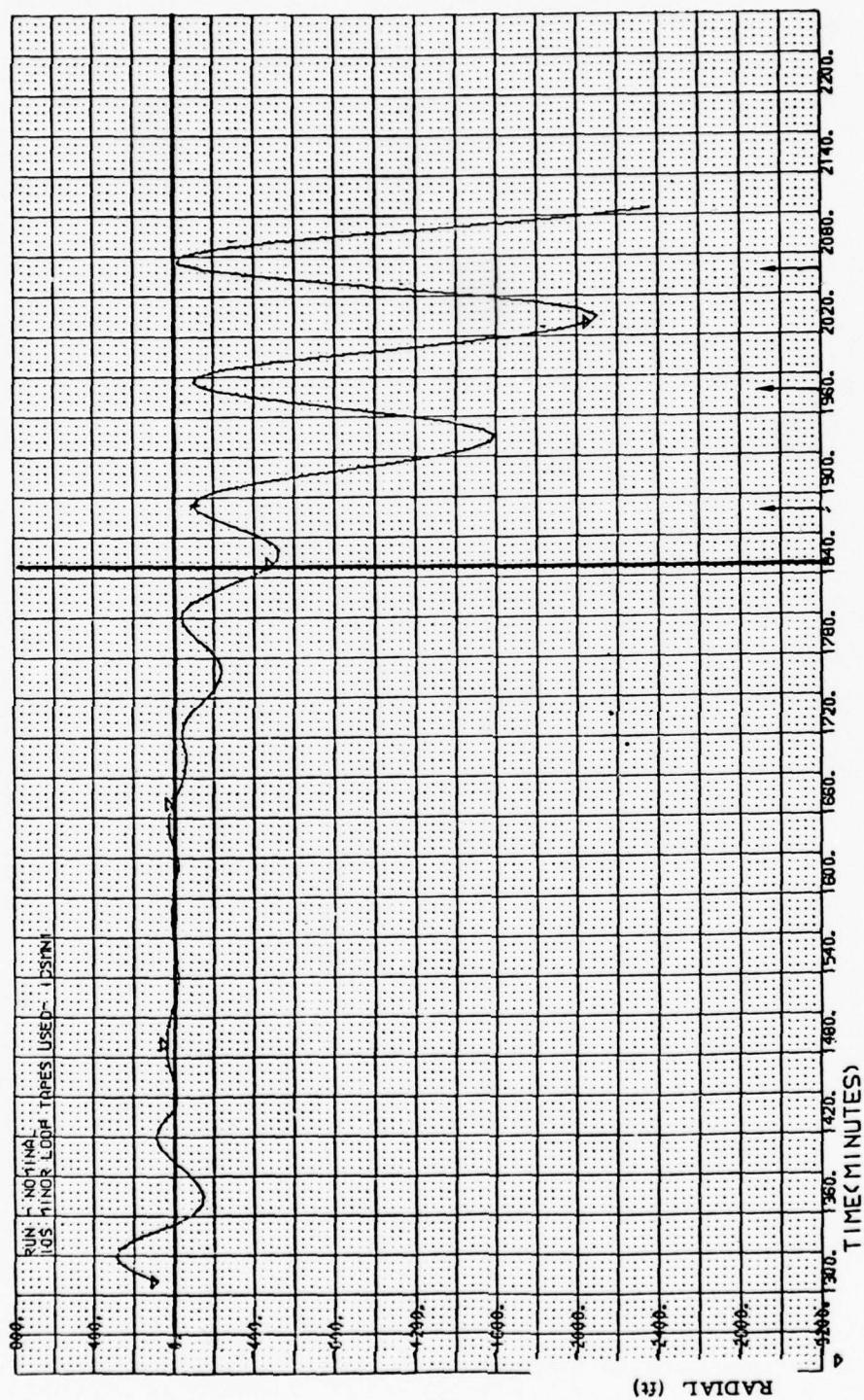
Fig. A-9. 'DENSEL (fit and predict) 502-510
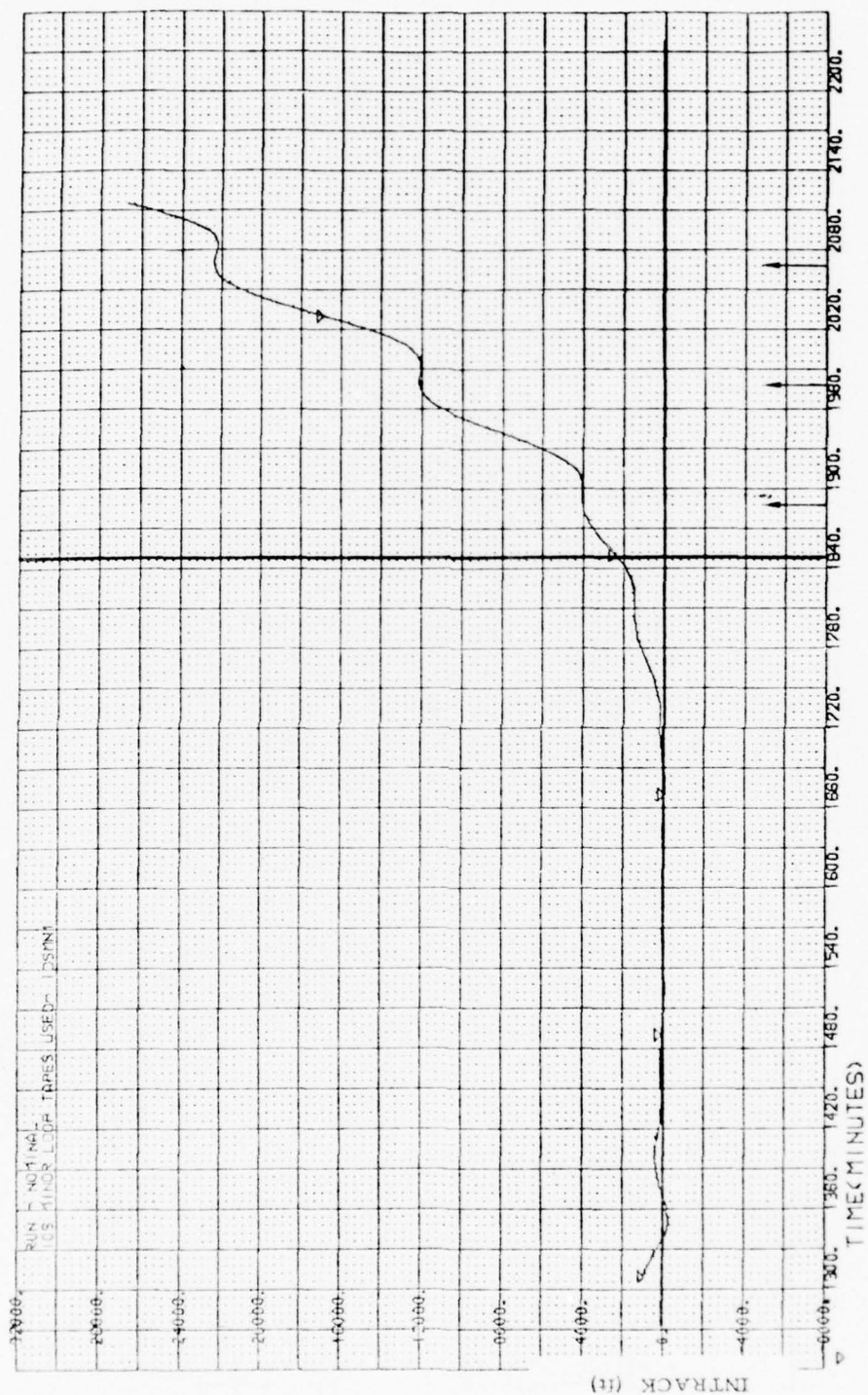
Fig. A-9. 'DENSEL (fit and predict) 502-510 (Continued)

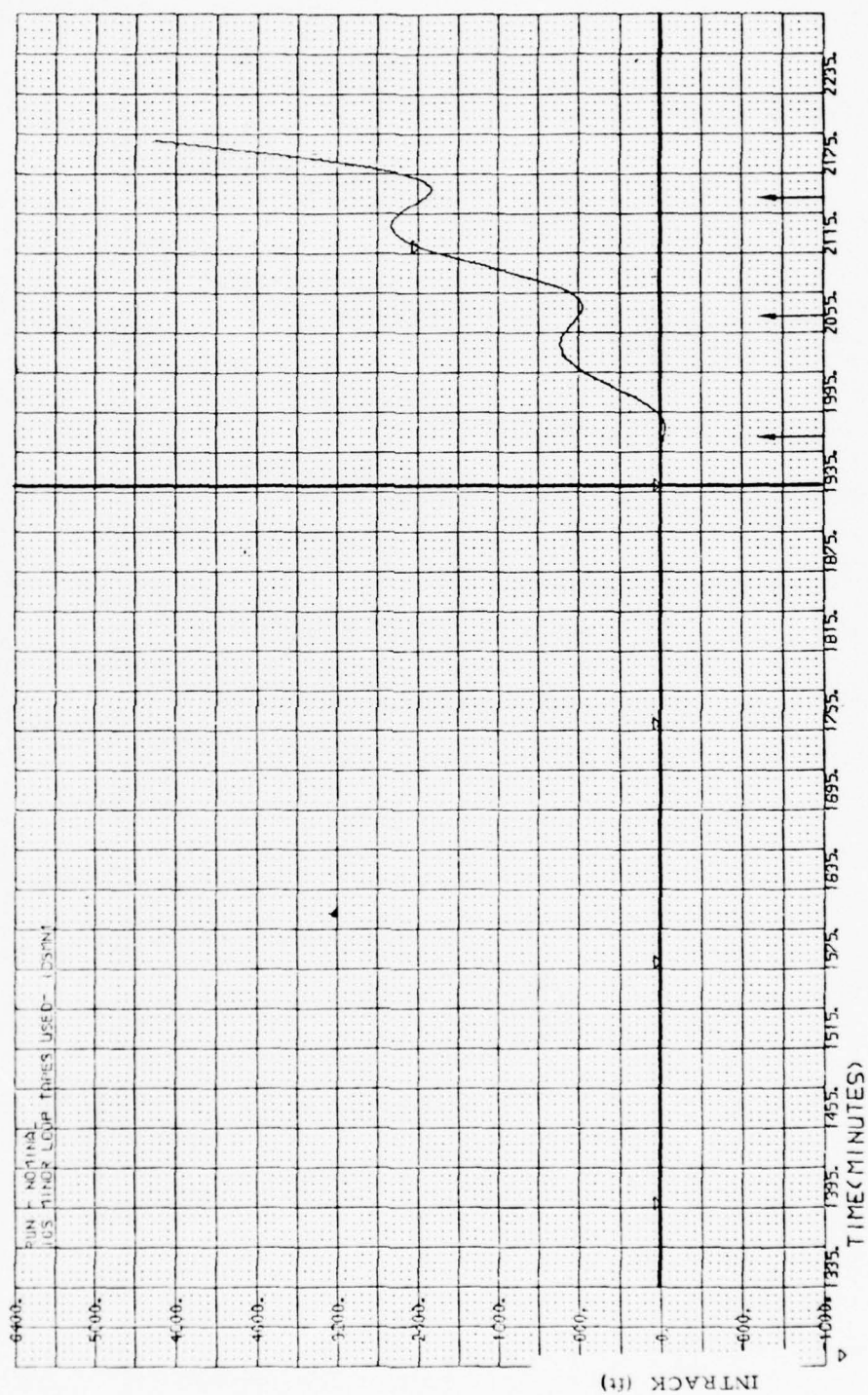Fig. A-10. Calorimeter (fit)/MODB (predict) 502-510

-66-
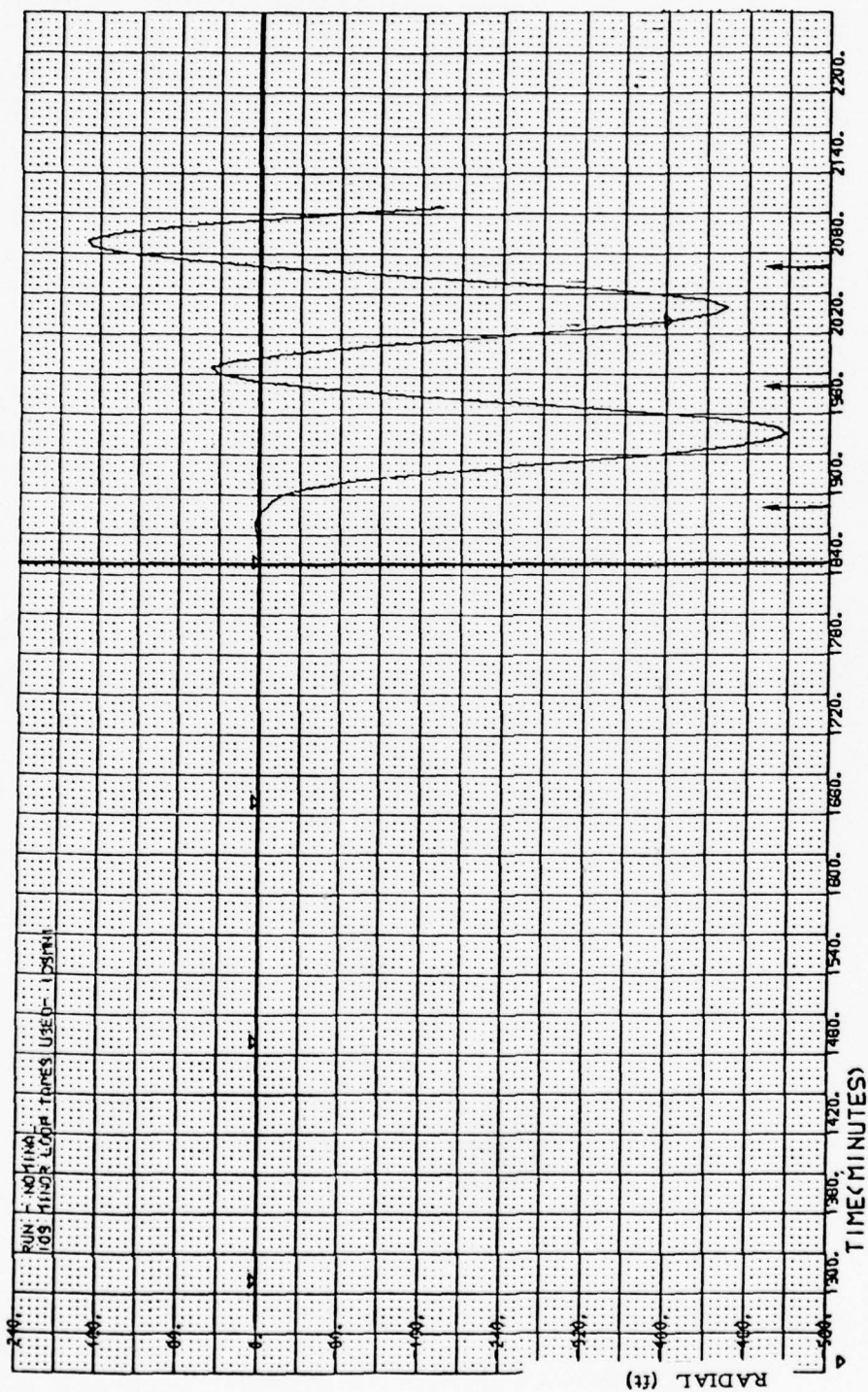
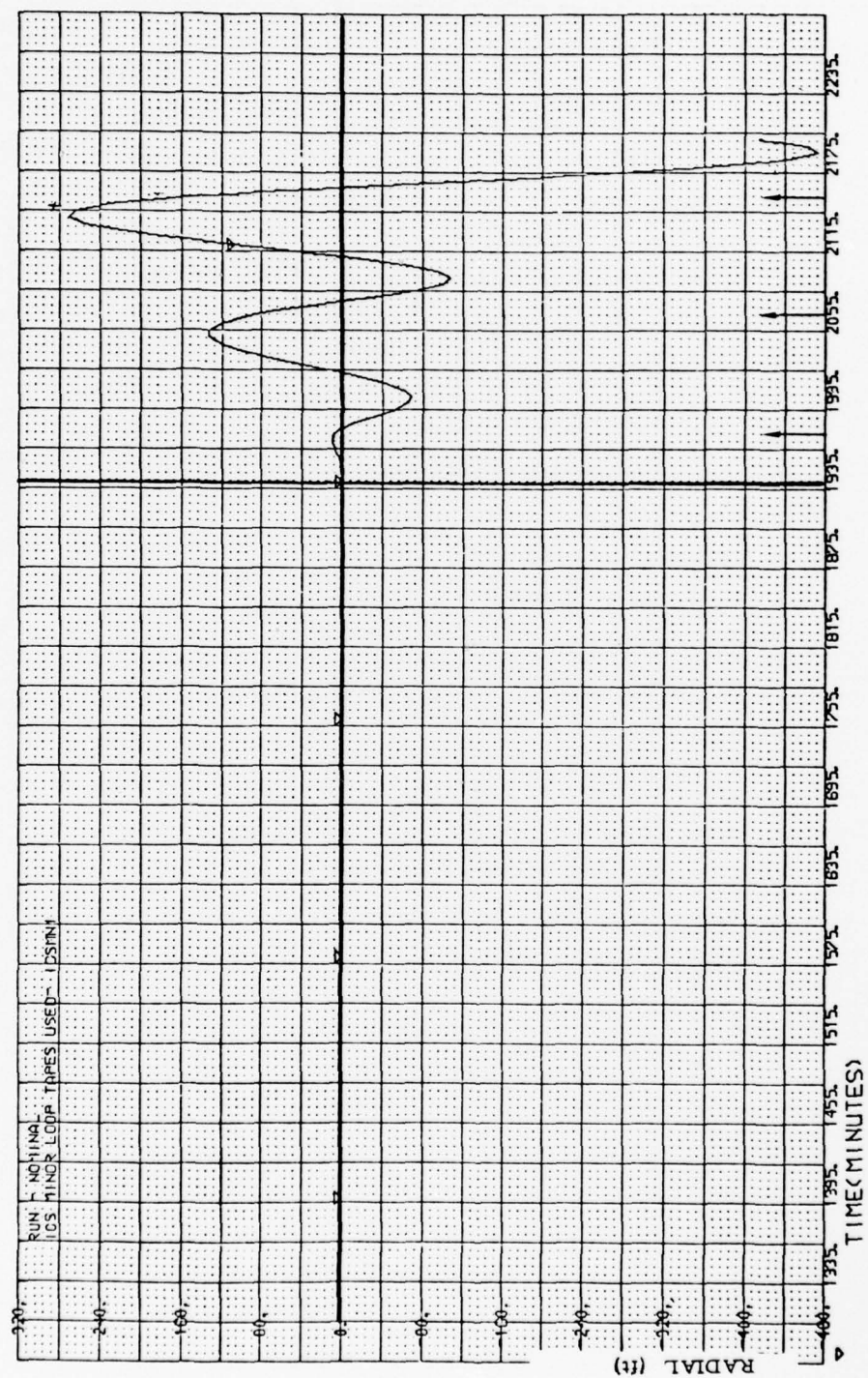Fig. A-10. Calorimeter (fit)/MODB (predict) 502-510 (Continued)

Fig. A-11. Calorimeter (fit)/MODC (predict) 502-510

-68-
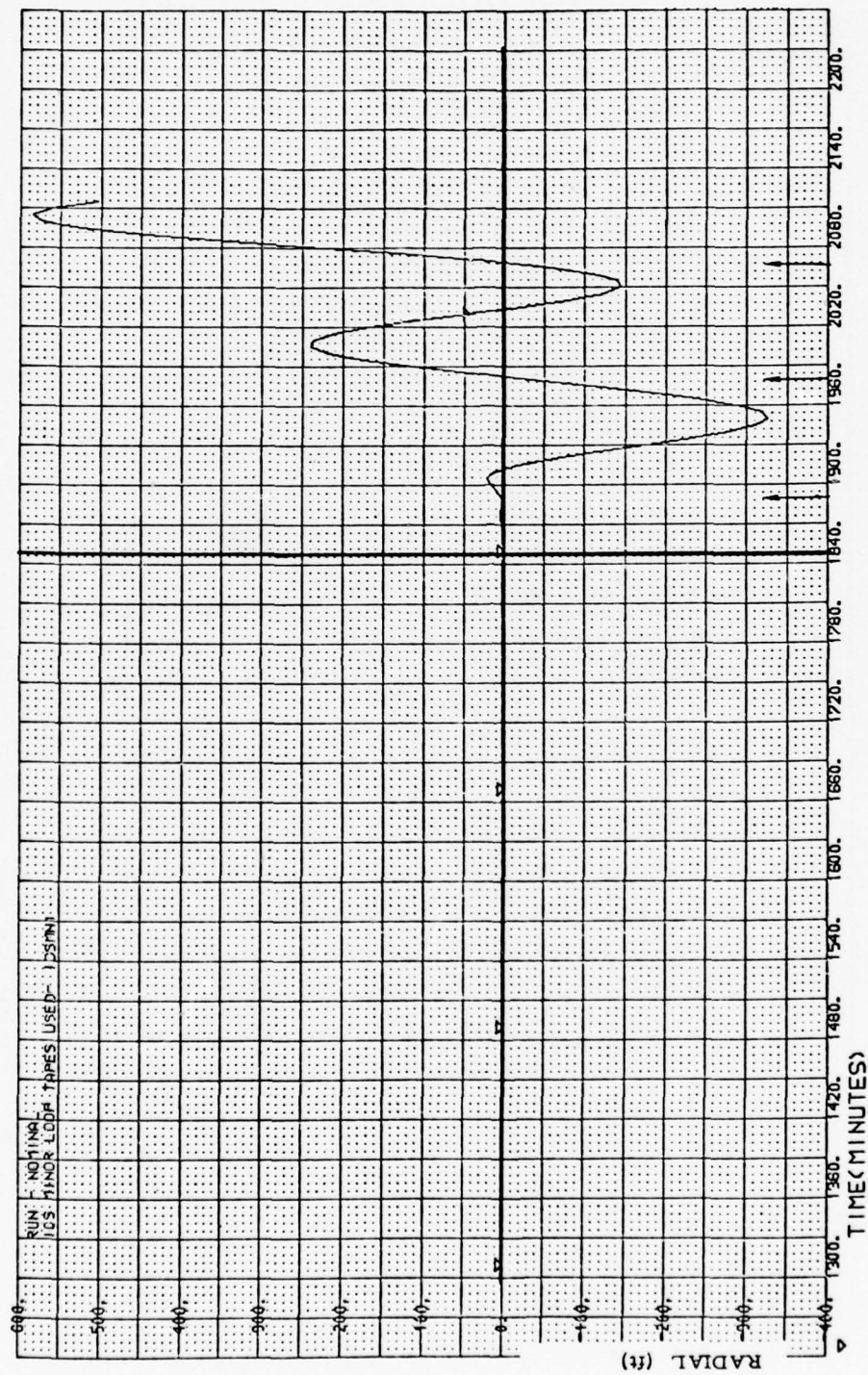
Fig. A-11. Calorimeter (fit)/MODC (predict) 502-510 (Continued)

Fig. A-12. Calorimeter (fit)/"DENSEL (predict) 502-510

-70-

Fig. A-12. Calorimeter (fit)/DENSEL (predict) 502-510 (Continued)

Fig. A-13. 'DENSEL (fit and predict) 761-769

Fig. A-13. "DENSEL (fit and predict) 761-769 (Continued)

Fig. A-14. Calorimeter (fit)/MODB (predict) 761-769

-74-

Fig. A-14. Calorimeter (fit)/MODB (predict) 761 769 (Continued)
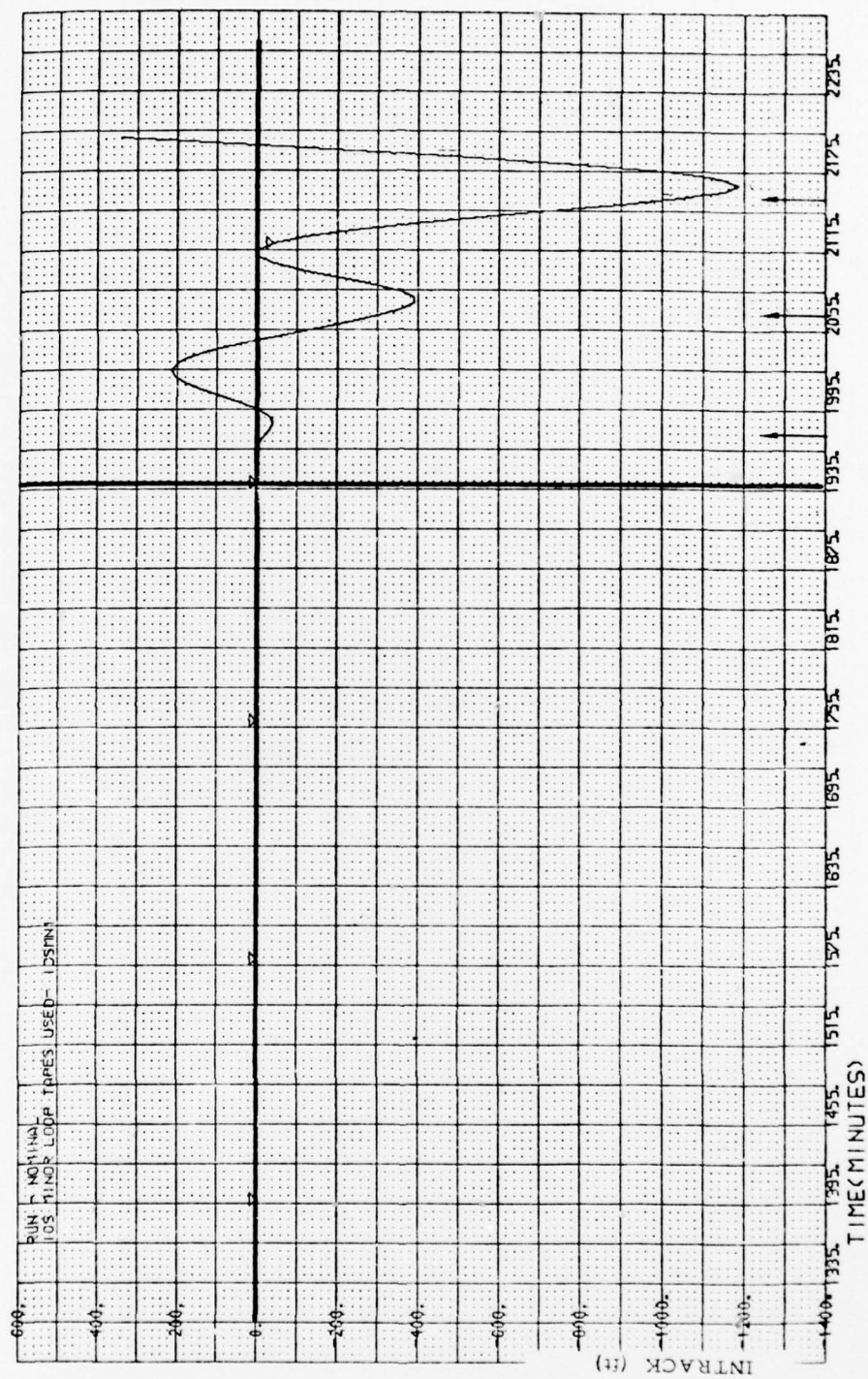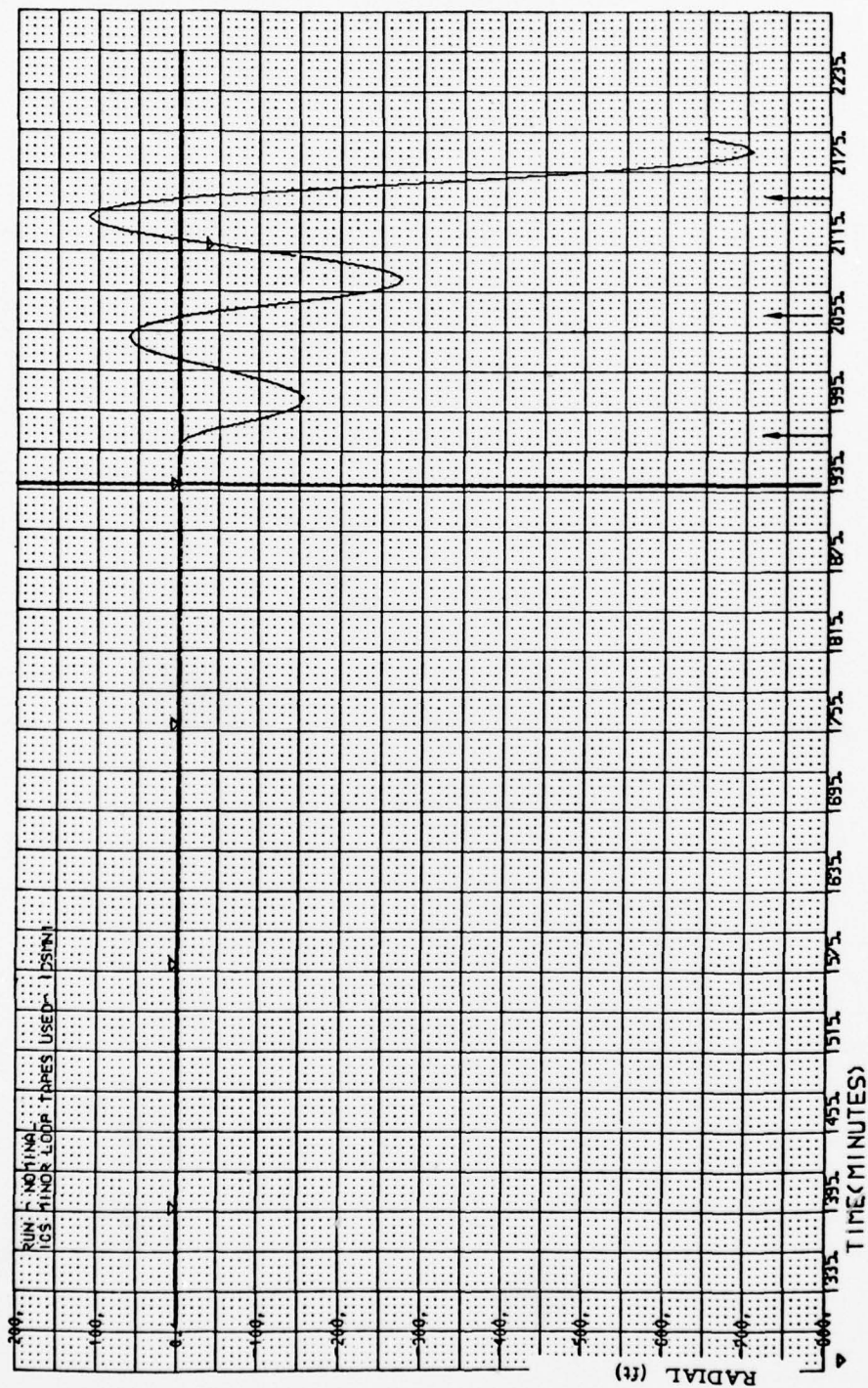
Fig. A-15. Calorimeter (fit)/MODC (predict) 761-769

-76-

RUN: NOMINAL
10S MINOR LOOP TAPES USED- 125MIN

TIME(MINUTES)

INTRACK (ft)

Fig. A-15. Calorimeter (fit)/MODC (predict) 761-769 (Continued)

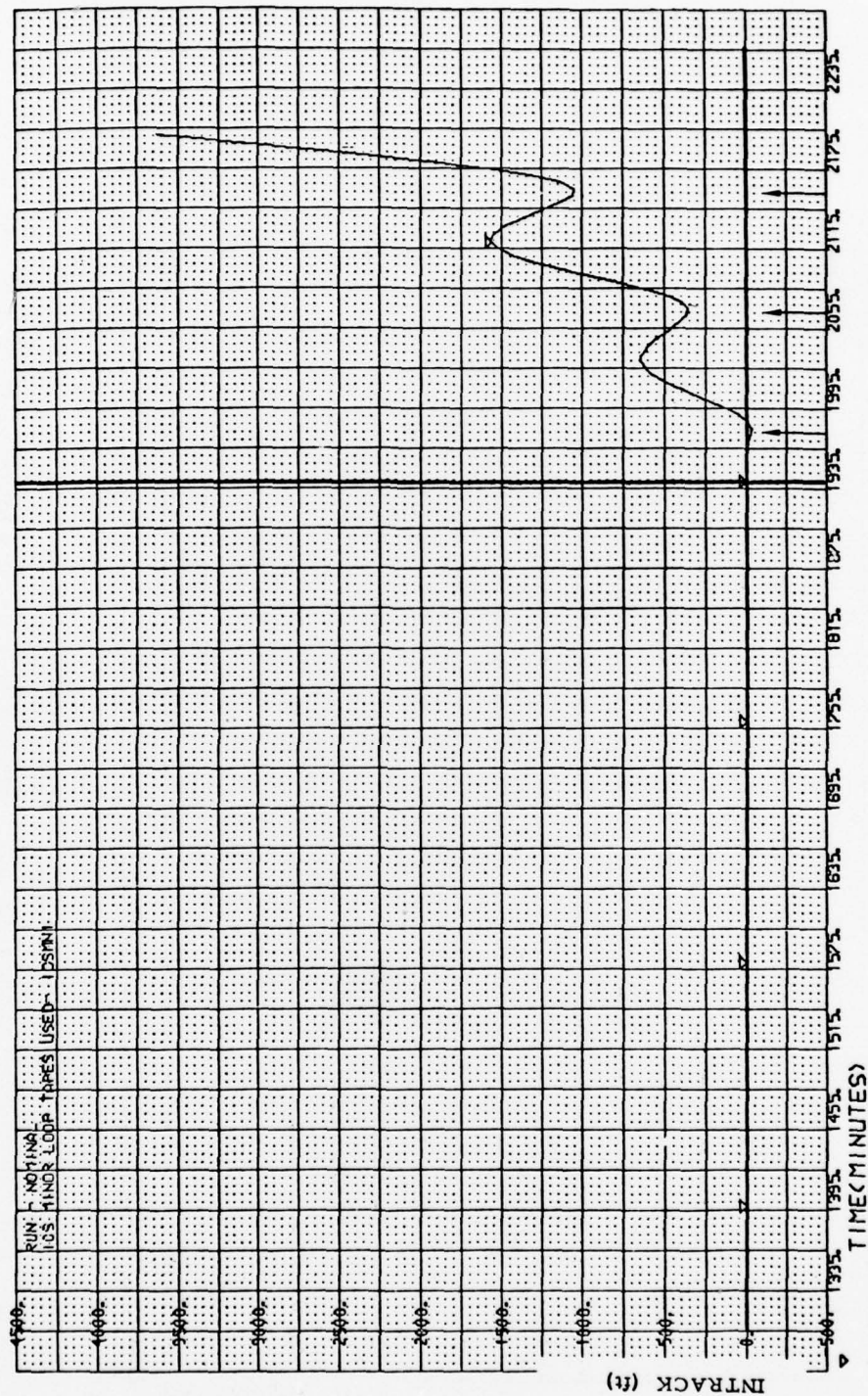Fig. A-16. Calorimeter (fit)/'DENSEL (predict) 761-769

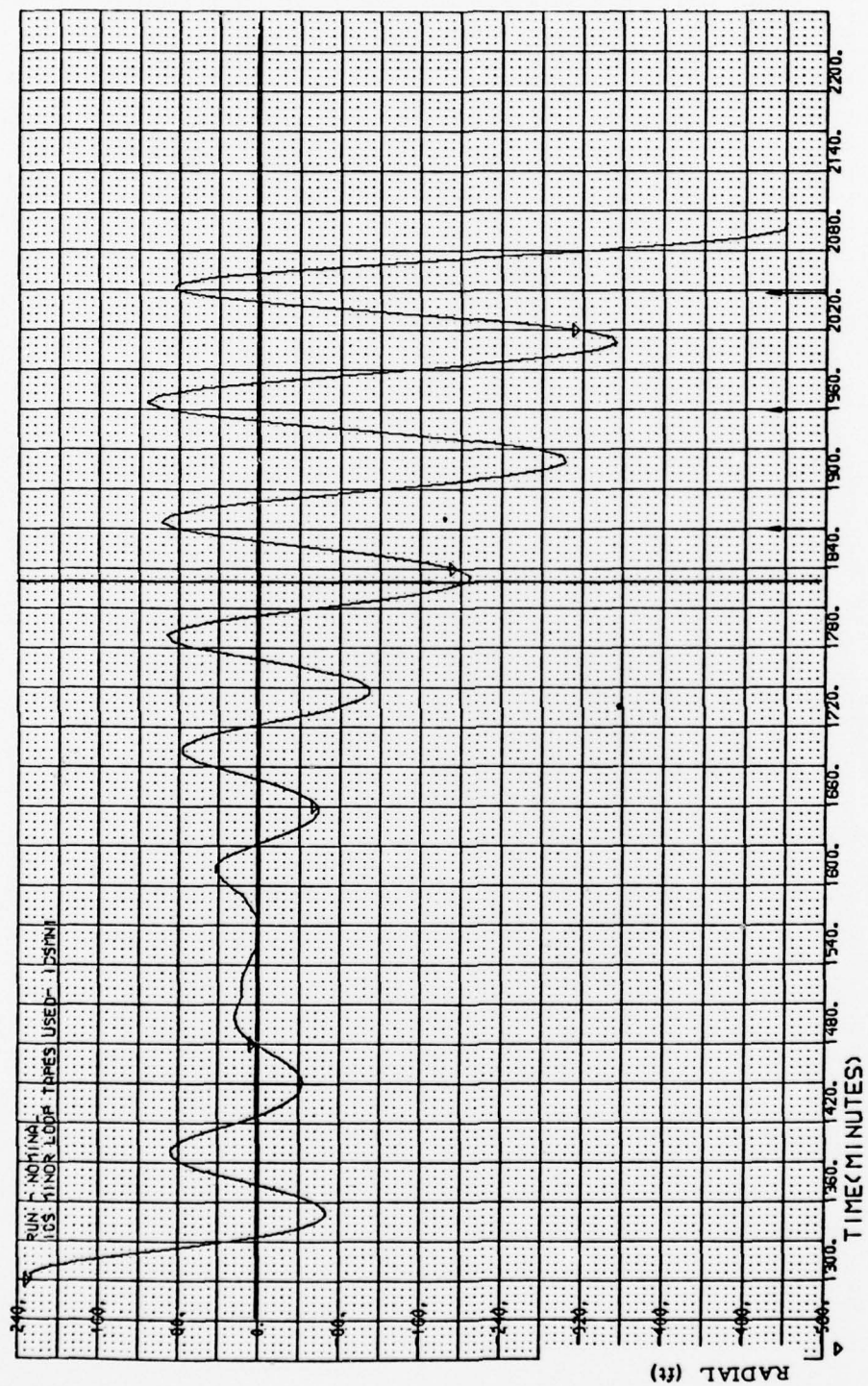Fig. A-16. Calorimeter (fit)/"DENSEL (predict) 761-769 (Continued)

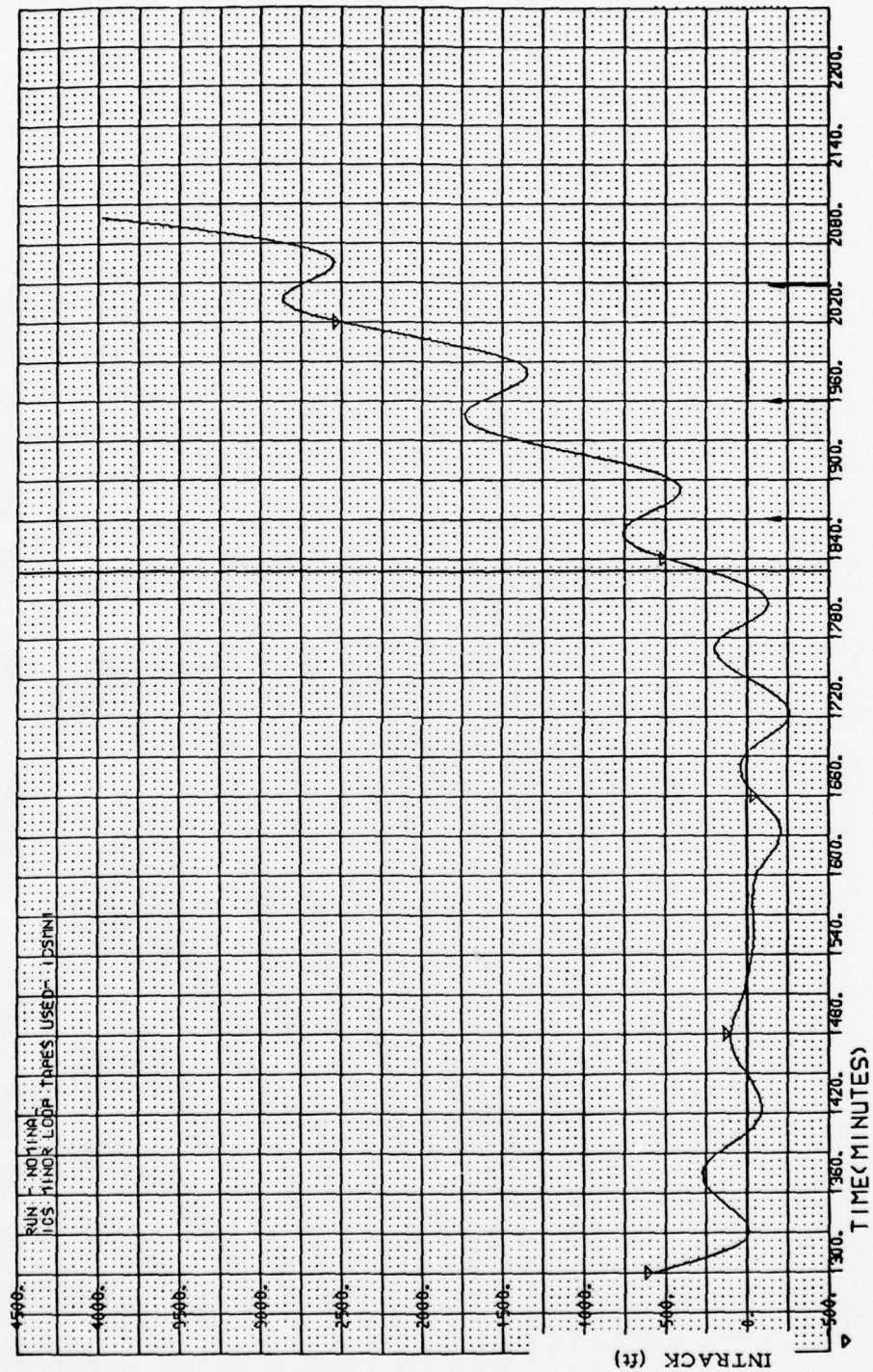Fig. A-17.   'DENSEL (fit and predict) 792-800

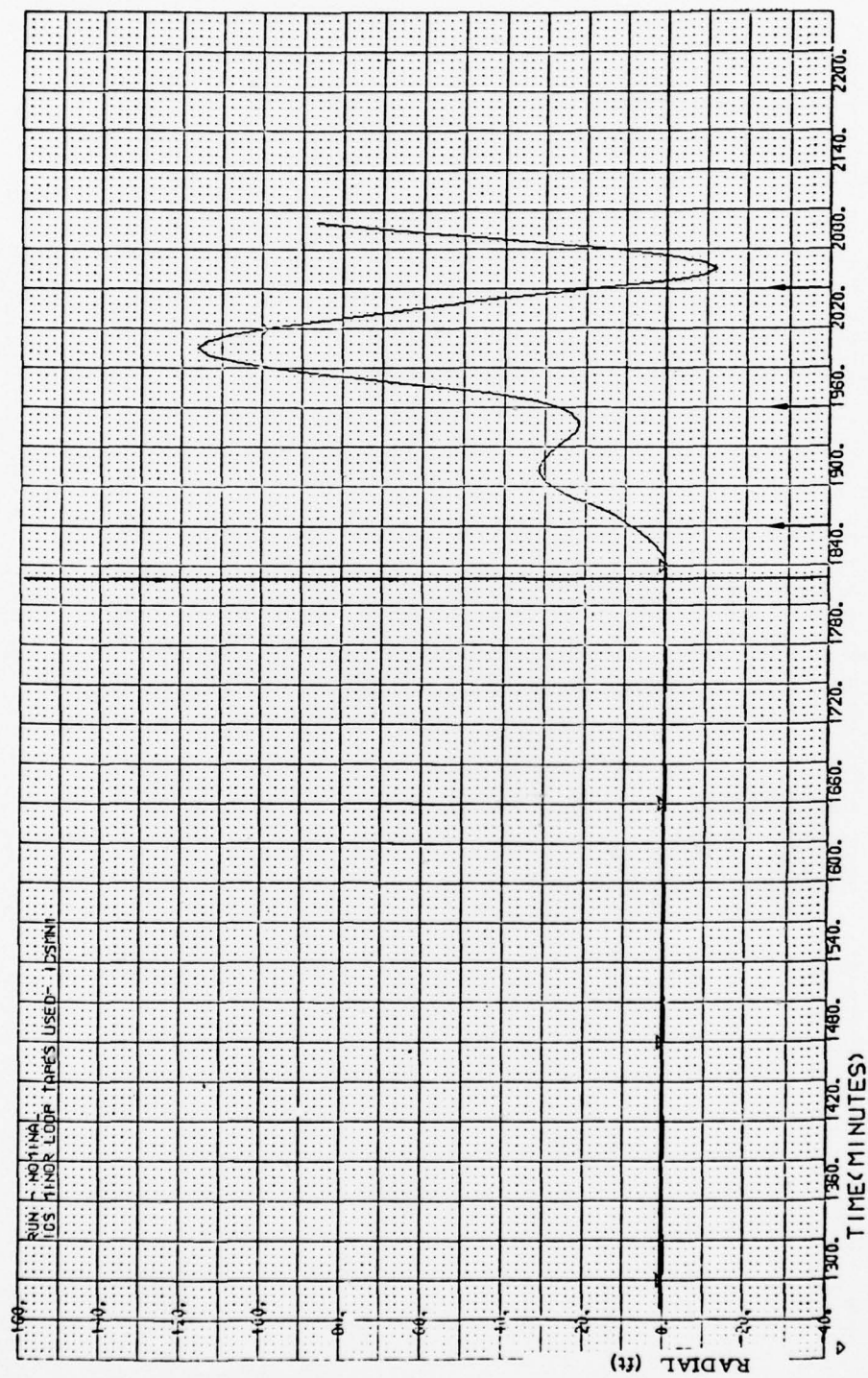Fig. A-17. 'DENSEL (fit and predict) 792-800 (Continued)

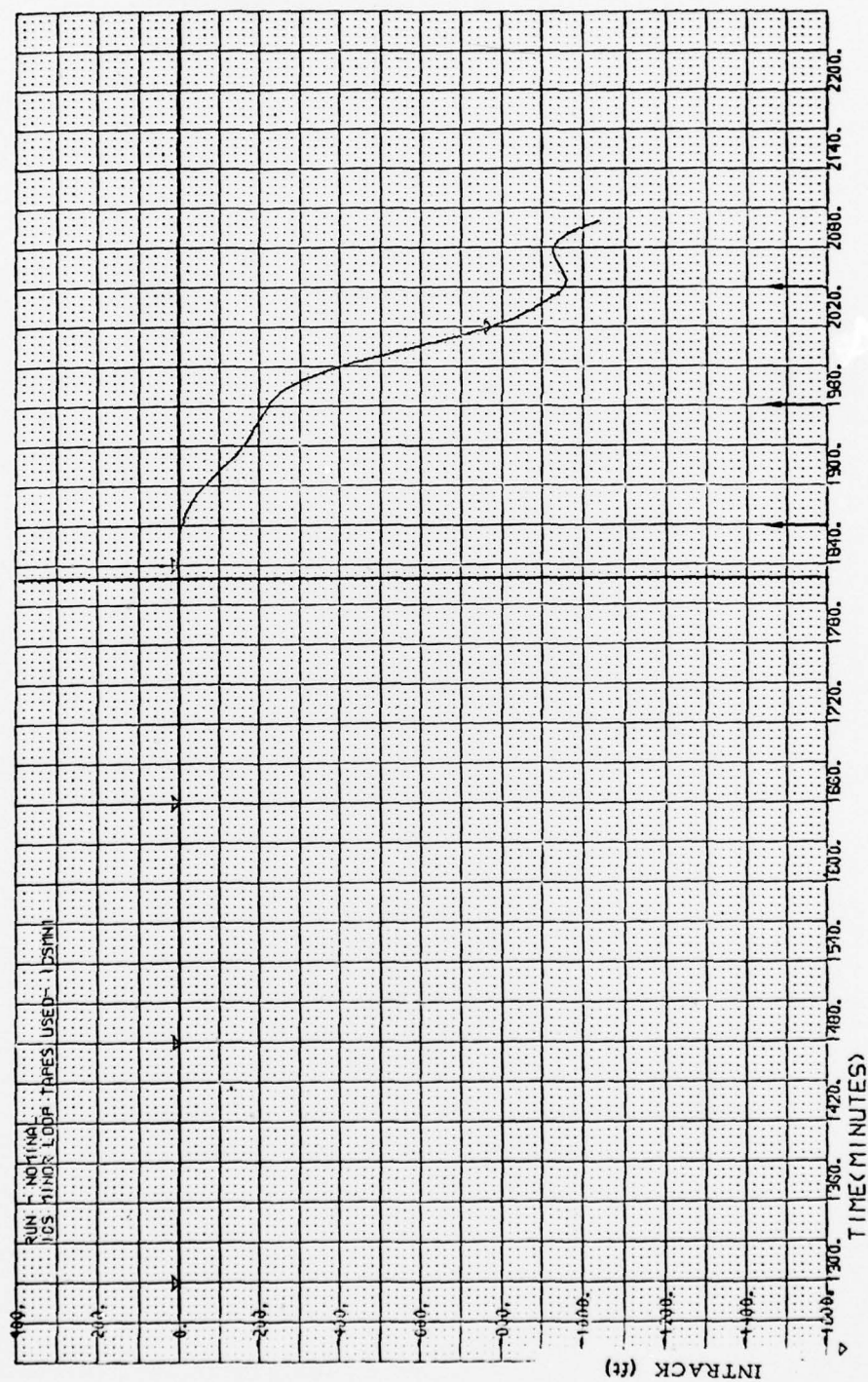Fig. A-18. Calorimeter (fit)/MODB (predict) 792-800

-82-

Fig. A-18. Calorimeter (fit)/MODB (predict) 792-800 (Continued)

-83-

RUN: SMOOTHING
JOB: MINOR LOOP TAPES USED(-) SPAN(-)

TIME(MINUTES)

300. 360. 420. 480. 540. 600. 660. 720. 780. 840. 900. 960. 1020. 1080. 1140. 1200.
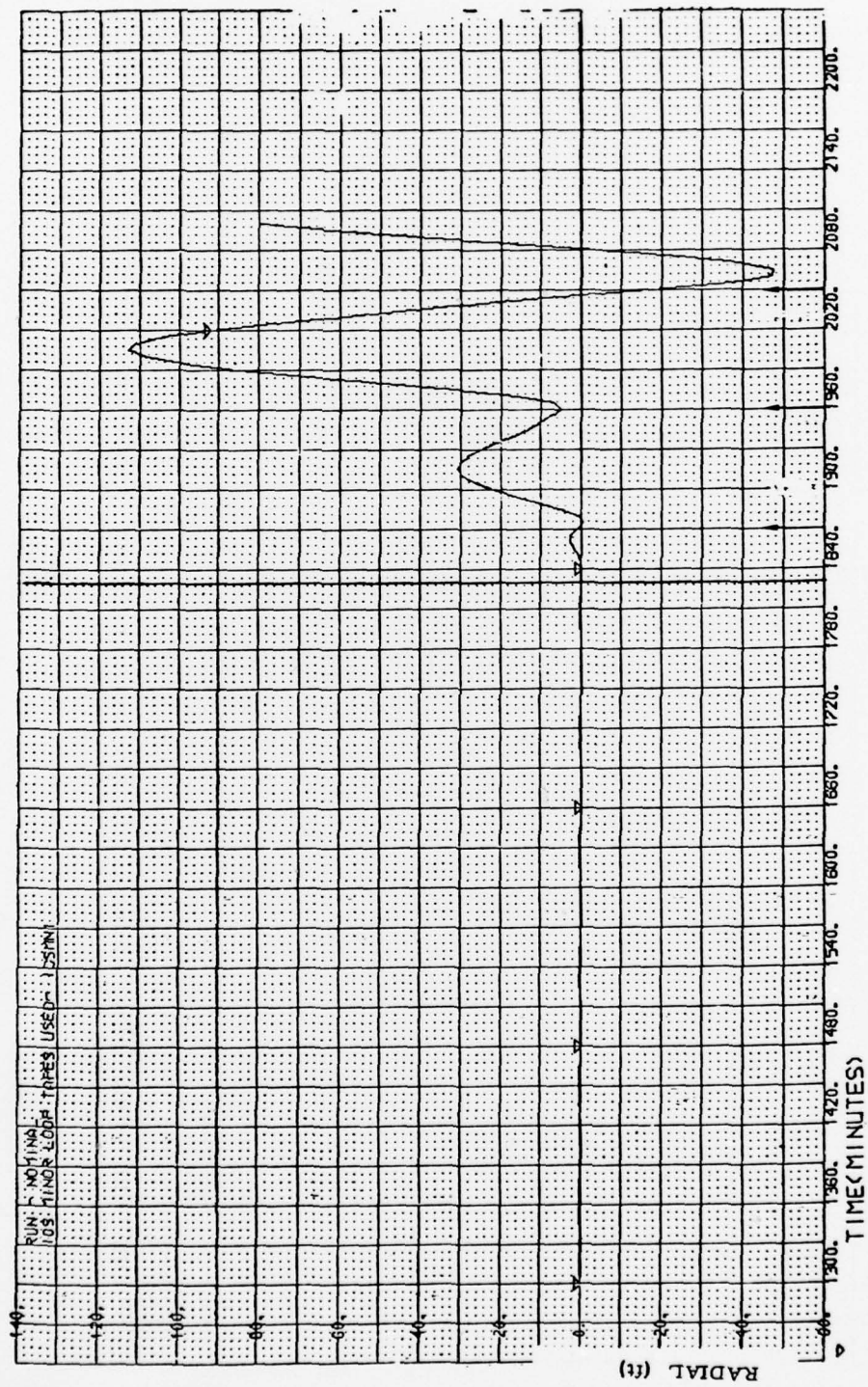
RADIAL (ft)

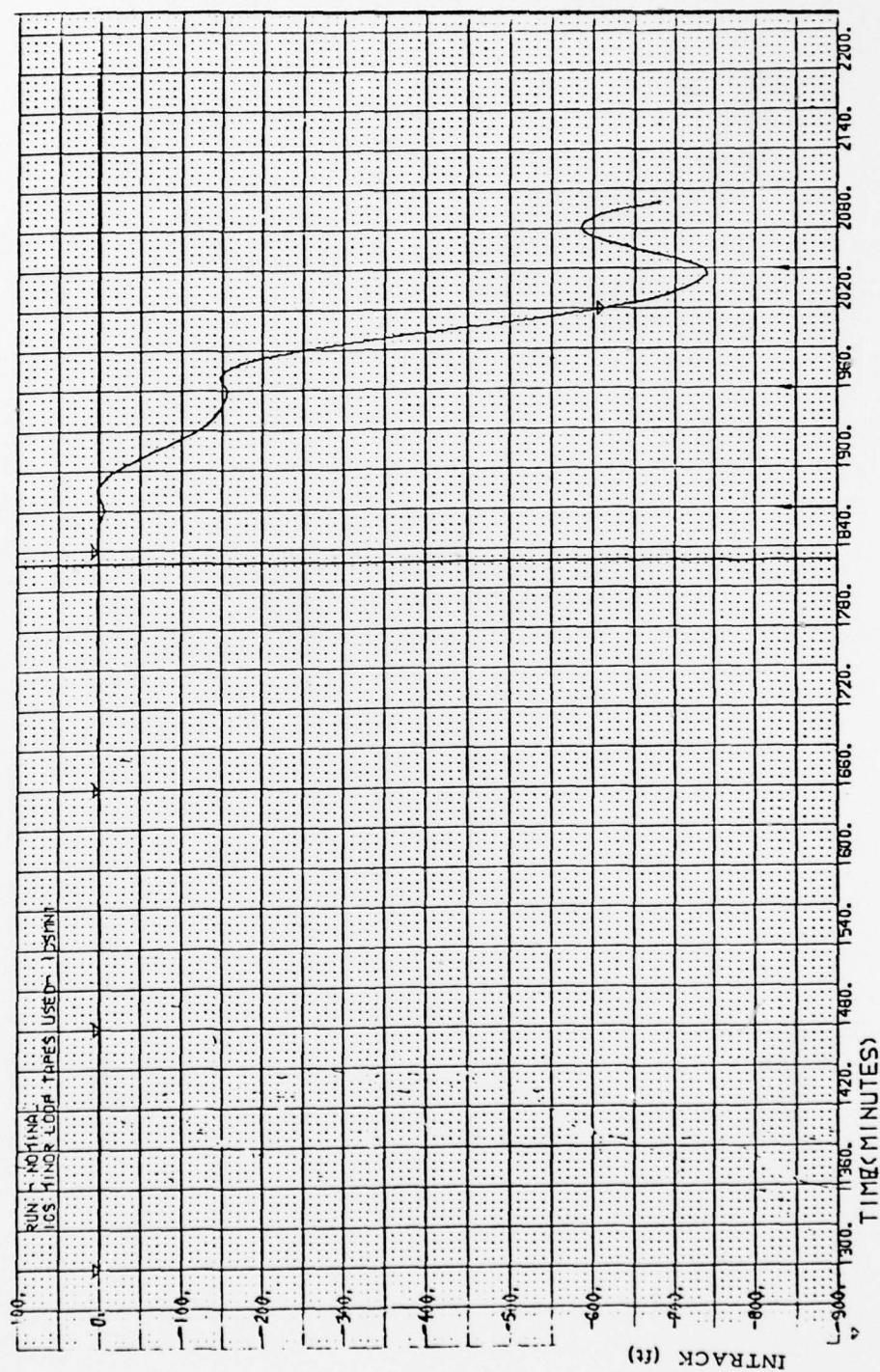Fig. A-19. Calorimeter (fit)/MODC (predict) 792-800

-84-

Fig. A-19. Calorimeter (fit)/MODC (predict) 792-800 (Continued)
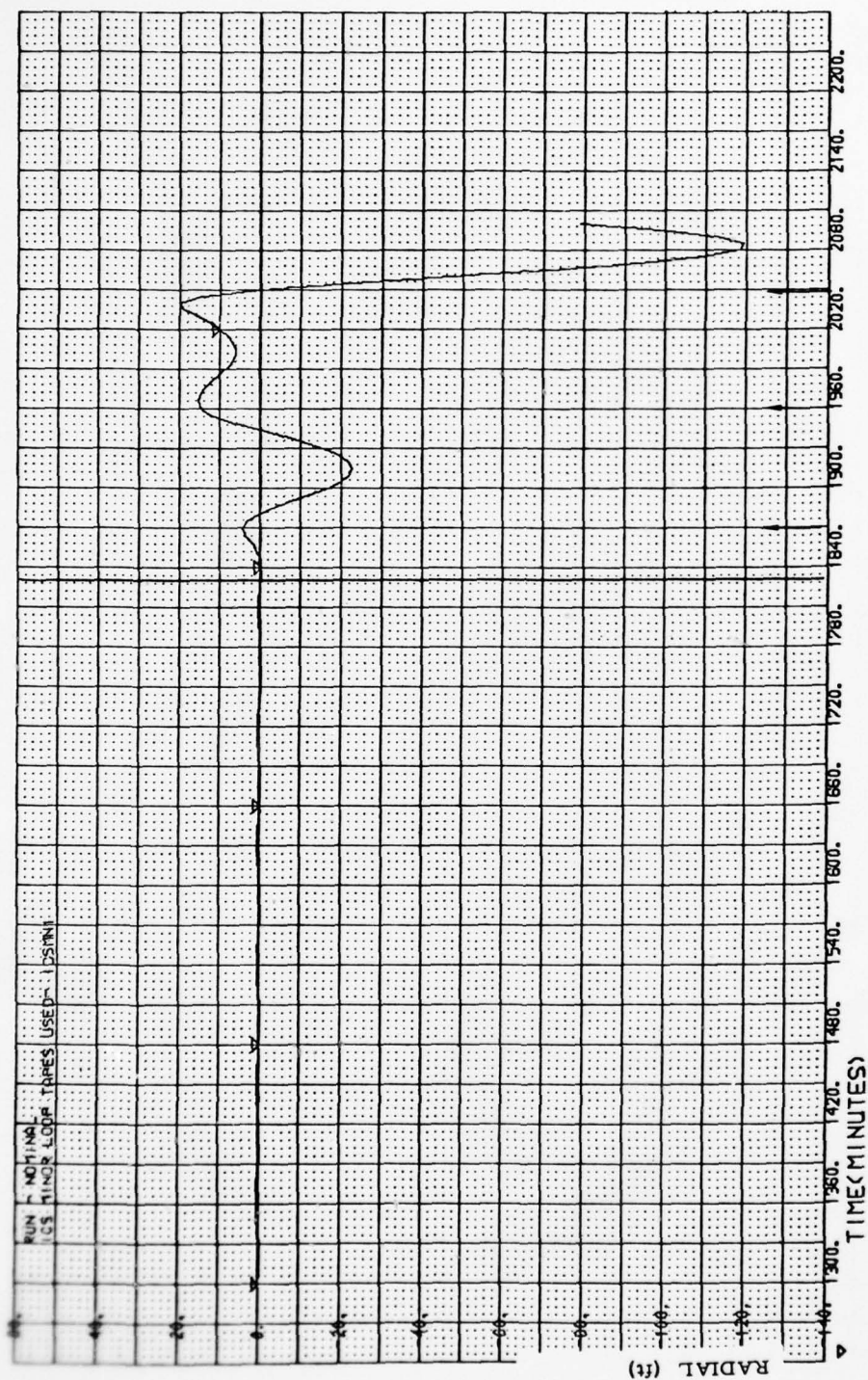
Fig. A-20. Calorimeter (fit)/"DENSEL (predict) 792-800
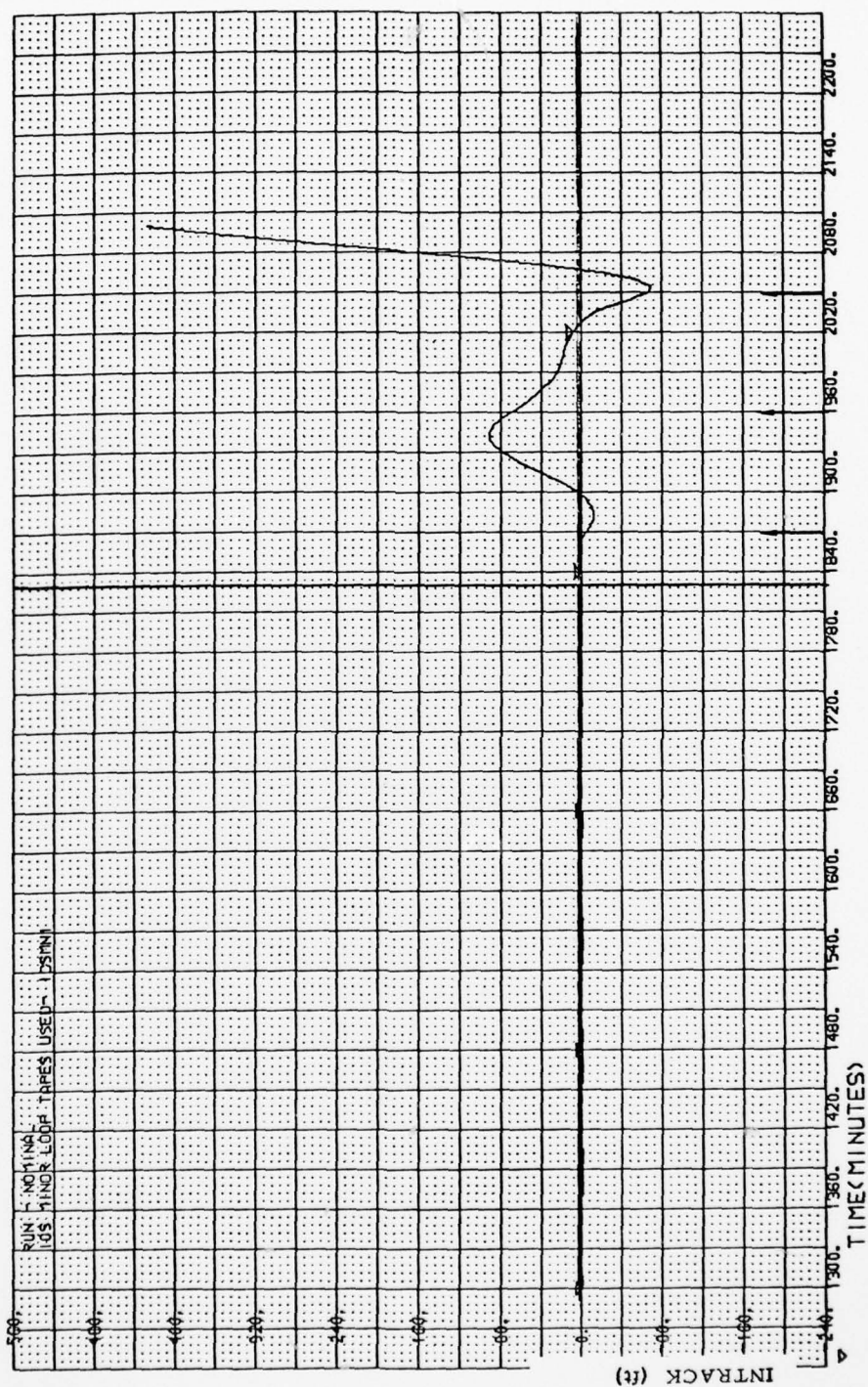
-86-

Fig. A-20. Calorimeter (fit)/"DENSEL (predict) 792-800 (Continued)

APPENDIX B. Altitude Normalization Procedure

The exponential altitude dependence of the density generally dominates over time- and horizontal space-dependent effects, and thus it is necessary to remove altitude effects in order to study atmospheric changes. A plot of the orbit-integrated density versus altitude of perigee is shown in Fig. B-1. A curve of the form

$$Y(z) = \exp\left[c_1 + c_2(z - z_0) + c_3(z - z_0)^2\right]$$

was fit to the data and is shown in the figure. In the expression above the c_i's are parameters of the fit, z is altitude, and z_0 is the reference altitude, chosen to be 70 nm.

For studies of time and horizontal space variations in the drag field, the orbit-integrated densities $Q_p(z_p)$ were reduced to the reference altitude z_0 using

$$Q_0(z_0) = Q_p(z_p) \cdot Y(z_0) / Y(z_p)$$
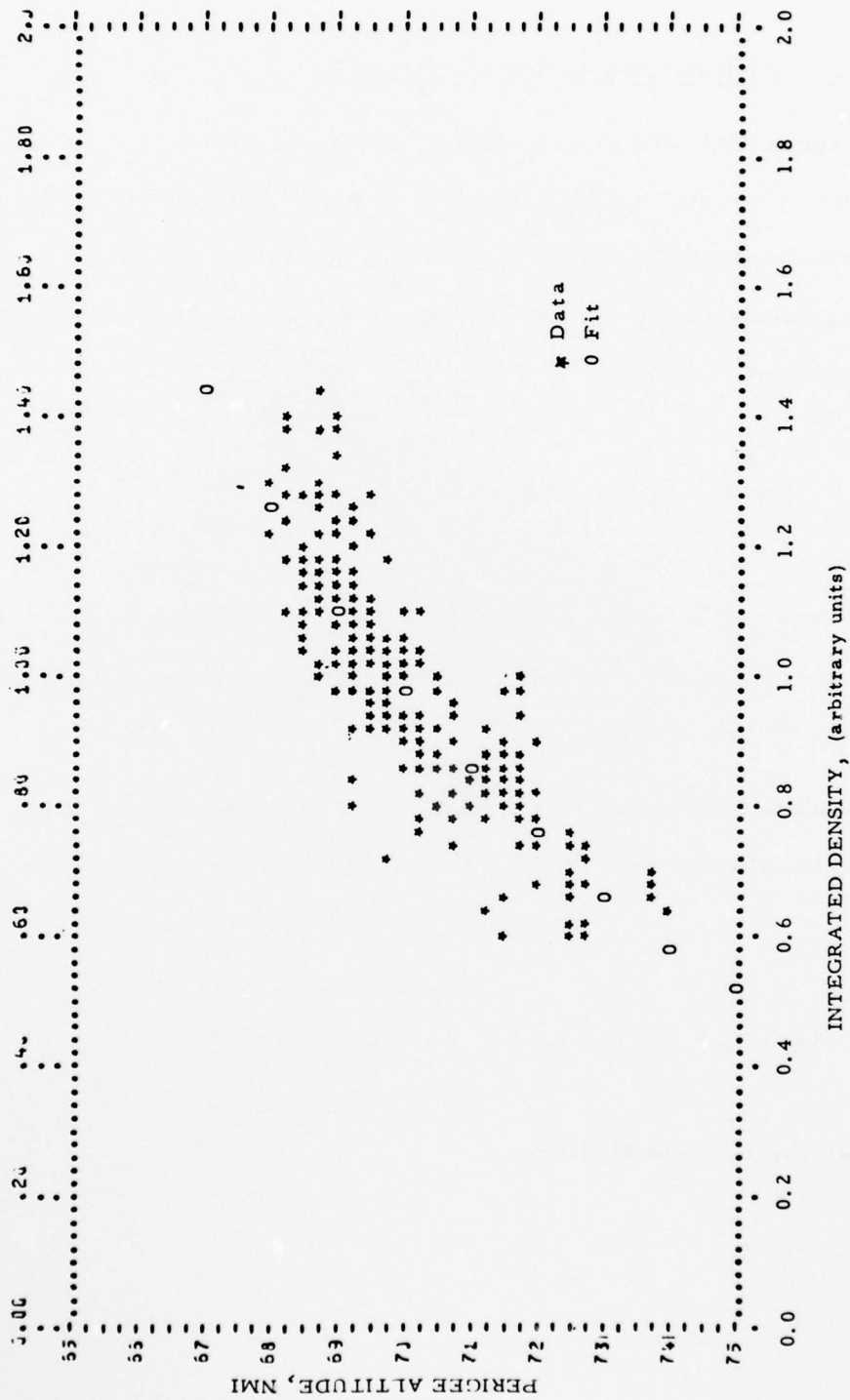
where z_p was the perigee altitude.

INTEGRATED DENSITY, (arbitrary units)

Fig. B-1. Orbit Integrated Density Vs. Altitude of Perigee

THE IVAN A. GETTING LABORATORIES

The Laboratory Operations of The Aerospace Corporation is conducting experimental and theoretical investigations necessary for the evaluation and application of scientific advances to new military concepts and systems. Versatility and flexibility have been developed to a high degree by the laboratory personnel in dealing with the many problems encountered in the nation's rapidly developing space and missile systems. Expertise in the latest scientific developments is vital to the accomplishment of tasks related to these problems. The laboratories that contribute to this research are:

Aerophysics Laboratory: Launch and reentry aerodynamics, heat transfer, reentry physics, chemical kinetics, structural mechanics, flight dynamics, atmospheric pollution, and high-power gas lasers.

Chemistry and Physics Laboratory: Atmospheric reactions and atmospheric optics, chemical reactions in polluted atmospheres, chemical reactions of excited species in rocket plumes, chemical thermodynamics, plasma and laser-induced reactions, laser chemistry, propulsion chemistry, space vacuum and radiation effects on materials, lubrication and surface phenomena, photosensitive materials and sensors, high precision laser ranging, and the application of physics and chemistry to problems of law enforcement and biomedicine.

Electronics Research Laboratory: Electromagnetic theory, devices, and propagation phenomena, including plasma electromagnetics; quantum electronics, lasers, and electro-optics; communication sciences, applied electronics, semiconducting, superconducting, and crystal device physics, optical and acoustical imaging; atmospheric pollution; millimeter wave and far-infrared technology.

Materials Sciences Laboratory: Development of new materials; metal matrix composites and new forms of carbon; test and evaluation of graphite and ceramics in reentry; spacecraft materials and electronic components in nuclear weapons environment; application of fracture mechanics to stress corrosion and fatigue-induced fractures in structural metals.

Space Sciences Laboratory: Atmospheric and ionospheric physics, radiation from the atmosphere, density and composition of the atmosphere, aurorae and airglow; magnetospheric physics, cosmic rays, generation and propagation of plasma waves in the magnetosphere; solar physics, studies of solar magnetic fields; space astronomy, x-ray astronomy; the effects of nuclear explosions, magnetic storms, and solar activity on the earth's atmosphere, ionosphere, and magnetosphere; the effects of optical, electromagnetic, and particulate radiations in space on space systems.

THE AEROSPACE CORPORATION
El Segundo, California
· · ·